ISSN 0917-1185

ANNUAL REPORT OF NATIONAL INSTITUTE FOR FUSION SCIENCE

April 2019 – March 2020

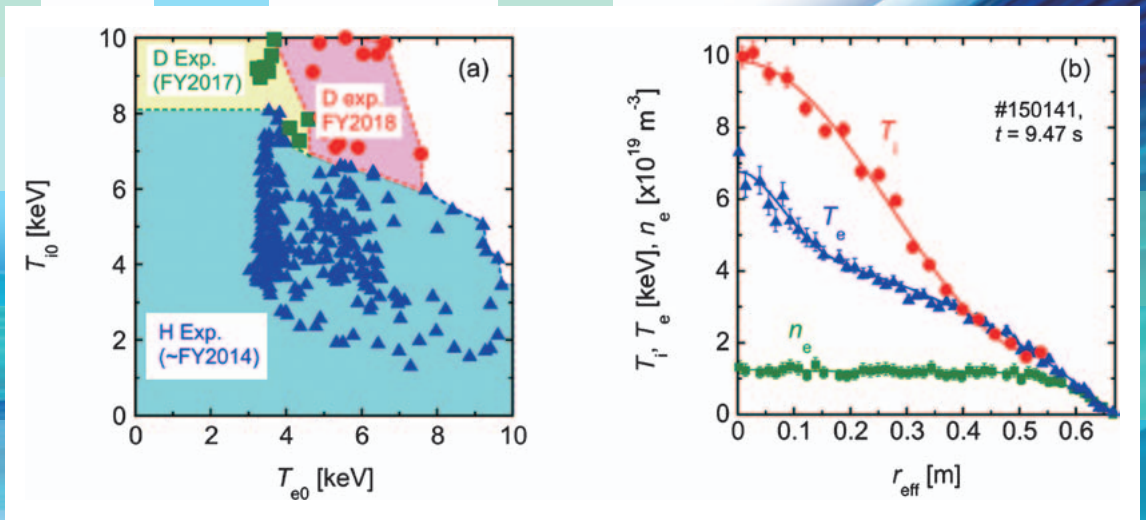

NATIONAL INSTITUTE FOR FUSION SCIENCE
TOKI CITY, JAPAN

Front Cover Caption:

Fig. (a) The operational map of high temperature plasmas, (b) the radial profiles of T_i, T_e, n_e of the typical plasma obtained in FY2018, of which T_i and T_e are simultaneously high.

H. Takahashi et al., presented in the 22nd International Stellarator Heliotron Workshop, Madison, USA, I-2 (2019).

Printer: Arakawa Printing Co., Ltd.
2-16-38 Chiyoa, Naka-ku, Nagoya-shi 460-0012, JAPAN
Phone: +81-52-262-1006, Facsimile: +81-52-262-2296

Printed in Japan, ISSN 0917-1185

ANNUAL REPORT OF NATIONAL INSTITUTE FOR FUSION SCIENCE

April 2019 – March 2020

December 2020

Inter-University Research Institute Corporation
National Institutes of Natural Sciences

NATIONAL INSTITUTE FOR FUSION SCIENCE

Address : Oroshi-cho, Toki-shi, Gifu-ken 509-5292, JAPAN
Phone : +81-572-58-2222
Facsimile : +81-572-58-2601
Homepage on internet : URL = http://www.nifs.ac.jp/

Contents

National Institute for Fusion Science
April 2019 – March 2020

The most inevitable issue for mankind in this century is energy security. Energy resources alternative to fossil fuels are indispensable for a sustainable society, since there is expanding demand for energy on a global scale due to the explosive population growth and economic development concentrated in developing countries. In addition, the increase in greenhouse gases such us carbon dioxide due to the continued use of fossil fuels and the depletion of fuel resources will become serious issues.

The realization of nuclear fusion energy can resolve the serious environmental and energy crisis which humans are now facing. The fuels for fusion can be obtained from seawater, therefore fusion energy is virtually inexhaustible. Furthermore, the fusion reaction does not emit carbon dioxide, thus fusion energy can be the ultimate clean energy. Fusion research around the world has progressed year by year based on the steady progress of basic science and advanced technology. On the other hand, critical scientific and technological issues which must be resolved to put this energy resource in our hands remain.

In order to promote the scientific and engineering research towards the realization of fusion energy, National Institute for Fusion Science (NIFS) conducts three major projects, the Large Helical Device (LHD) Project, the Numerical Simulation Reactor Research Project and the Fusion Engineering Research Project. These three pillars collaborate and stimulate each other to contribute to the progress of the comprehensive fusion science. In addition to the above three major projects mentioned above, NIFS also supports interdisciplinary and basic research, and promotes the coordinated research for ITER-BA cooperation, laser cooperation and academic-industrial cooperation.

This annual report summarizes achievements of research activities concerning the fusion research at NIFS from April 2019 to March 2020. NIFS is an inter-university research organization which conducts collaboration research programs under three frameworks, i.e., General Collaboration Research, LHD Collaboration Research and Bilateral Collaboration Research. More than 500 collaborating research topics were proposed by collaborators in universities or institutes across the country. Proposals from abroad were also included.

Finally, I would like to emphasize one more important role of NIFS, the development of human resources. NIFS is pouring energy into education for graduate students who will realize fusion power generation and our society. For this purpose, NIFS provides the advanced education system through the Graduate University for Advanced Studies (Sokendai). Educational collaboration with partner universities across the nation is also conducted by accepting their graduate students to NIFS.

Yasuhiko Takeiri
Director-General
National Institute for Fusion Science

1. Large Helical Device (LHD) Project

The Large Helical Device (LHD) project conducts fusion-grade confinement research in a steady-state machine to elucidate important research issues in physics and engineering for the helical-type fusion reactor.

The LHD is one of the largest helical devices, with major and averaged minor radii of 3.6 – 4.0 m and 0.6 m, respectively. A double helical coil and three pairs of poloidal coils are all superconducting, by which maximum magnetic field strength at the plasma center is 3 T. For plasma heating, three negative-ion-based 180 – 190 keV neutral beams with total heating power of 8 – 16 MW are injected tangentially to the plasma.

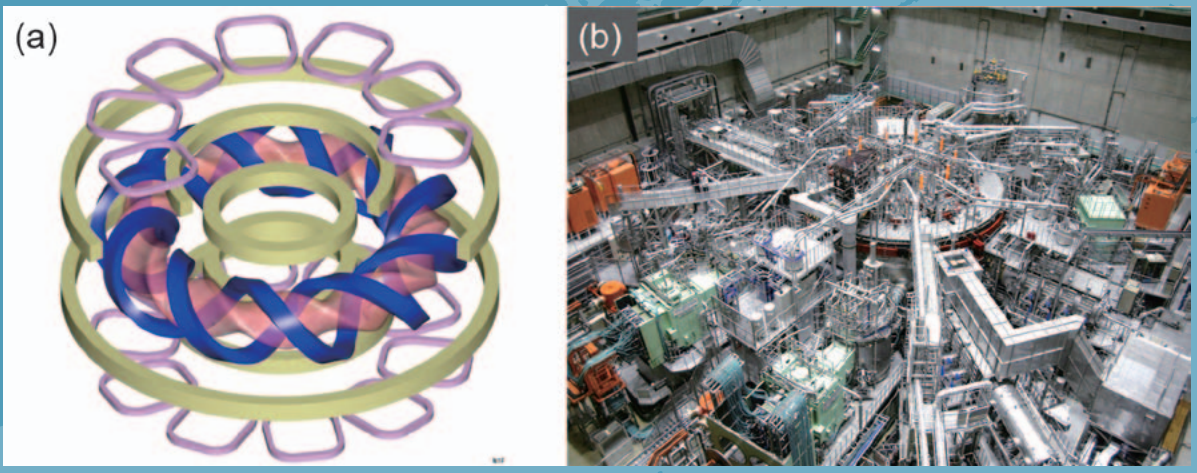

Fig. 1 (a) Coil configuration of LHD. Superconducting helical coils (blue), poloidal coils (yellow) and normal conducting RMP coils, together with plasma. (b) LHD torus hall.

Two positive-ion-based 40 – 80 keV neutral beams with total heating power of 6 – 18 MW are also injected perpendicular to the plasma. In addition, electron cyclotron resonance heating with total heating power of ~ 5.5 MW is also available. For fuelling, LHD is equipped with four gas puff valves and two pellet injectors.

Since 2018, LHD has performed the deuterium experiment in which plasma is expected to improve its performance, thanks to the "isotope effect". Achieved plasma parameters to date are summarized in Table 1.

Table 1 A Achieved plasma parameters (1990 – 2018)

Parameters	Achieved	Key physics	Target
T_i	10 keV ($n_e = 1.3\times10^{19}$ m^{-3})	Ion ITB Impurity hole	10 keV ($n_e = 2\times10^{19}$m^{-3})
T_e	20 keV (2×10^{18} m^{-3}) 10 keV (1.6×10^{19} m^{-3})	Electron ITB	10 keV (2×10^{19}m^{-3})
Density	1.2×10^{21}m^{-3} ($T_e = 0.25$ keV)	Super dense core	4×10^{20} m^{-3} ($T_e = 1.3$ keV)
β	5.1 % ($B_T = 0.425$ T) 4.1 % (1 T)	MHD in current-free plasmas	5 % ($B_T = 1$ - 2 T)
Steady-state operation	54min. 28sec (0.5MW, 1keV, 4×10^{18}m^{-3}) 47min. 39sec. (1.2MW, 2keV, 1×10^{19}m^{-3})	Dynamic wall retention	1 hour (3 MW)

(T. Morisaki)

High Performance Plasma

Highlight

Extension of high temperature operational regime

In future reactors, the fusion reaction is expected to be sustained under the electron heating dominant condition, where both the ion temperature (T_i) and the electron temperature (T_e) are high. Thus not only the investigation of the confinement improvement but also the characterization of the thermal transport for the plasmas, of which T_i and T_e are simultaneously high, are necessary. In the present status, such a plasma condition is realized by the combination heating of a neutral beam injection (NBI) and an electron cyclotron resonance heating (ECRH).

In the Large Helical Device (LHD), the deuterium (D) experiment was initiated in March 2017 in order to seek higher performance plasmas and to study the mechanism of the increased performance by isotope effect. In the first D experiment campaign in 2017, we successfully attained the T_i of 10 keV [1]. The achievement of the T_i value is a milestone toward realizing a helical reactor, which has an intrinsic advantage for steady state operation, because the T_i value is one of the important ignition conditions. In the FY2018 experimental campaign, we focused on the performance integration of high temperature plasmas and the investigation of confinement characteristics of plasmas, of which T_i and T_e is simultaneously high. As a representative result, high temperature operation regime could be successfully extended. The extended operation regime and the typical temperature and electron density (n_e) profiles are shown in Fig. 1 (a) and (b), respectively. The extended high temperature regime was realized due to the suppression of EIC (Energetic ion driven interchange) modes and the control of the T_e/T_i in the moderate range, where the ion thermal confinement does not degrade [2].

(H. Takahashi)

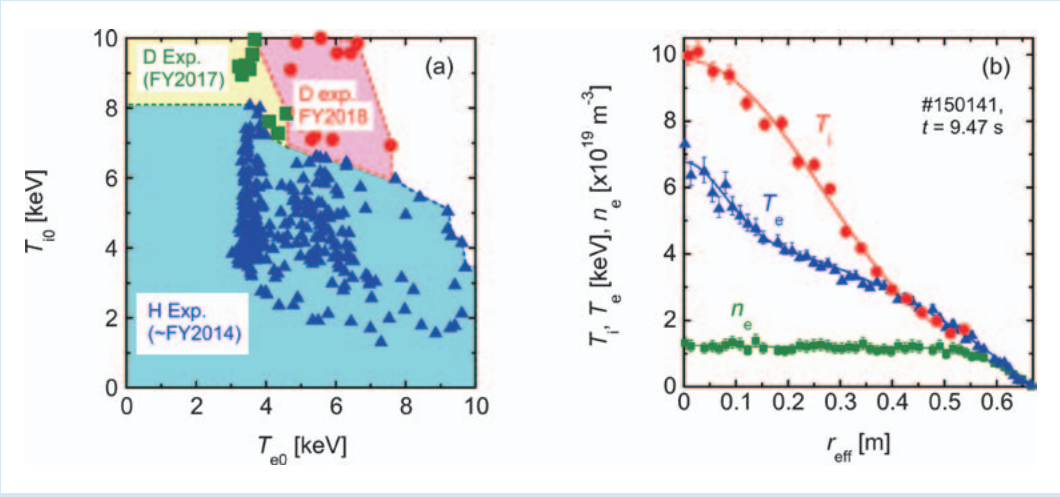

Fig. 1 (a) The operational map of high temperature plasmas, (b) the radial profiles of T_i, T_e, n_e of the typical plasma obtained in FY2018, of which T_i and T_e are simultaneously high [2].

Realization of higher ion temperature due to the suppression of EIC using ECRH

In the D experiments initiated in the LHD from 2017, the simultaneous high T_i and high T_e regime has been successfully extended mainly due to the suppression of the EIC modes and control of the T_e/T_i value. The EIC is triggered by helically trapped ions at lower order magnetic resonant surface and the EIC causes loss of high energy ions, leading to the decrease in T_i [3]. The mode width of EIC depends on $T_e^{-1/2}$ thus the increase in T_e at resonant surface is expected to be effective to suppress the EIC.

Figure 2 shows the comparison of the time evolution of (a) the heating power, (b) the line-averaged-electron density n_{e_fir}, (c) the poloidal magnetic fluctuation amplitude B_θ, (d) the neutron emission rate S_n, (e) the central electron temperature T_{e0}, (f) the central ion temperature T_{i0}, and the radial profiles of (g) the T_e and (h) the T_i in the plasmas which the highest T_i was achieved in the FY2017 and the 2018 experimental campaign. The NBI power was similar (~30 MW). The t_0 in the horizontal axis represents the plasma start-up timing. In the plasma obtained in FY2017, the EIC event occurred and the significant drop in the S_n was observed. This represents the loss of the high energy particles from the plasma. On the other hand, the EICs were clearly suppressed in #150133 using the superposed ECRH. Due to the suppression of the EICs, T_{i0} exceeded the previous record of 10 keV [2].

(H. Takahashi)

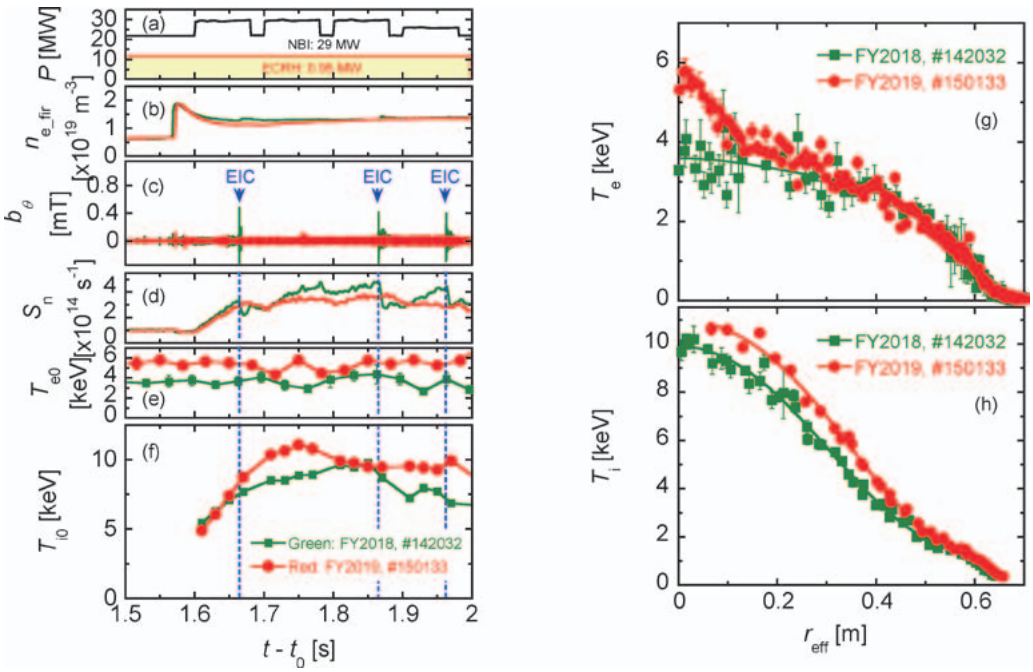

Fig. 2 Time evolution of (a) the heating power, (b) the line-averaged-electron density n_{e_fir}, (c) the poloidal magnetic fluctuation amplitude B_θ, (d) the neutron emission rate S_n, (e) the central electron temperature T_{e0}, (f) the central ion temperature T_{i0}, and the radial profiles of (g) the T_e and (h) the T_i in the plasmas which the highest T_i was achieved in the FY2017 and the 2018 experimental campaign [2].

Isotope effect in the internal transport barrier strength

In order to unveil the isotope effect in the internal transport barrier (ITB), a measure of the ITB strength newly defined. The ITB strength deuterium (D) and hydrogen (H) plasmas is compared, and it is found that the ITB strength is systematically high in D plasmas than H plasmas.

Unlike the case of tokamak plasmas, there is no generally accepted criterion for the ITB strength in stellarators/heliotrons. Here, a new criterion for the ITB strength is proposed by defining a unique scalar coefficient. The typical L-mode plasmas in LHD are characterized by the dome-shaped temperature profile with the diffusion coefficient being proportional to the temperature to the power of a factor α, i.e., $\chi \propto T^{\alpha}$, where $\alpha = 1$ is widely applicable. The reference L-mode profile $T_L^{ref}(r)$ is defined by extrapolating the edge temperature profile to the core according to the solution of the thermal diffusion equation with $\chi \propto T^{\alpha}$. By comparing the volume integral of $n_e(r)T_L^{ref}(r)$ with the electron kinetic stored energy, the profile gain factor $G_{1.0}$ is defined as a measure of the ITB strength [4] to be

$$G_{1.0} = \frac{\int_0^a n_e(r) T_i(r) V' dr}{\int_0^a n_e(r) T_i^{ref}(r) V' dr},$$

where V' is the radial derivative of the plasma volume and a is the plasma minor radius.

In LHD, the ITB in the ion temperature profile is typically formed when an intense neutral beam heating is applied to low electron density plasmas. Figure 3 compares the high and low electron density discharges in D plasmas. Symbols and curves correspond to the measured data and $T_L^{ref}(r)$, respectively. Stronger ion temperature ITB is formed in the low electron density plasma with $G_{1.0} \sim 1.47$ compared to the high electron density plasma with $G_{1.0} \sim 1.01$.

The proposed method is applied to both D and H discharges with the line averaged density scan in the shot-to-shot basis (fig. 4). When the line averaged density ($\bar{n}_e$) is high, $G_{1.0} \sim 1$ that corresponds to the L-mode, and decreasing $\bar{n}_e$ leads to a non-monotonic increase in $G_{1.0}$. Larger $G_{1.0}$ is routinely observed in D plasmas in $\bar{n}_e < 2\times10^{19}$ m^{-3} [5]. The isotope difference in the ITB strength is much distinguishable compared to the isotope difference in the confinement scaling [6].

Another dedicated set of experiments was performed to identify a slowing down MHD mode for triggering a collapse of the ITB in electron temperature profile. The ITB collapse event is observed in the neutral beam switching experiments, in which the core rotational transform profile is forced to be reversed or flattened by the toroidal return current. The mode radial width expands as the rotation frequency decays after its emergence. By this mode activity, the central electron temperature gradient is gradually

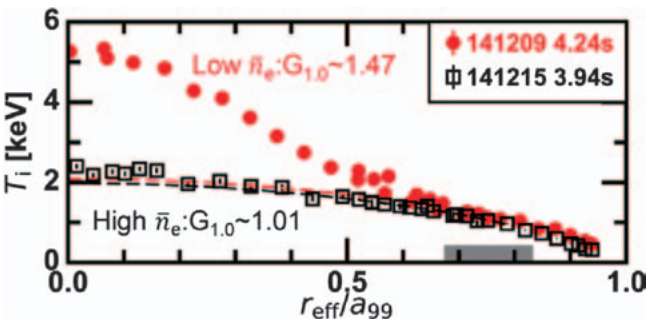

Fig. 3 Radial profiles of ion temperatures (symbols) and reference L-mode profiles (dashed curves) in low and high electron density discharges [5].

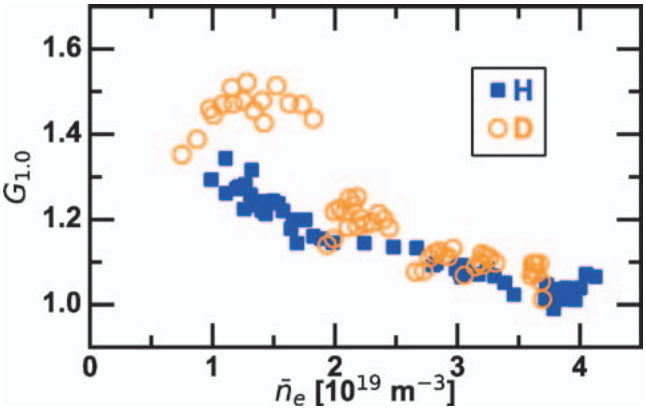

Fig. 4 Line averaged density dependence of the profile gain factor $G_{1.0}$ for D and H plasmas [5].

weakened. The mode is found to have two phase inversion points in radius, which we call the double-odd-parity. Advanced motional Stark effect (MSE) spectroscopy diagnostics suggests a possible role of the reversed or flattened iota profile for the mode excitation and the ITB collapse [7].

(T. Kobayashi)

[1] H. Takahashi *et al*., Nucl. Fusion **58**, 106028 (2018).
[2] H. Takahashi *et al*., presented in the 22nd International Stellarator Heliotron Workshop, Madison, USA, I-2 (2019).
[3] K. Ogawa *et al*., Nucl. Fusion **58**, 044001 (2018).
[4] T. Kobayashi *et al*., Plasma Phys. Control. Fusion **61**, 085005 (2019).
[5] T. Kobayashi *et al*., Sci. Rep. **9**, 15913 (2019).
[6] H. Yamada *et al*., Phys. Rev. Lett. **123**, 185001 (2019).
[7] T. Kobayashi *et al*., Nucl. Fusion **60**, 036017 (2020).

Transport and Confinement

Highlight

Isotope effect on energy confinement and thermal transport in NBI-heated plasmas in LHD

It has been recognized that thermal transport in toroidal plasmas is dominated by the turbulence with the characteristic scale of ion gyro-radius. However, while this gyro-Bohm model predicts $\chi \propto \rho^* \propto M^{1/2}$, major experimental observations in tokamak have shown better confinement in deuterium(D) with heavier mass M than in hydrogen(H). This isotope effect remains a long-standing mystery in fusion research. Extensive and elaborated comparisons of H and D plasmas in LHD have unveiled the co-existence of the gyro-Bohm nature and significant mass dependence.

The regression analysis of thermal energy confinement time has shown $\tau_{E,th}^{scl} \propto M^{-0.02} B^{0.89} \bar{n}_e^{0.75} P_{abs}^{-0.90}$. Here no significant dependence on M is distinguished and this expression is inconsistent with the gyro-Bohm model suggesting $M^{-0.5}$ dependence. However, this scaling expression rephrased into the dimensionless form yields $\tau_{E,th}^{scl} \Omega_i \propto M^{0.98} \rho^{*-2.99} \nu^{*0.21} \beta^{-0.35}$. It should be noted that the gyro-Bohm nature is described as $\tau_E \Omega_i \propto M^0 \rho^{*-3}$. Additional clear M dependence is identified here, which compensates unfavorable negative dependence on M in the gyro-Bohm model while the gyro-Bohm dependence of ρ_*^{-3} persists.

Then thermal diffusivity in dimensionally similar plasmas has been compared. Since the three operational parameters B, $\bar{n}_e$, and P_{abs} are controllable in the experiment, dimensionally identical conditions in terms of ρ^*, ν^*, and β can be fulfilled for plasmas with different M [1]. Normalized thermal diffusivity χ/Ω_i is expected to be the same between these dimensionally similar plasmas. However, Fig. 1 shows that $\chi_e/(S_{2/3}\Omega_i)$ is improved robustly in D from H by a factor of around 2, which may implicate $1/M$. Therefore, reduction of thermal diffusivity in D is consistent with the significant mass dependence seen in the dimensionless expression of $\tau_{E,th}^{scl}$.

[1] H. Yamada *et al.*, Phys. Rev. Lett. **123**, 185001 (2019).

(H. Yamada, The University of Tokyo)

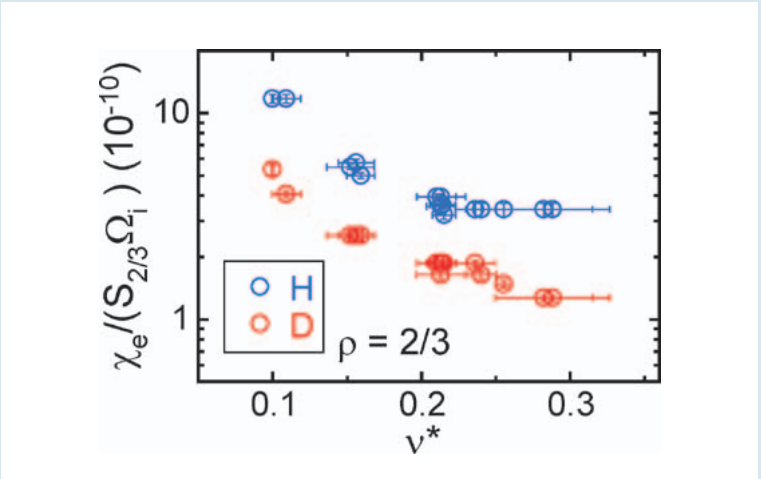

Fig. 1 Comparison of dimensionally similar plasmas. The thermal diffusivity at ρ=2/3 normalized by the corresponding surface area $S_{2/3}$ and Ω_i as a function of ν^*.

Isotope-mixing and non-mixing states in hydrogen-deuterium mixture plasmas

Transition between isotope-mixing and non-mixing states in hydrogen-deuterium mixture plasmas is observed in the isotope (hydrogen and deuterium) mixture plasma in LHD. In the non-mixing state, the isotope density ratio profile is non-uniform when the beam fueling isotope species differs from the recycling isotope species and the profile varies significantly depending on the ratio of the recycling isotope species. Bulk charge exchange spectroscopy system [1] has been installed in LHD to measure the radial profiles of hydrogen fraction $n_H/(n_H+n_D)$ in the plasma from H_α and D_α lines emitted by the charge exchange reaction between the bulk ions and the neutral beam injected. The transition from non-mixing state to isotope-mixing state is observed after H and D pellet injections [2]. Before the pellet injection the H density profile is much more peaked than the D density profiles due to the H beam fueling and D dominating recycling as seen in Fig. 1 (a), and the hydrogen fraction is non-uniform (isotope non-mixing state). After the pellet injection, the hydrogen fraction becomes uniform (isotope mixing state) as seen in Fig. 1 (b).

Figure 2 (a) (b) shows the density fluctuation spectrum integrated from edge to core along the laser beam line of the central chord of phase contrast imaging (PCI) for non-mixing and isotope-mixing states and the linear growth rates calculated with gyrokinetic simulation code GKV for TEM and ITG turbulence. The fast transition from non-mixing state to isotope-mixing state (nearly uniform profile of isotope ion density ratio) is observed associated with the change of electron density and its profile (with peaked with hollow) by the pellet injection near the plasma periphery. The transition from non-mixing to isotope-mixing state strongly correlates with the increase of turbulence and the transition of turbulent state from TEM to ITG mode as predicted by gyrokinetic simulation.

This results shows that non-mixing and the isotope-

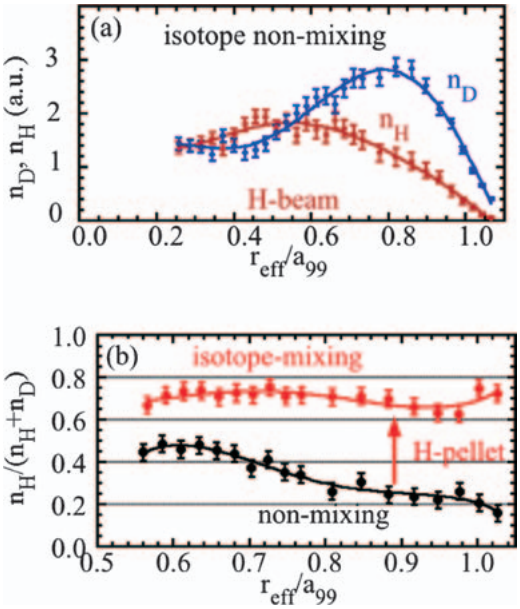

Fig. 1 Radial profiles of (a) hydrogen and deuterium density in isotope non-mixing state and (b) hydrogen fraction before and after the H-pellet injection.

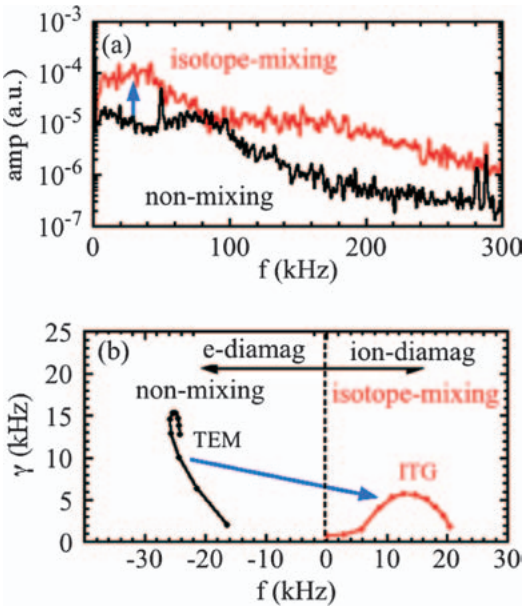

Fig. 2 (a) Density fluctuation spectrum measured with PCI and (b) the linear growth rate at r_{eff}/a_{99}=0.8 for the isotope non-mixing and mixing states calculated with GKV.

mixing states depend on the turbulent state and give the essential knowledge for predicting the isotope density profiles in the D-T mixture plasma in JET and ITER.

[1] K.Ida, *et.al.*, *Rev. Sci. Instrum.* **90**, (2019) 093503.
[2] K.Ida, *et.al.*, *Phys. Rev. Lett.* **124**, (2020) 025002.

(K. Ida)

Improved performance of ECRH by perpendicular injection [1]

Adjustments of launcher settings of electron cyclotron resonance heating (ECRH) are necessary to produce high-performance plasma. The precise evaluation of deposition profiles is also essential for transport studies. For such purposes, a method of perpendicular injection on the horizontally elongated cross section was developed to improve performance of ECRH in LHD. Perpendicular injection to the ECR layer can be more insensitive to the effect of refraction in comparison to the conventional oblique injection. However, the perpendicular injection had not been performed and the oblique injection had been standard in LHD. This is because the unabsorbed wave by perpendicular injection will damage divertor tiles and heat the cryo-sorption panel in closed divertors. Thus, the interlock system for gyrotron power output was developed to avoid injection to extremely low n_e plasma in which the EC wave is less absorbed.

Achieved T_e profiles were compared between the two kinds of injection of 1 MW without modulation. Plasmas were sustained by another two 154 GHz gyrotrons with 1 MW injection power each. As shown in Fig. 1, T_{e0} increased from 4 keV by the standard oblique injection up to 6 keV by the newly developed perpendicular injection at $n_{e,avg} = 1\times10^{19}$ m^{-3}. This will contribute to extending high T_i-T_e regime. Modulation ECRH experiments indicate that perpendicular injection shows better central heating than oblique injection. Refraction and Doppler-shifted absorption in oblique propagation of the EC wave cause broadening of the deposition profiles, in particular at high n_e.

Such an improved ECRH performance has opened up a new operational region in ECRH plasma. As shown in Figs. 2 (a1)~(d1), high density plasma of $n_{e0} \sim 8\times10^{19}$ m^{-3} was successfully sustained after injection of three consecutive hydrogen ice pellets for the first time only by ECRH in LHD. Two 154-GHz gyrotrons for standard oblique injection and one 77-GHz gyrotron for perpendicular injection were used for plasma sustainment. Hollow n_e profiles by

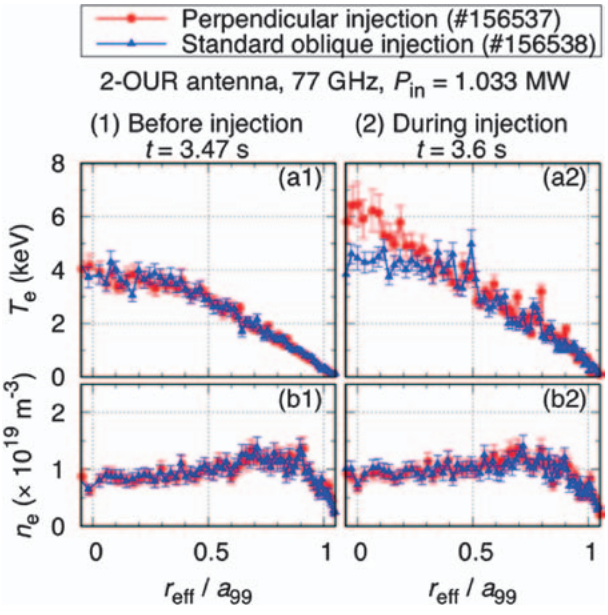

Fig. 1 Comparisons of radial profiles of (a) T_e and (b) n_e (1) before and (2) during perpendicular/oblique injection [1].

gas puffing changed to rather peaked profiles after the pellet injection. Equipartition heating was significant in the high-n_e region: $T_{i0} \sim T_{e0} \sim 1$ keV at $n_{e0} \sim 8\times10^{19}$ m^{-3} and $T_{i0} \sim T_{e0} \sim 2$ keV at $n_{e0} \sim 5\times10^{19}$ m^{-3} were achieved. τ_E at the W_p peak is estimated to be 0.2 s. On the other hand, in the case of oblique injection for the 77-GHz ECRH, high n_e plasma was radiatively collapsed due to the increase of radiation, as shown in Figs. 2 (a2)~(d2). Accumulated database of high n_e discharges with a wide range of n_e by perpendicular injection of higher P_{ECRH} will contribute to comparative studies between different devices such as W7-X, as well as for isotope effect studies.

[1] T. Ii Tsujimura *et al.*, Nucl. Fusion to be submitted.

(T. Tsujimura)

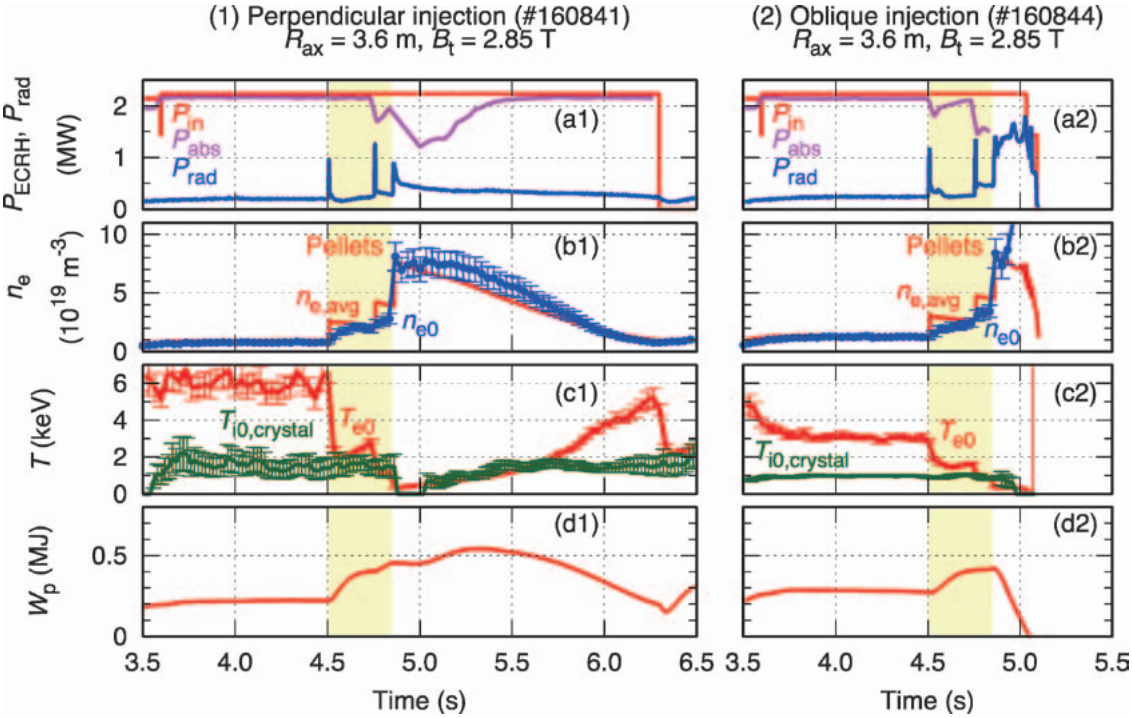

Fig. 2 Comparisons of time evolution of (a) injection power P_{in} and absorption power P_{abs} of ECRH, radiation power P_{rad}, (b) n_{e0}, $n_{e,avg}$, (c) T_{e0}, T_{i0} measured with the crystal spectrometer, and (d) W_p between (1) perpendicular injection and (2) oblique injection [1].

Edge/Divertor/Atomic and Molecular Processes

Highlight

The Impurity Powder Dropper was installed and employed in dedicated experiments

Wall conditioning techniques with low-Z impurities such as boron (B) or lithium are fundamental for accessing low collisionality plasmas, and are employed routinely on tokamaks and stellarators. The Impurity Powder Dropper (IPD), designed and built by PPPL, allows the injecting of low-Z impurities in the form of sub-millimeter powder grains into the plasma, potentially performing a real-time wall-conditioning of the plasma facing components, without interruption of plasma operation.

To investigate the viability of this technique in steady-state operation, the IPD has been installed in LHD sector 2.5 (Fig. 1). A first series of dedicated experiments has been performed, where controlled amounts of B and boron nitride (BN) powder have been injected in a variety of plasma conditions, featuring different species (H and He), heating schemes and magnetic configurations, in discharges of a duration ranging from 4 seconds to 9 minutes.

The successful injection of the powder grains into the plasma is confirmed by multiple diagnostics, such as visible cameras (Fig. 2), UV and charge exchange spectroscopy. Preliminary results show a reduction of wall fueling both on a shot-to-shot basis and even in real time for longer discharges. The intrinsic level of impurities (oxygen and carbon) was also observed to decrease after cumulative injection of B, when the powder injection was performed in the absence of a standard glow discharge boronization.

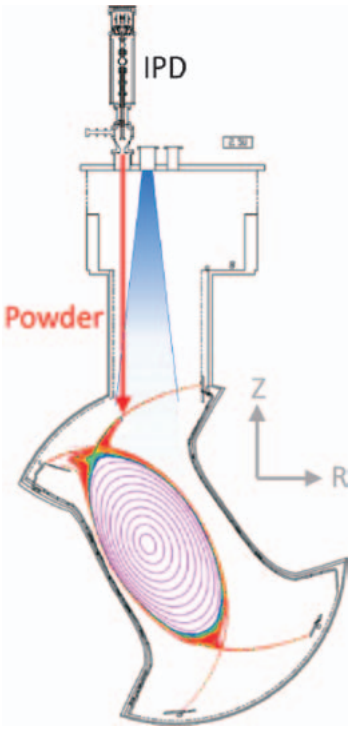

Fig. 1 Position of the IPD on the LHD vacuum vessel with the corresponding plasma poloidal cross section, and field of view of the visible camera.

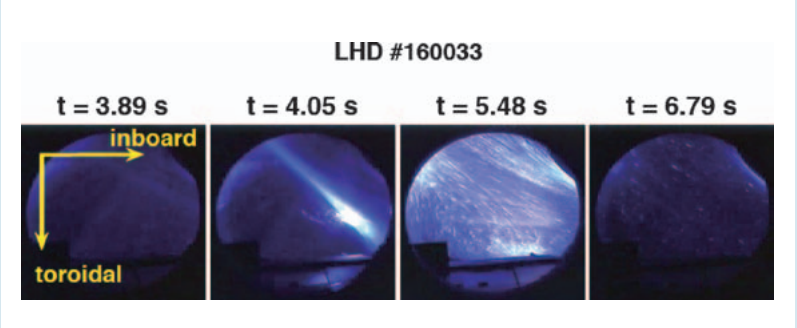

Fig. 2 Visible camera imaging of boron powder injection in LHD plasma.

Steady-state sustainment of divertor heat load reduction with multi-species impurity seeding in LHD

To manage the power exhaust in fusion reactors, a radiation enhancement is required not only in the divertor region but also in the upstream region with suppression of dilution and contamination. Multi-species impurity seeding is a candidate to realize the radiation enhancement in the edge plasma region, and divertor heat load reduction.

Superimposed seeding of higher-Z (Kr) and lower-Z (Ne) impurities have been applied to the LHD plasma [1]. As shown in Fig. 1, although reduction of divertor heat flux, q_{div}, is not significant after Kr seeding at 4.1 s, q_{div} decreases by ~ 85% after Ne seeding at 4.5 s. While the q_{div} reduction only using Ne seeding disappears 0.4 s after the seeding, the q_{div} reduction in Kr+Ne seeded plasma can be sustained for 1 s until termination of NBI heating. T_e decreases at $|r_{eff}/a_{99}| > 0.8$ due to the Ne seeding as shown in Fig. 2 (b). The T_e reduction enhances the emission from the pre-seeded Kr. Negative E_r is formed in the edge plasma and sustained until termination of deuterium gas puff. The negative E_r should be a key for the enhancement of the Kr emission and the sustainment of the heat load reduction. As shown in Fig. 2 (c), the radiation profile in the Kr+Ne seeded plasma can be shifted to upstream region compared with the profile of the only Ne seeded plasma with the same radiation fraction. These results indicate the availability of multi-species impurity seeding with different cooling rate.

[1] K. Mukai *et al.*, Plasma Fusion Res. **15**, 1402051 (2020).

(K. Mukai)

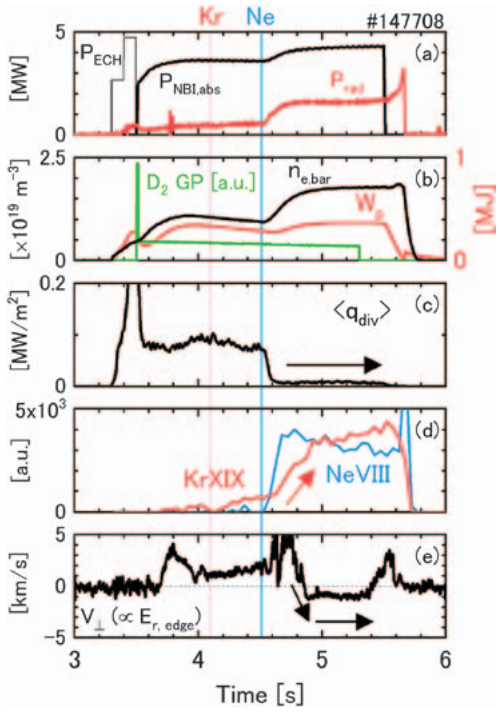

Fig. 1 Waveform of Kr+Ne seeded plasma in LHD. (a) Heating power and plasma radiation power, (b) line-averaged electron density, deuterium gaspuff, and plasma stored energy, (c) divertor heat flux, (d) Line emission of NeVII and KrXIX, and (e) radial electric field at edge plasma.

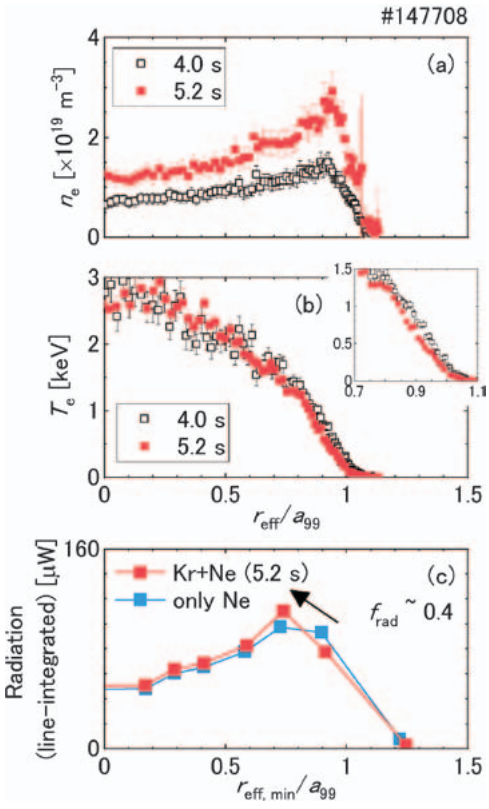

Fig. 2 Radial profiles of Kr+Ne seeded plasma in LHD. (a) electron density, (b) electron temperature, and (c) plasma radiation.

Multi-wavelength spectroscopic observation of line emissions from tungsten ions with a wide range of charge states

Spectroscopic studies for emissions released from tungsten (W) ions ranging from low to high charge states have been intensively conducted in LHD for contribution to the impurity transport study in fusion devices with plasma facing components made of W such as ITER and DEMO, and for the expansion of experimental database of W line emissions. In order to observe the line emissions released from W ions efficiently, W ions are distributed in the LHD plasma by injecting a pellet consisting of a small piece of W metal wire enclosed by a carbon tube. Figure 1 shows ionization energy of W ions, E_i, as a function of charge state, q^+. Ranges of the electron temperature, T_e, of the ITER core plasmas and the LHD core plasmas with W pellet injection are illustrated together for a rough guideline of the distribution of charge states. As shown in the figure, from the neutral atoms, W^0, to the highly-ionized ions up to W^{45+} are observed simultaneously by applying the spectroscopic diagnostics for extreme-ultraviolet (EUV), vacuum-ultraviolet (VUV), and visible wavelength ranges. Figure 2 shows a typical waveform of the W pellet injection experiment in LHD. After the tungsten pellet injection at 4.1 s, the central electron temperature, T_{e0}, once decreases, and then T_{e0} recovered up to around 3 keV by a superposition of ECH for 4.2~4.7 s. At 5.3 s, T_{e0} decreases down to the minimum value with switching the NBIs from the negative ion-sourced NBI (n-NBI) to the positive ion-sourced NBI (p-NBI). In the low T_{e0} phase, the T_e profile is extremely hollow, the so-called "temperature hole" [1]. Even though T_{e0} becomes close to zero, finite value of low T_e is distributed within the confinement region, so it is still possible for W ions to be distributed with releasing emissions. Figure 3 shows wavelength spectra including W line emissions observed in high T_{e0} (= 2.7 keV) and low T_{e0} (~0 keV) phases, which were obtained in the red and blue-hatched periods in Fig. 2, respectively. As shown in Fig. 3 (a-c), W^{41+}, W^{42+}, W^{43+}, W^{45+} lines and W^{24+} ~ W^{33+} ,W^{24+} ~ W^{29+} unresolved-transition arrays (UTAs) are observed in the EUV range as well as the magnetic dipole forbidden transitions of W^{26+} and W^{27+} in the visible range are observed in the high T_{e0} phase [2,3]. On the other hand, W^{6+} and W^{5+} lines are observed in the EUV and VUV ranges, respectively, in the low T_{e0} phase as shown in Fig. 3 (d, e) [4]. Thus, variation in the dominant charge states of W ions against T_{e0} has been successfully demonstrated in a single discharge. This observation can contribute as a fundamental dataset for evaluation of W concentration in the plasmas even in the cases that W ions are sputtered from the plasma facing components.

[1] C. Suzuki *et al.*, Plasma Phys. Control. Fusion **59**, 014009 (2017).
[2] Y. Liu *et al.*, Plasma Fusion Res. **13**, 3402020 (2018).
[3] S. Morita *et al.*, Journal of Physics: Conf. Series **1289**, 012005 (2019).
[4] T. Oishi *et al.*, Phys. Scr. **91**, 025602 (2016).

(T. Oishi)

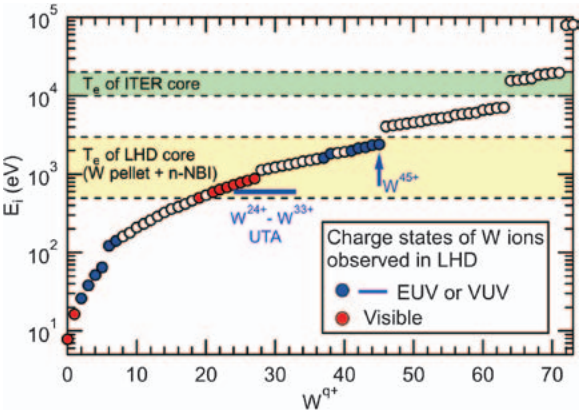

Fig. 1 Ionization energy, E_i, of W ions as a function of charge state, q^+. Green and yellow-hatched regions indicate electron temperature range at $T_e = E_i$ for ITER core plasmas and LHD core plasmas with W pellet injection, respectively.

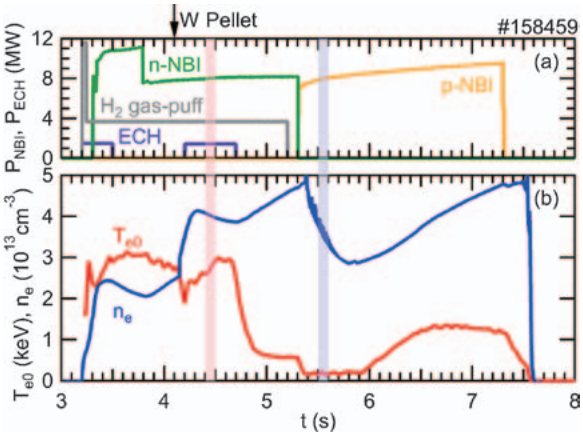

Fig. 2 Typical waveform of the W pellet injection experiment in LHD. (a) Injection power of NBI and ECH and (b) central electron temperature, T_{e0}, and line-averaged electron density, n_e.

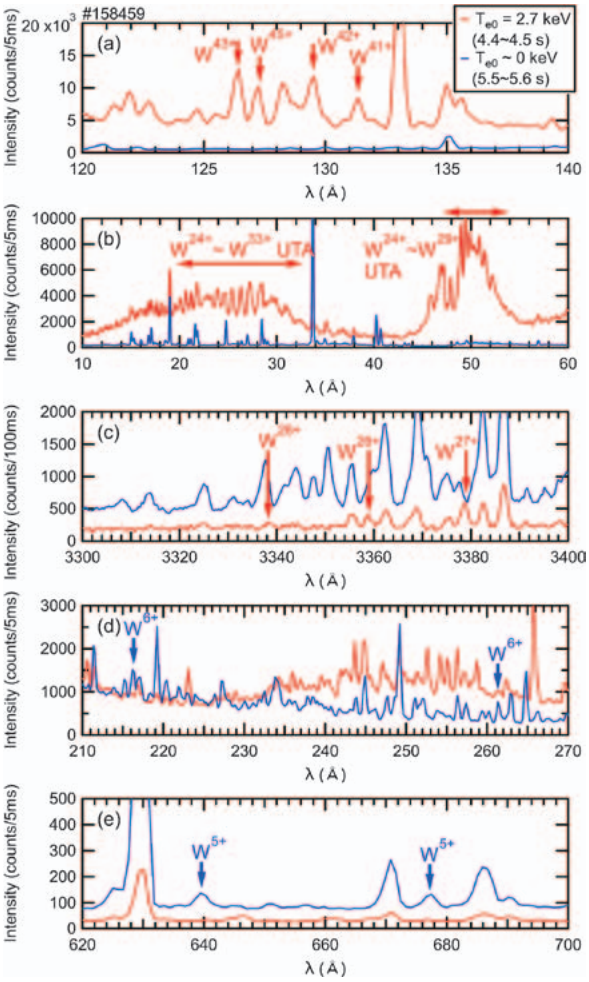

Fig. 3 Wavelength spectra including line emissions released from W ions observed in high T_{e0} (= 2.7 keV) and low T_{e0} (~0 keV) phases. (a) W^{41+}, W^{42+}, W^{43+}, W^{45+} lines, (b) W^{24+} ~ W^{33+} and W^{24+} ~ W^{29+} UTAs in the EUV range and (c) the magnetic dipole forbidden transitions of W^{26+} and W^{27+} in the visible range are observed in the high T_{e0} phase. (d) W^{6+} lines in EUV range and (e) W^{5+} lines in VUV range are observed in the low T_{e0} phase.

High-beta/MHD/Energetic Particles

Highlight

High-beta plasma production examined in Deuterium experiment

An aim of the LHD project is the realization of the reactor-relevant high-beta plasma, where the volume averaged beta, $\langle\beta\rangle$, is 5%, at B = 1~2 T. In the hydrogen experiment before the 19th campaign, the beta value achieved 3.4% and 4.1%, which are the quasi-steady state by the gas puffing and the transient by the pellet injection, respectively. However, in the deuterium experiment, due to the power degradation of the tangential NBI, the plasma start-up in the low field was impossible. For solving that problem, in the 21st campaign, only one tangential NBI keeps the hydrogen operation for expecting the high heating power. Then the high-beta production examined comparing with the hydrogen plasma.

Figure 1 shows the dependency of the achieved beta value on the line averaged density. The circle symbol indicates the quasi-steady state discharge by the gas puffing, and the triangle symbol indicates the transient discharge by the pellet injection. The color indicates the pre-set vacuum magnetic axis. For both quasi-steady state and transient discharges, the highest beta values were achieved at R_{ax} = 3.55 m. For discharges of the gas puffing, it seems the degradation due to the increased density, but for the pellet injection, there is no degradation by the increased density. The fine-tuning of the density is the next step.

(Y. Suzuki)

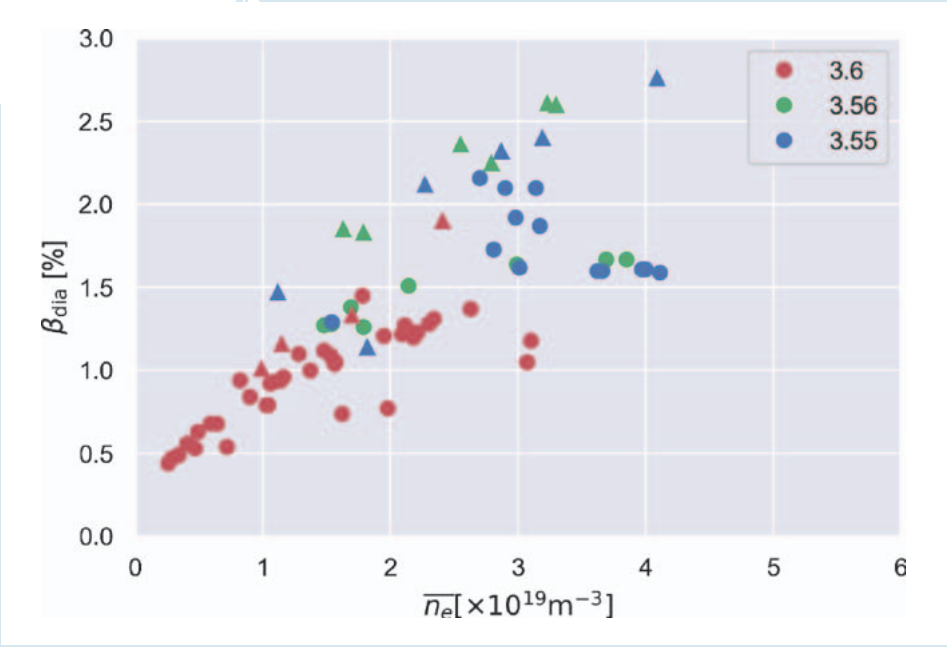

Fig. 1 the dependency of the achieved beta value on the line averaged density.

Energetic Particle Transport by Helically-trapped Energetic-ion-driven Resistive Interchange Mode in LHD

In high-ion temperature experiment performed in relatively low-density plasma with intense positive-ion-source based perpendicular neutral beam injections (P-NBI) in the Large Helical Device (LHD), the helically-trapped energetic-ion-driven resistive interchange mode (EIC) is often observed [1,2] and limits sustainment of the high-ion-temperature state [3]. To sustain the high-ion-temperature state for a longer period, a study of energetic ion transport due to EIC was performed using neutron diagnostics in LHD [4].

We used two vertical neutron cameras (VNCs) to measure the time evolution of the neutron profile. VNC1 [5] characterized by a high spatial resolution based on stilbene fast-neutron detector and VNC2 characterized by high detection efficiency based on EJ410 fast-neutron scintillator were installed under the floor concrete of the torus hall. VNC1 and VNC2 were installed in the vertical elongated poloidal cross section and the diagonal poloidal cross section, respectively. Figure 2 shows the typical density profile of helically-trapped beam ion created by P-NB injection in relatively low-density plasma calculated by MORH code [6] with sightlines of VNCs.

Figure 3 shows line-integrated neutron profiles measured by VNC1 and VNC2 before and after the EIC burst.

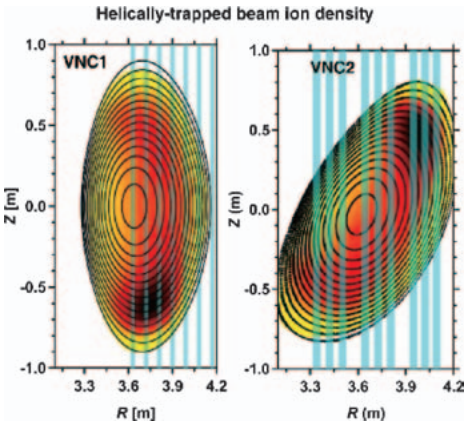

Fig. 2 Helically trapped beam ion density created by P-NB injection and sight lines of VNCs.

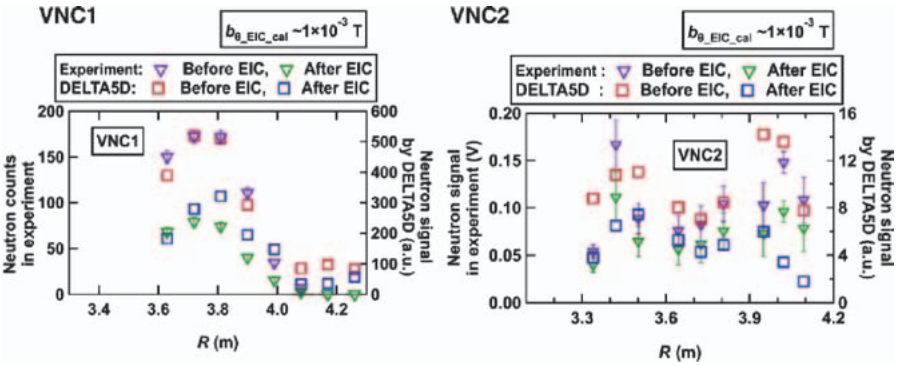

Fig. 3 Line-integrated neutron profile before and after the EIC burst.

Here, the neutron counts measured by VNC1 at a time interval of 20 ms and the averaged signals over 20 ms measured by VNC2 are plotted. These results showed that the neutron profiles were substantially changed due to the EIC burst. Guiding-center orbit-following simulations, including EIC fluctuations, were performed to understand the helically-trapped beam ion transport due to EIC. A comparison of the line-integrated neutron profile before and after the EIC burst measured in the experiment and obtained by the numerical simulation is shown in Fig. 3. The neutron profile for VNC1 shows a single peak appeared at R of approximately 3.75 m, which is nearly equal to the peak position measured in the experiment. The neutron counts for VNC1 at the central channel (R from 3.6 m to 3.9 m) becomes almost one-half after the EIC burst, as measured in the experiment. Although there are relatively wide peaks for line-integrated neutron profile for VNC2 compared with the experiment, the neutron signal shows two peaks in numerical calculation. A decrease in the neutron signal due to the EIC burst at two peaks corresponding to helical ripple valley is reproduced.

[1] Du X. D. *et al.*, 2015 Phys. Rev. Lett. **114**, 155003.
[2] Du X. D. *et al.*, 2015 Nucl. Fusion **56**, 016002.
[3] Takahashi H. *et al.*, 2018 Nucl. Fusion **58**, 106028.
[4] Isobe M. *et al.*, 2018 IEEE Trans. Plasma Sci. **46**, 2050.
[5] Ogawa K. *et al.*, 2018 Rev. Sci. Instrum. **89**, 113509.
[6] Seki R. *et al.*, 2015 Plasma Fusion Res. **10**, 1402077.

(K. Ogawa)

Observation of the Transported Particles Using an Upgraded Neutral Particle Analyzer during TAE Burst in the Large Helical Device

The bursting toroidal Alfvèn eigenmodes (TAEs) [1] are often observed in relatively low magnetic field experiments in the Large Helical Device (LHD). In previous studies, by measuring the transported neutral particles by the TAE burst using the E-parallel-B type neutral particle analyzer (E‖B-NPA) [2] and using the lost ion using scintillator-based fast-ion loss detector (FILD), the existence of the hole-clump pairs was suggested in real space [3–5]. To measure the time evolution of the energetic particles transported by TAE bursts in more detail, the E‖B-NPA was upgraded. The time duration of the observed single TAE burst is approximately 0.5 ms with the frequency chirping down. Therefore, the measurement time resolution is important for measuring the detailed structure of the transported energetic particles during the TAE burst. The measurement electronic circuits of the E‖B-NPA were updated, and the time resolution was improved up to 100 kilo samples per second [6].

During the tangential neutral beam (t-NB) #1 injection in the magnetic field at the magnetic axis is 0.6 T, TAE bursts were observed by the Mirnov coils and the E‖B-NPA. Figure 4 shows the (a) signal of the Mirnov coil, (b) the spectrogram of the magnetic fluctuations, and (c) the energy spectrum of the particle flux Γ observed by E‖B-NPA. The TAE bursts were observed with the time intervals of approximately 10 ms. During and after the TAE bursts, the transported particles were observed by E‖B-NPA. Figure 5 shows the result of the conditional averaging technique for the amplitude of the magnetic fluctuation and the changing of the observed particle flux $\Delta\Gamma$ measured by E‖B-NPA with using 72 TAE bursts. The peak amplitude of the magnetic fluctuation of 70 kHz is set to 2.0 ms. By the conditional averaging technique, the structure of the transported particles is clearly con-

firmed during and after the TAE burst. The highest detected energy of the transported particles is 150 keV, which is less than the injection beam energy of 180 keV. The energy slowing down time was 1.0–1.5 ms during the TAE burst, and 6–8 ms after the TAE burst. The energy slowing down during the TAE burst is considered to be related to the TAE burst frequency chirping down, and the energy slowing down after the TAE burst can be considered as the classical energy slowing down time.

[1] Cheng C. Z. and Chance M. S. 1986 Phys. Fluids **29**, 3695.
[2] Medley S. S. and Roquemore A. L. 1998 Rev. Sci. Instrum. **69**, 2651.
[3] Osakabe M. *et al.*, 2006 Nucl. Fusion **46**, S911-S917.
[4] Ogawa K. *et al.*, 2009 J. Plasma Fusion Res. SERIES **8**, 655.
[5] Ogawa K. *et al.*, 2010 Nucl. Fusion **50**, 084005.
[6] Fujiwara Y. *et al.*, 2020 JINST **15**, C02021.

(S. Kamio)

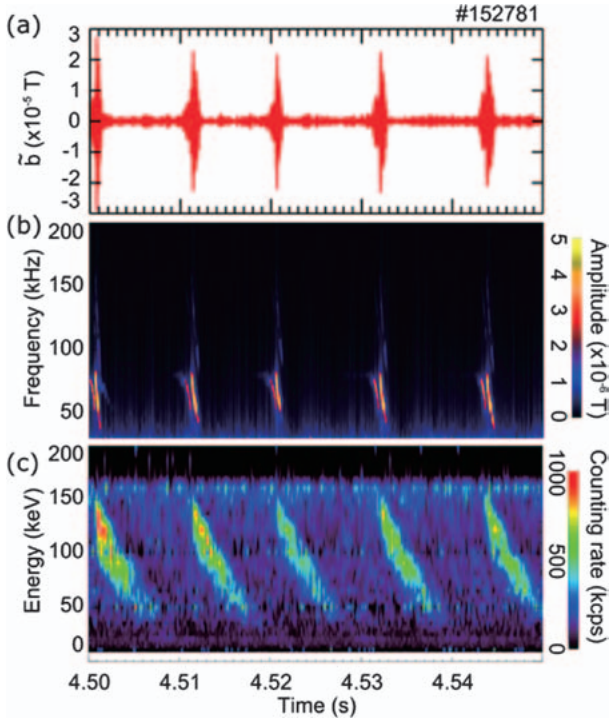

Fig. 4 Time evolutions of (a) the signal of the Mirov coil, (b) the spectrogram of the magnetic fluctuations, and (c) the energy spectrum of the particle flux Γ observed by E‖B-NPA.

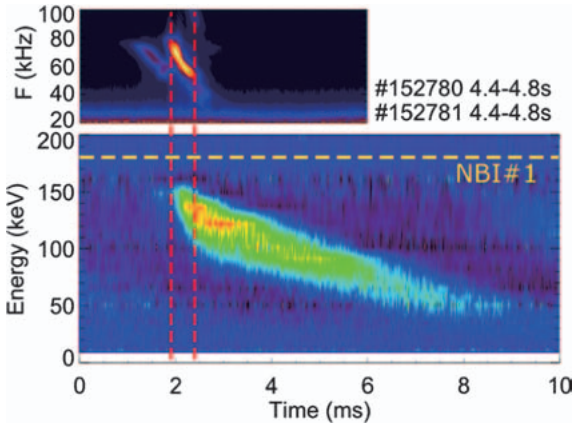

Fig. 5 The conditional averaged spectrogram of the magnetic fluctuation and the ΔΓ observed by E‖B-NPA. Red dashed lines are the timing of the start and the end of the TAE bursts. Yellow dashed line is the injection energy of the NB #1.

2. Fusion Engineering Research Project

The Fusion Engineering Research Project (FERP) started in FY2010 at NIFS. Along with the conceptual design studies for the helical fusion reactor FFHR, the FERP has been developing technologies of key components, such as the superconducting magnet, blanket, and divertor. The research is also focused on materials used for blankets and divertors, the interaction between the plasma and the first wall including atomic processes, handling of tritium, plasma control, heating, and diagnostics. The FERP is composed of 13 tasks and 44 sub-tasks with domestic and international collaborations. Cooperation with the Large Helical Device Project, the Numerical Simulation Reactor Research Project, and the Task Force for Next Research Project are also promoted. (T. Muroga)

Design Studies for The Helical Fusion Reactor

Regarding the fusion reactor design study, the step-by-step strategy towards the helical fusion power plant FFHR-d1 has been proposed. Currently, three intermediate step devices has been considered before the construction of FFHR-d1: FFHR-c1 (experimental/prototype reactor for the demonstration of steady-state operation of the power plant system, FFHR-b1 (volumetric neutron source for the early utilization of fusion fast neutrons) and FFHR-a1 (non-nuclear system for the examination of improved magnetic configuration and advanced engineering concepts). In this fiscal year, reexamination of the primary design parameters of FFHR-b1 has been conducted. The major radius was enlarged from 3.9 m (just the same as LHD) to 5.46 m (1.4 times larger than LHD) to increase the neutron output and to ensure sufficient thickness of the neutron shielding blanket. The helical coil current density and the maximum field on the helical coil are decreased, resulting in the relaxation of the engineering design requirement. In the last fiscal year, the pitch modulation parameter of the helical coil α was changed from 0.1 to 0.0 to achieve simultaneous improvement in the MHD stability and energy confinement property [1]. This improvement effect has been confirmed through the analysis using the finite-beta MHD equilibrium data obtained by the HINT code (Figs. 1 and 2). According to this analysis, the helical pitch modulation of $\alpha = 0.0$ has been selected for FFHR-b1. In response to these changes in the design parameter, the new design of the volumetric fusion neutron source has been defined as FFHR-b2. The related works on the engineering design concepts have also been advanced. The three-dimensional shape of the blanket modules has been reexamined and the replacement of the modules by a robotic arm has been examined using a 3-D printing model. Regarding the advanced divertor system using a pebble flow and the self-cooled liquid breeder blanket system, adoption of new materials for the improvement of thermal efficiency has been proposed. Regarding the high-temperature superconducting magnet system, improvement of the cooling efficiency using cryogenic coolants other than helium gas is also considered. Resolution of the design issues and enhancement of the design attractiveness are expected by advancing the examination of these new concepts.

[1] T. Goto *et al.*, Nucl. Fusion **59**, 076030 (2019).

(T. Goto)

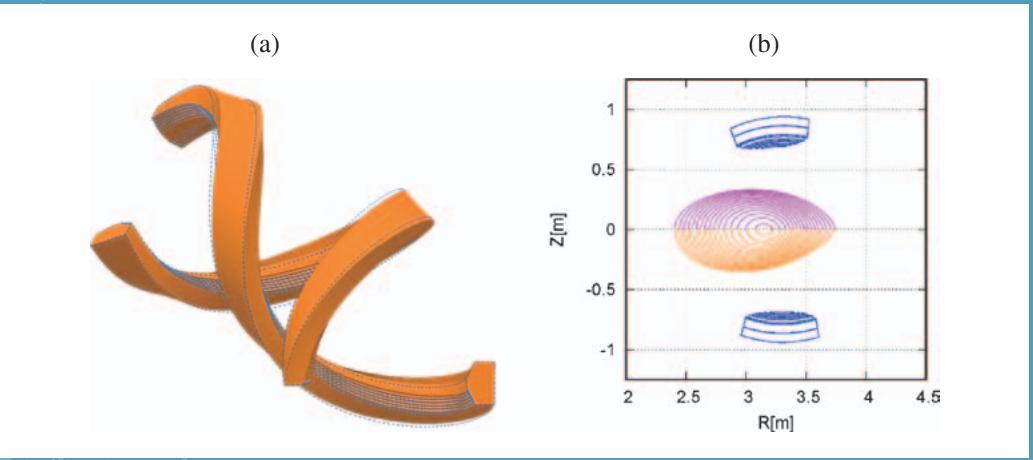

Fig. 1 (a) Variation of the helical winding path with a helical pitch modulation parameter α of 0.1 (blue dotted-curves) and 0.0 (orange block). (b) Cross-sectional shape of the magnetic surfaces (calculated by the HINT code with a peak beta value of 3%) and helical coils at the horizontally-elongated plasma cross-section with a helical pitch modulation parameter α of 0.1 (upper) and 0.0 (lower).

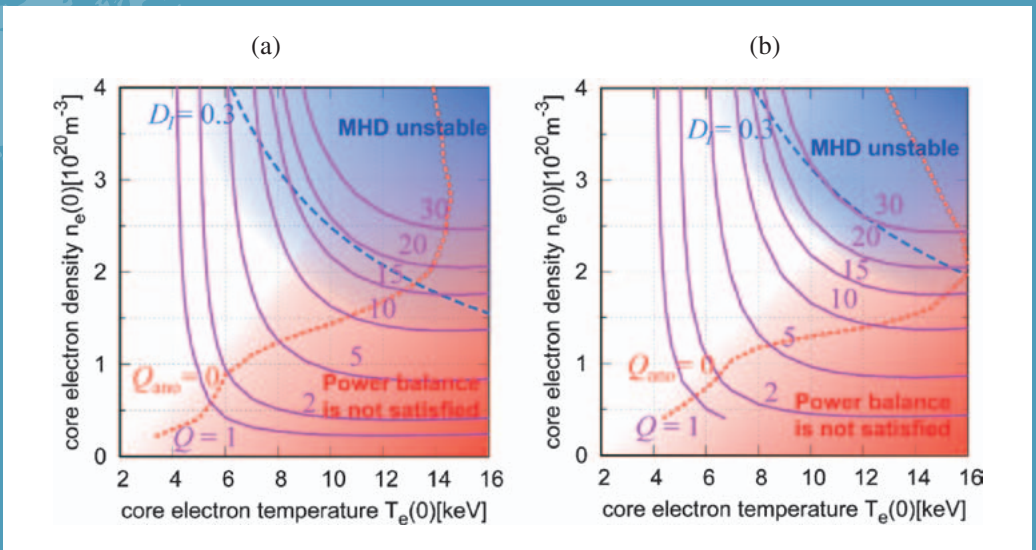

Fig. 2 Comparison of the achievable operation region (the white area without shades) in the diagram of core electron temperature and core electron density for cases of (a) α = 0.1 and (b) 0.0.

Highlight

Enhancement of Link between Design and R&D

Visualization of the link between the critical issues in the helical fusion reactor design and the ongoing R&Ds has been conducted (Fig. 12). All R&Ds has been sorted by research area and “status bars” theme that specify the goal, the member, the execution plan, the current progress and the related budget for each R&D have been made. Regarding the design issue, 22 items have been identified and the “design issue flip boards” that describe the related design parameters assumed in the design study of FFHR-c1 and FFHR-b2 and the necessary knowledge to solve the issues has been made. These status bars and design issue flip boards are linked each other using the reference numbers. The status bars will be continually updated and actively utilized as a research communication tool for the creation of new research field based on the wide-ranged research of the fusion engineering as well as the acceleration of the reactor design activity and the extension of the R&Ds including the cooperative research.

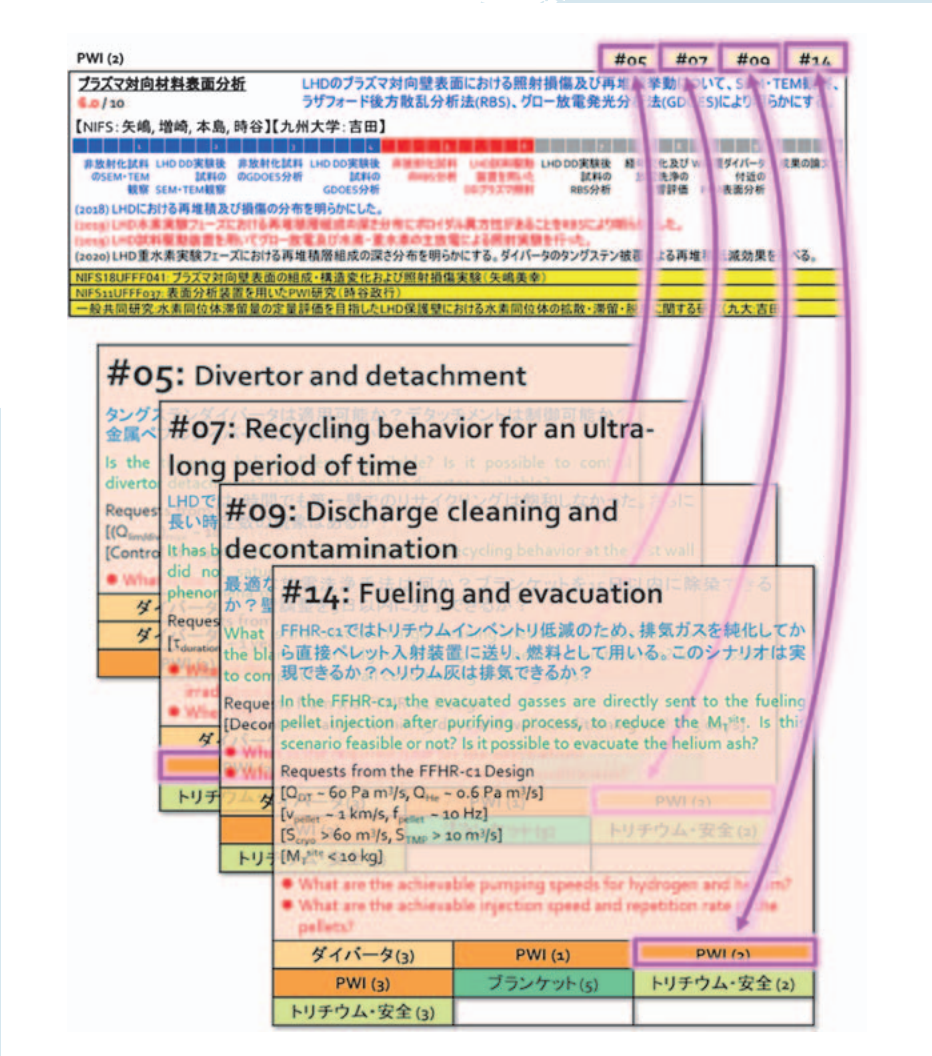

Fig. 12 Example of the visualization of the link between design issues and R&Ds. The design issue flip boards (upper) and the R&D status bars (lower) are linked each other.

(T. Goto and J. Miyazawa)

Highlight

Topology Optimization of the Coil Supporting Structure

Electromagnetic forces generated by superconducting coils in fusion reactors reaches the order of several tens of MN/m. The supporting structure needs to be strong enough to support this huge force. The conventional design of the supporting structure for the FFHR-c1, the helical fusion reactor aiming to realize steady electrical self-sufficiency, assumes a stainless steel 316LN plate with a basic thickness of 200 mm. The total weight of the supporting structure is estimated to exceed 7,800 tons in this case. In the present study, the "topology optimization", which enables innovative designs that overturn conventional design common sense, was applied to the design of the helical fusion reactor to reduce the heavy amount of the supporting structure. Consequently, unnecessary regions were removed, and total weight was significantly decreased as shown in Fig. 13. From the verification analysis applied for the optimized model, it is confirmed that the stress is in an acceptable level. Furthermore, as a derivative of this research, an effort in structural design of coil supporting structure can be reduced. The topology optimization can be applied to any original shape. For instance, assume that the block covers the entire coil but excludes the space occupied by in-vessel components. The shape obtained by topology optimization is close to the assumed toroidal shape as shown in Fig. 14. By preparing an arbitrary block with the necessary access ports open, it becomes possible to conduct design almost automatically.
This research result was published as H. Tamura *et al.*, J. Phys.: Conf. Ser. 1559, 012108 (2020).

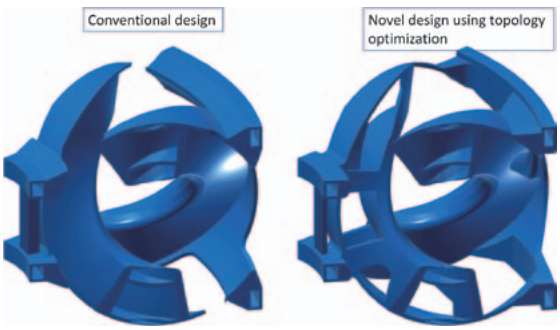

Fig. 13 The shape of the coil support structure obtained by applying the topology optimization (right figure). The figure on the left is based on the conventional design method. Arranging 10 of these structures in the circumferential direction gives the torus-like overall shape. Weight reduction from the conventional design is approximately 2,000 tons.

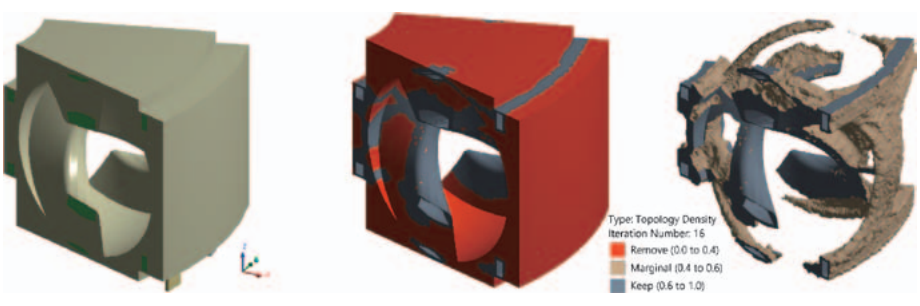

Fig. 14 Example of a design using topology optimization. Left figure is an initial setting, and right one is the optimization result. Red color in the middle figure is the removed region.

(H. Tamura)

Research and Development on the Blanket

The FLiNaK/LiPb twin loop system Oroshhi-2 (Operational Recovery Of Separated Hydrogen and Heat Inquiry-2) is being operated at NIFS as a collaboration platform for integrated experiments on the liquid blanket technologies. In FY2019, two new testing sections have been installed in Oroshhi-2: (i) a test chamber for demonstration of continuous and high efficiency hydrogen isotope recovery from LiPb by the vacuum sieve tray (VST) technique and (ii) a test section for evaluation of heat removal performance of a molten salt flow under an intense magnetic field.

The demonstration of the hydrogen isotope recovery is being conducted by a collaboration with Kyoto University under the LHD-Project Research Collaboration program. In the VST method proposed by the Kyoto University group [1], small droplets of liquid LiPb are made in 0.6 mm diameter nozzles in a vacuum chamber (Fig. 3). Hydrogen isotopes contained in LiPb are quickly released from surfaces of the droplet into vacuum. Circulation of LiPb through the VST chamber has already been confirmed in the test experiment. The world's first demonstration of continuous and high-efficiency hydrogen isotope recovery from LiPb will be performed with the VST chamber in FY2020.

In the design studies of self-cooled molten-salt blanket systems for helical reactors, acquisition of experimental

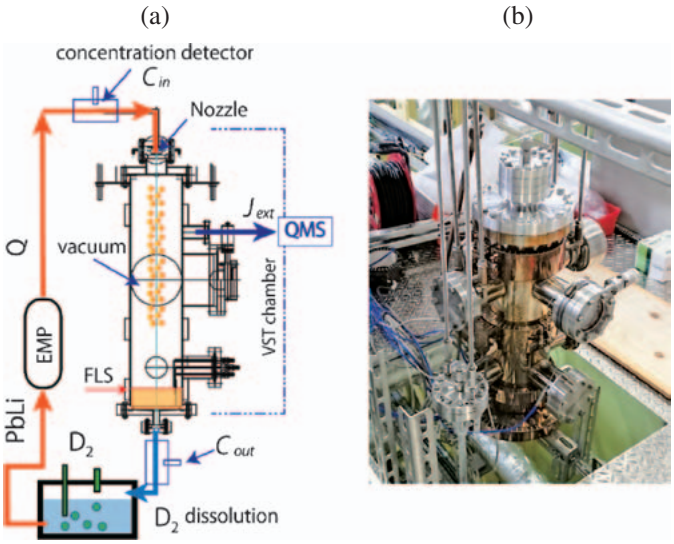

Fig. 3 (a) A schematic drawing of the vacuum sieve tray (VST) technique for continuous and high efficiency hydrogen isotope recovery from LiPb [1], and (b) a photo of the VST chamber installed in Oroshhi-2 in FY2019.

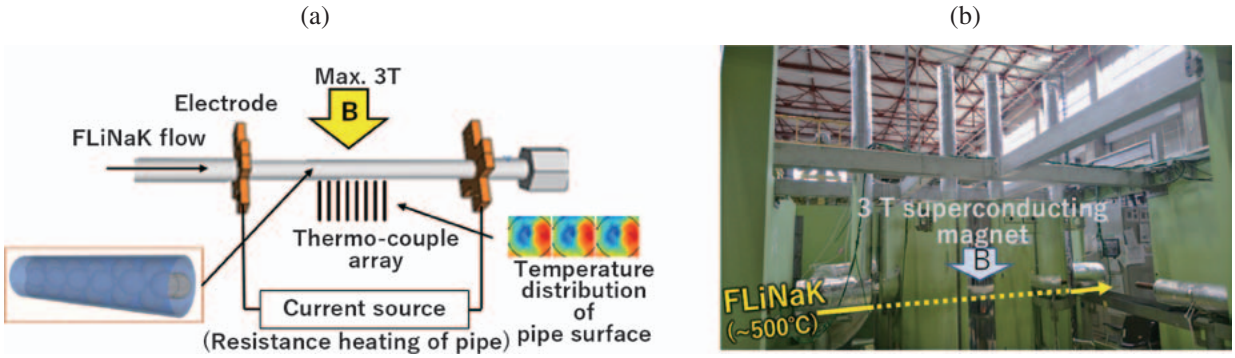

Fig. 4 (a) Schematic drawing of the vacuum sieve tray (VST) technique for continuous and high efficiency hydrogen isotope recovery from LiPb. (b) Photo of the VST chamber installed in Oroshhi-2 in FY2019.

data on heat removal performances of the molten salt coolant flows under intense magnetic field is being required over many years. This is because previous simulation studies indicate that turbulent flow of molten-salts would be suppressed under intense magnetic field and the heat removal performance would be degraded [2]. The test section to evaluate the heat removal performance has been designed and installed at the 3-T superconducting magnet section of the FLiNak loop by a collaboration with Tohoku University in FY2019 (LHD-Project Research Collaboration). Temperature distribution of the surface of the Inconel tube penetrating the magnet body is measured using thermo-couple arrays (Fig. 4). From the changes in the temperature distribution, changes in the heat removal performances due to the applied magnetic field can be evaluated. The FLiNaK circulation and acquisition of data will be started in FY2020 and this will be the world's first evaluation of heat removal performances of molten-salts under intense magnetic field.

[1] F. Okino *et al.*, Fusion Eng. Des. **146**, 898 (2019).
[2] S. Satake *et al.*, Fusion Eng. Des.i **81**, 367 (2006).

(T. Tanaka, Y. Hamaji)

Development of advanced structural materials for fusion reactor blanket

For vanadium alloys, which are leading the world's development of low-activation blanket structural materials, various investigations for dissimilar-metals bonding technologies are ongoing to connect the blankets with the out-vessel components. While the direct melt-welding between the low-activation vanadium alloy NIFS-HEAT-2 and the nickel-based Hastelloy-X alloy is known to be impossible, the casual weld cracking due to intermetallics precipitation has been successfully suppressed by the non-melt explosive welding process under collaboration studies with Kumamoto University, Qilu University of Technology in China, and others. It is indicated that a high-entropy solid solution, which is attractive as a strong and radiation-resistant material, possibly forms in the alloys of weld mixture (Fig. 5). Further investigations will prove whether its solid-solution state can be stable or not during the long-term operation at high temperature.

[1] S. N. Jiang et al., J. Nucl. Mater. 539 (2020) 152322.

(T. Nagasaka)

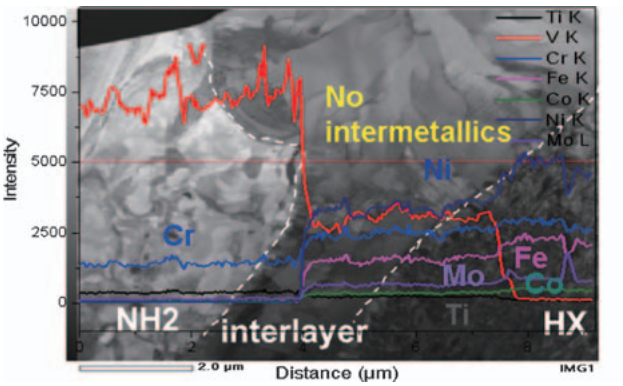

Fig. 5 The transmission-electron microscope image at the interlayer produced by the explosive-weld mixture between the low-activation vanadium alloy NIFS-HEAT-2 (NH2) and the nickel-based Hastelloy-X alloy (HX). Neither intermetallics particles nor homogeneous element distribution are observed in the multi-component interlayer, which is considered to prove formation of high-entropy solid solution [1].

Research and Development on the Divertor

The advanced brazing technique between oxide-dispersion-strengthened copper (ODS-Cu) (GlidCop®) and tungsten (W) with BNi-6 (Ni-11%P) filler material has been developed for fabricating a divertor heat removal component [1,2], and optimization of the procedures were greatly progressed in the last fiscal year [3]. By further enhancing the optimized advanced brazing technique, we newly developed a joint between ODS-Cu and ODS-Cu (ODS-Cu/ODS-Cu), and between stainless steel (SS) and ODS-Cu (SS/ODS-Cu) [4,5]. This newly developed joint has two special features. The first is that these joints have leak tightness against fluids. The second is that the multiple brazing heat treatment can be applicable for fabricating a single divertor component because the prior bonding layer is not affected by the subsequent brazing heat treatment. The superior fabrication procedures for divertor heat removal component, "Advanced Multi-Step Brazing (AMSB)", was newly developed by applying these special features. The prototype AMSB component with the rectangle shaped cooling flow path and the "V-shaped staggered rib" structure has been successfully produced as shown in Fig. 6, in which a pre-processed rectangle shaped cooling flow path in the ODS-Cu heat sink is sealed by a SS lid with a leak tight condition.

A high heat flux test facility named ACT2 (Active Cooling Test stand 2) has been used for the heat load test of plasma facing components since 2015. ACT2 is capable of performing a reactor relevant heat loading test (>20 MW/m^2) on a large surface area of >1,000 mm^2. Several types of the produced AMSB components have been tested in ACT2. For a representative heat loading experiment, a steady state heat loading test was carried out up to the heat flux of ~30 MW/m^2 at a water-cooled condition (flow rate: 15 L/min, pressure: ~0.5 MPa). The heat loading area is depicted in the photograph of Fig. 6 (a). The thermocouples of Channel 4 to 6 were embedded in the positions shown in Fig. 6 (b). Fig. 7 shows the temperature dependence of CH 4 to 6 during a heat loading. The temperature increase during the heat loading of up to ~30 MW/m^2 is acceptable from the viewpoint of structural reliability. The AMSB component shows an extremely high heat removal capability under the reactor relevant condition.

New oxide dispersion strengthened tungsten (DS-W), which applies mechanical alloying (MA)-hot isostatic pressing (HIP) process shown in Fig. 8 (a), is being studied for the development of an advanced plasma facing material (PFM). The initial materials of W and titanium carbide are alloyed using a planetary-type ball mill, consisting of balls of 1.6-mm and 3.0-mm diameter. The mechanically alloyed powders are then pre-sintered. The pre-sintered W alloys are then sintered by HIP at 1,750 degrees Celsius for 1.5 hrs with a pressure of 186 MPa. The HIPed-materials made by this process were evaluated for their mechanical properties at high temperature. In Fig. 8 (b), it is shown that a DS-W after MA using 3.0-mm-diameter balls maintained the hardness and the grain size after annealing temperature of up to 1,900 degrees Celsius, whereas the hardness of a DS-W after MA using 1.6-mm-diameter balls decreased with an increase of the grain size. This result exhibits that the alloying process of DS-W affects the thermal properties after sintering.

The electron beam ion trap (CoBIT) is used for conducting spectroscopy studies of highly-charged ions to provide data necessary for the analysis of fusion plasma emission spectra. In the previous study, we successfullyobserved strong forbidden transitions, with a probability of about 10 billion times smaller than that for the allowed transitions, which is called the "Electric octupole transition (E3)" from highly-charged tungsten ions for the first time in the world [1]. In FY2019, we predicted that the same phenomenon may occur for rhenium multiply-charged ions with an isoelectronic series, and successfully observed it. The spectrum is shown in Fig. 9.

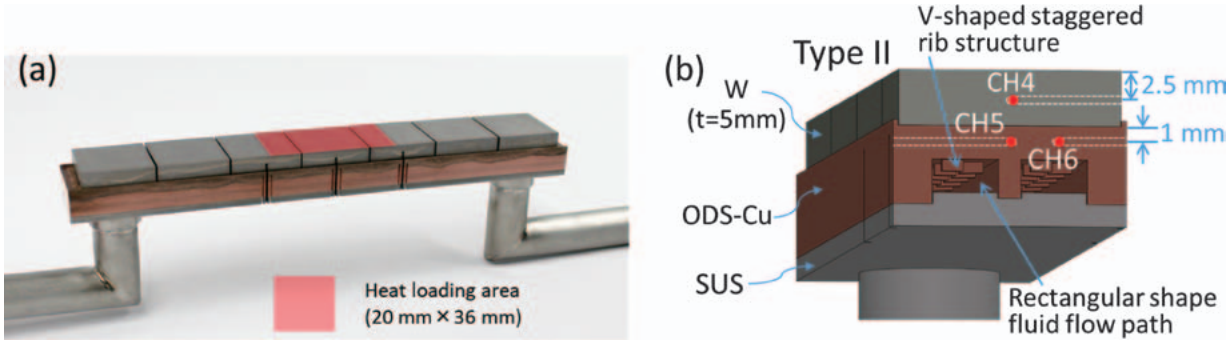

Fig. 6 (a) Photograph of the AMSB divertor heat removal component with the heat loading area for the ACT2 experiment. (b) Schematic cross-sectional view of the AMSB divertor heat removal component at the central region of heat loading area of (a).

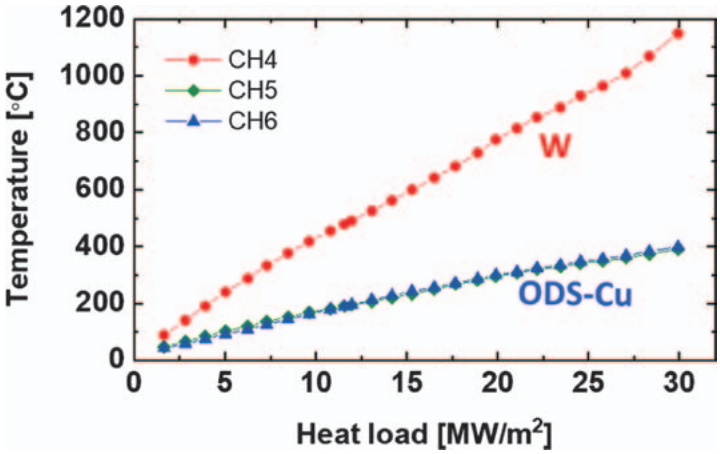

Fig. 7 Temperature dependence of the embedded thermocouples (CH4 to 6) under a steady state heat loading condition in ACT2. The positions of the thermocouples from CH 4 to 6 correspond to the red marker points in Fig. 6 (b).

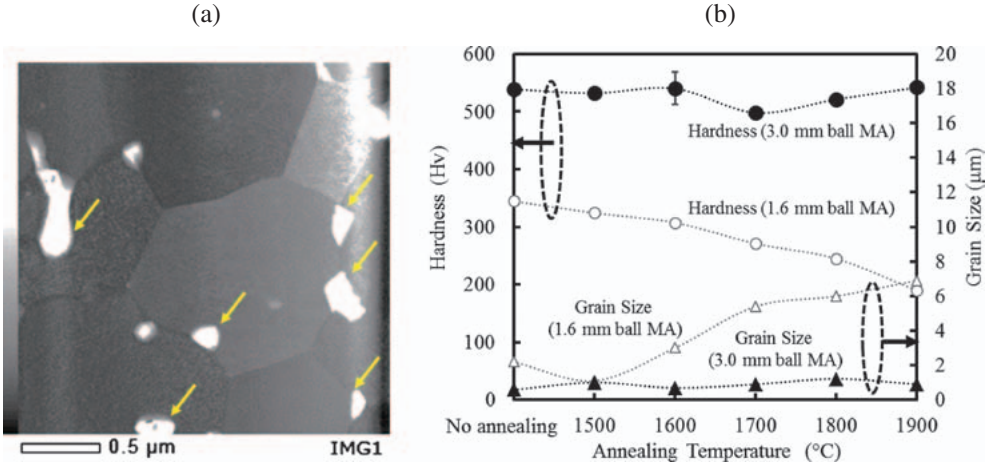

Fig. 8 (a) Transmission Electron Microscope (TEM) image of nano-titanium oxide at grain boundaries after annealing at 1800°C. (b) Relationship between hardness and grain size of DS-W samples made by the MA and HIP process.

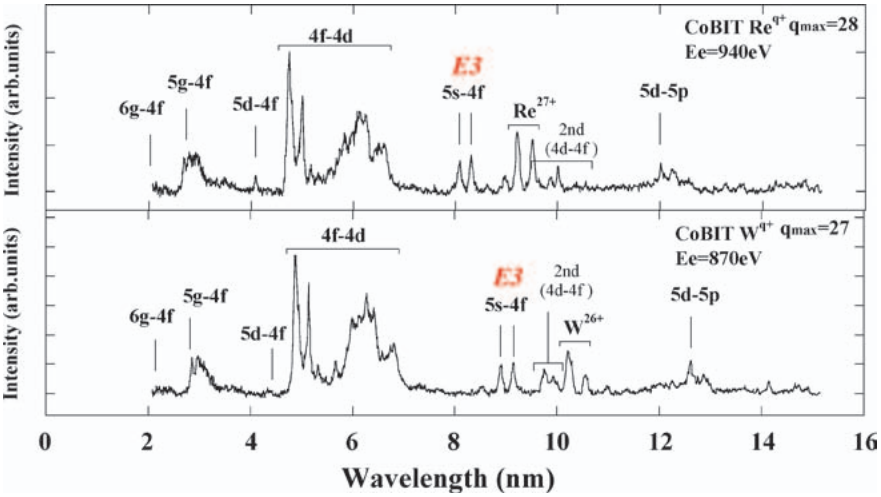

Fig. 9 Extreme ultraviolet spectra of tungsten and rhenium multiply-charged ions observed in CoBIT.

[1] M. Tokitani *et al.*, Plasma Fusion Res. **10**, (2015) 340503.
[2] M. Tokitani, *et al.*, Nucl. Fusion **57**, (2017) 076009.
[3] M. Tokitani *et al.*, Fusion Eng. Des. **146**, (2019) 1733-1736.
[4] M. Tokitani *et al.*, Fusion Eng. Des. **148**, (2019) 111274.
[5] M. Tokitani *et al.*, J. Nucl. Mater. (2020) in press, doi.org/10.1016/j.jnucmat.2020.152264.
[6] H. A. Sakaue *et al.*, Physical Review A100, 052515 (2019)

(M. Tokitani, Y. Hamaji, H. Noto and H. Sakaue)

Research and Development on the Superconducting Magnet

For the helical fusion reactor, FFHR, High-Temperature Superconductor (HTS) is considered to apply to the magnet system. Various types of large-current capacity HTS conductors are being designed and developed combining the second generation REBCO HTS tapes. For this purpose, an international collaboration experiment was carried out between Massachusetts Institute of Technology (MIT) in US and NIFS for testing the Twisted Stacked-Tape Cable (TSTC) HTS conductor. A one-turn coiled sample, made of a TSTC conductor, was designed and fabricated at MIT, transported to NIFS, and installed into the superconductor testing facility (Fig. 10), which is equipped with a large-bore (700 mm), high magnetic field (13 T), large sample current (50 kA), and temperature control capability (4.2–50 K). The experiment was carried out two times in FY2018. On this occasion, self-field measurements of the TSTC conductor were conducted using Hall sensors, and the detailed analysis was completed in FY2019. Based on the measurement results, the current distribution of the TSTC conductor was analyzed using analytical models. The calculation results indicate that the current distribution of the TSTC is uniform when the operating current is maintained at 10 kA and the temperature is controlled at 34 K. On the other hand, the current distribution is not uniform at the charging and discharging phases with the ramp rate of 50 A/s. Additionally, the current distribution of the TSTC is stable and uniform when the temperature is increased from 29.5 K to 33.5 K at the operating current of 10 kA. To confirm occurrence of a shielding current with a long time constant, self-fields of the TSTC after the discharging were investigated. As a result, a shielding current with a long time constant was not observed in the single turn coil wound with a TSTC conductor.

As an extension of the ITER technology based on the LTS magnet concept, the development of the internal

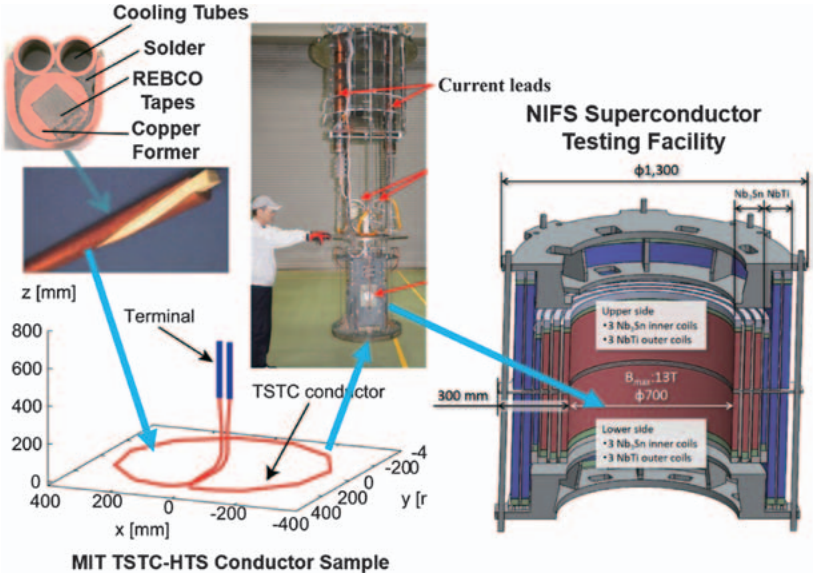

Fig. 10 Experimental setup of the MIT's TSTC-HTS conductor sample in the NIFS superconductor testing facility.

matrix-reinforced Nb_3Sn multifilamentary wires using ternary Cu-Sn alloys have been progressing. We succeeded in fabricating Nb_3Sn multifilamentary wires using Cu-Sn-Zn and Cu-Sn-In ternary alloy matrices, such as shown in Fig. 11 (a). After the synthesis process of Nb_3Sn, the ternary alloy matrices were transformed to a Cu-system solid solution, and they contributed in the improvement of mechanical strength. When a Cu-Sn-In ternary alloy is used as the matrix material, the stress value that gives the maximum critical current is found to exceed that of the CuNb reinforced Nb_3Sn wire, as shown in Fig. 11 (b) [5].

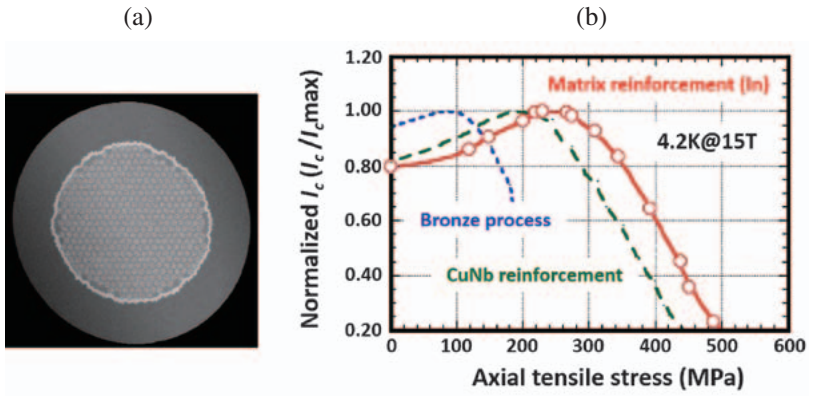

Fig. 11 (a) Typical cross-sectional image of the internally reinforced Nb_3Sn multifilamentary wire. (b) Dependence of the critical current (normalized by each maximum value) on the axial tensile stress for various Nb_3Sn wires.

[1] S. Imagawa *et al.*, Plasma Fusion Res. **10**, 3405012 (2015).
[2] J. Hamaguchi *et al.*, Plasma Fusion Res. **10**, 3405020 (2015).
[3] M. Takayasu *et al.*, IEEE Trans. Appl. Supercond. **26**, 6400210 (2016).
[4] T. Obana *et al.*, Cryogenics **105**, 103012 (2020).
[5] Y. Hishinuma *et al.*, IEEE Trans. Appl. Supercond. **30**, 6001104 (2020).

(N. Yanagi, T. Obana and Y. Hishinuma)

LHD-Project Research Collaboration

The LHD Project Research Collaboration program has been contributing to enhancing both the scientific and the technological foundations for the research related with the LHD project as well as the future helical fusion reactors. The characteristics of this collaboration program are that the researches are performed at universities and/or institutions outside NIFS. In the research area of fusion engineering, the following ten subjects were approved and conducted in FY2019:

1. Development of irradiation-resistant NDS-Cu alloys for helical reactor divertor
2. Engineering study on lithium isotope enrichment by ion exchange
3. New R&D facility for supercritical CO_2 (sCO_2) gas system as secondary cooling
4. Establishment of high susceptible detection assay for biomolecule response and estimation of the biological effects of low-level tritium radiation by utilizing its assay
5. Development of highly ductile tungsten composite systems
6. Fundamental engineering of tritium recovery process for liquid blanket of helical reactor
7. Development of new rapid-heating and quench processed Nb_3Al large-scaled cables for the helical winding due to the react-and-wind method
8. Field estimation for improvement of environmental tritium behavior model
9. Evaluation of Heat-transfer-enhanced Channel under High Magnetic Field for Liquid Molten Salt Blanket Development
10. Evaluation of multi hydrogen isotope transfer behavior on plasma driven permeation for plasma facing materials
11. Development of effective heat removal method from liquid metal free-surface with local heating under strong magnetic field and its demonstration by Oroshhi-2

From the above ten research items, two of them (3 and 7) are briefly described below:

3. New R&D facility for supercritical CO_2 (sCO_2) gas system as secondary cooling in FFHR

In FFHR, supercritical CO_2 (sCO_2) gas system is considered to apply to the secondary cooling system for electricity generation considering the advantages of compact design and higher thermal efficiency under the operational temperature of molten-salt blanket using the FLiNaBe. It is unavoidable that a small amount of tritium is permeated into the secondary cooling system via heat exchangers. Hence, understanding of mass transfer phenomena of gas components including hydrogen isotope in interfaces between sCO_2 and structural materials is necessary. In this study, constructions of sCO_2 experimental setup were done (Fig. 15), and then the analysis of reaction products in high temperature and high pressure CO_2 was done. Using this new facility, sCO_2 condition was successfully operated and CO, H_2, CH_4 were detected as reaction products during hydrogen permeations. These Concentrations of reaction products were observed to increase with a rise of temperature [1].

7. Development of new rapid-heating and quench processed Nb3Al large-scaled cables for the helical winding due to the react-and-wind method

The large helical coils of the helical fusion reactor FFHR-d1 have three-dimensional complex architecture so that the “React and Wind (R&W)” process of the superconductor is preferable to be applied. In this respect, we

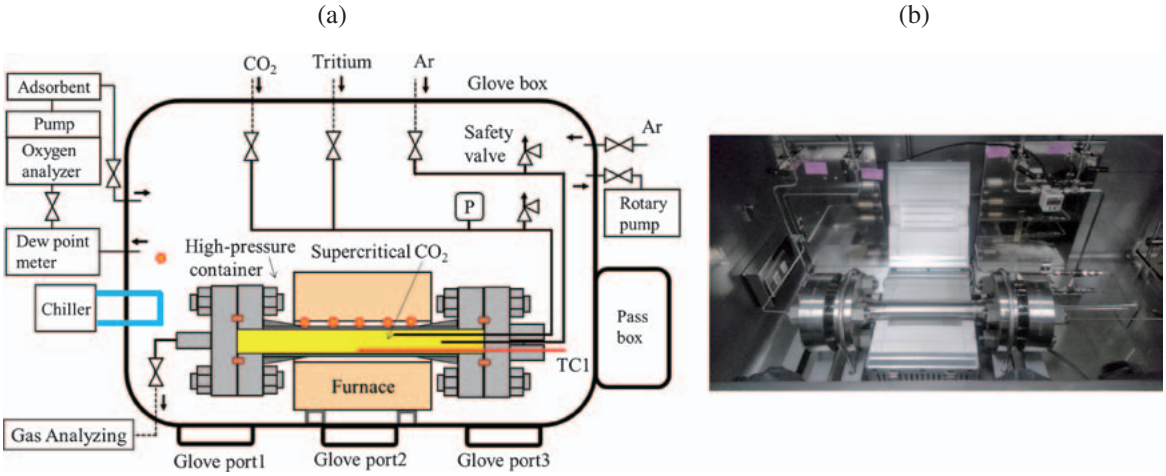

Fig. 15 (a) Design of Supercritical CO_2 gas facility. (b) Photograph of supercritical CO_2 gas facility.

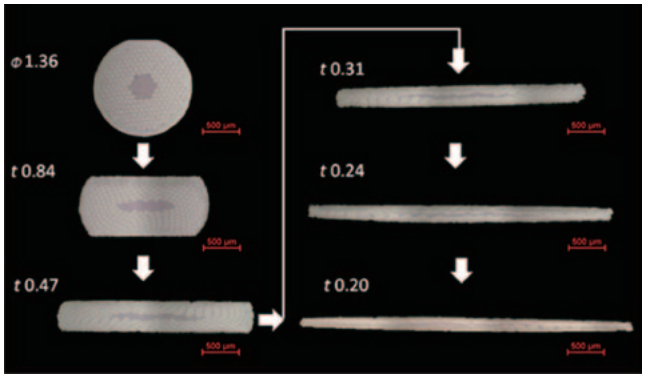

Fig. 16 Fabrication procedure of the tape-shaped RHQT Nb3Al conductor (final thickness $t = 0.20$ mm) starting from a wire-shaped conductor (diameter $\phi = 1.36$ mm).

should note that the A15 superconductors, such as Nb_3Sn, are brittle intermetallic compounds, and the critical current properties of these materials are sensitive to thermal and mechanical strains. However, the Nb_3Al conductor shows an excellent strain tolerance compared to that of Nb_3Sn, and it is suitable for applying the "R&W" process. We investigated a tape-shaped Nb_3Al conductor made by the rapid-heating and quench (RHQT) technique for further improving the mechanical strain tolerance of Nb_3Al shown in Fig. 16 [1]. The bending strain dependence on the critical current property was evaluated. No deterioration of the critical current property was observed even if a bending strain was applied above 0.6%.

[1] K. Katayama, N. Ashikawa, T. Chikada, "Mass Transfer at the interface between stainless steel and supercritical carbon dioxide", ICFRM (2019) poster presentation.
[2] K. Yamada *et al.*, presented at 10th ACASC / 2nd Asian-ICMC / CSSJ, (2020), 7P-20.

(N. Ashikawa and K. Katayama (Kyushu University),
Y. Hishinuma, K. Takahata and A. Kikuchi (National Institute for Materials Science))

3. Numerical Simulation Reactor Research Project

Fusion plasmas are complex systems which involve a variety of physical processes interacting with each other across wide ranges of spatiotemporal scales. In the National Institute for Fusion Science (NIFS), we are utilizing the full capability of the supercomputer system, Plasma Simulator, and propelling domestic and international collaborations in order to conduct the Numerical Simulation Reactor Research Project (NSRP). Missions of the NSRP are i) to systematize understandings of physical mechanisms in fusion plasmas for making fusion science a well-established discipline and ii) to construct the Numerical Helical Test Reactor, which is an integrated system of simulation codes to predict behaviors of fusion plasmas over the whole machine range.

The Plasma Simulator is to be replaced in July 2020 to a new model (Fig. 1). It consists of 540 computers, each of which is equipped with 8 "Vector Engine" processors. The 540 computers are connected with each other by a high-speed interconnect network. The computational performance of the new Plasma Simulator is 10.5 petaflops. The capacities of the main memory and the external storage system are 202 terabytes and 32.1 petabytes, respectively. The nickname of the new Plasma Simulator is "Raijin (雷神)" which means a god of thunder.

Presented below in Figs. 2 and 3 are examples of successful results from collaborative simulation researches in 2019–2020 on ballooning and kink modes in the PLATO tokamak and on nonlinear saturation mechanism of toroidal ETG turbulence. Also, highlighted in the following pages are achievements of the NSRP on energetic-particle physics, neoclassical and turbulent transport, peripheral plasma transport, multi-hierarchy physics, and simulation science basis.

(H. Sugama)

Fig. 1 The new Plasma Simulator, "Raijin (雷神)"

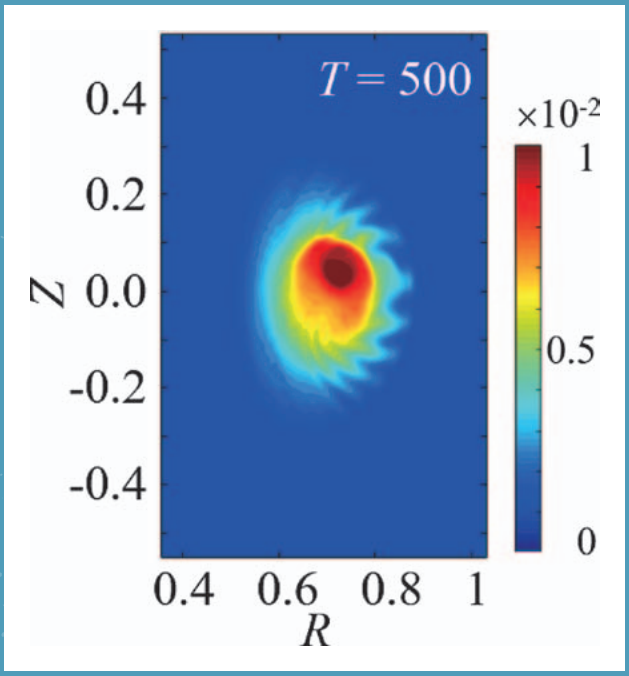

Fig. 2 Emergence of kink instability with existence of ballooning instability on the poloidal cross section of the PLATO tokamak obtained by nonlinear MHD simulation using the MIPS code [presented by N. Kasuya (Kyushu University)]. Reference: S. Tomimatsu, *et al.*, Plasma Fusion Res. (2020) in press.

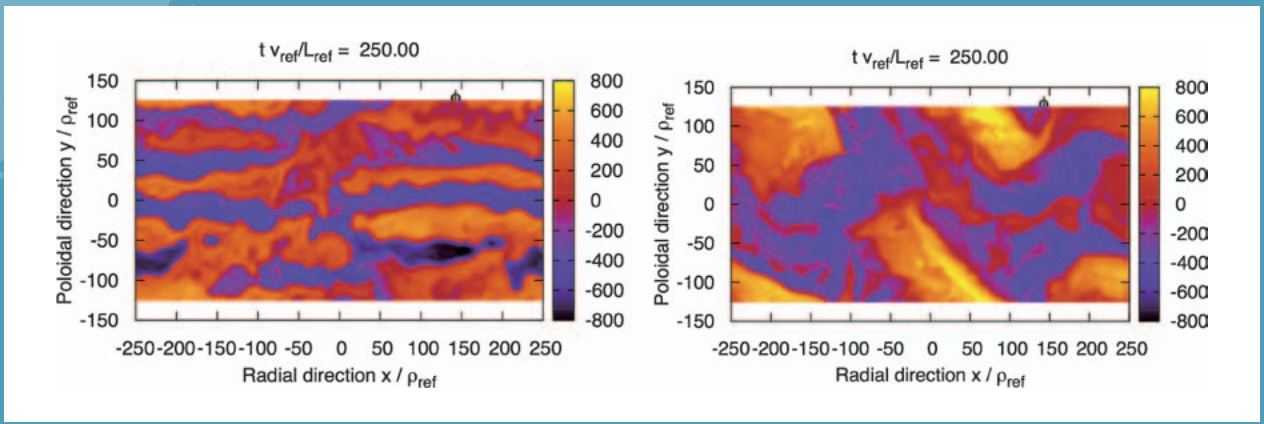

Fig. 3 Snapshots of the electrostatic potential in the nonlinear saturation phase of the toroidal ETG turbulence obtained by gyrokinetic simulation using the GKV code for the cases with "adiabatic" (left) and kinetic (right) ions [presented by T.-H. Watanabe (Nagoya University)]. In the latter case, finite radial wavenumber modes strongly modulate the ETG streamers.

Energetic Particle Physics

Highlight

Extended kinetic magnetohydrodynamic hybrid simulations with thermal and fast ions clarify the fast-ion transport due to multiple Alfvén eigenmodes

The closure problem of magnetohydrodynamics (MHD) remains unresolved for collisionless high-temperature plasmas. A new hybrid simulation model where the gyrokinetic particle-in-cell simulation method is applied to both thermal and fast ions has been developed [1]. The new simulation model was implemented and applied to fast-ion driven instabilities in tokamak plasmas. Energy channeling from fast ions to thermal ions through the interaction with Alfvén eigenmodes (AEs) was demonstrated by the simulations. The real frequency and the spatial profile of the AEs are in good agreement with those given by the standard hybrid simulation for energetic particles interacting with an MHD fluid.

The distribution functions of fast ions and thermal ions are analyzed in detail during the nonlinear evolution of the multiple AEs. Figure 1 compares the fast-ion distribution function perturbations among the linear growth phase of the primary AE, the saturation phase of the primary AE, the nonlinear phase with the growth of the secondary AE, and the final phase for co-going and counter-going particles to the plasma current. The resonant orbits are also shown in Fig. 1 with the resonance poloidal numbers labeled in the figure. We see in Fig. 1 (c) and (g) that the poloidal mode number of the distribution function perturbations are different from those for the linear growth phase shown in Fig. 1 (a) and (e). This indicates that the secondary mode is excited leading to the further transport of fast ions and the global flattening of the distribution functions shown in Fig. 1 (d) and (h).

[1] Y. Todo *et al.*, "Extended magnetohydrodynamic hybrid simulations with kinetic thermal and fast ions for instabilities in toroidal plasmas", in the 46th European Physical Society Conference on Plasma Physics (July 8–12, 2019, Milan, Italy).

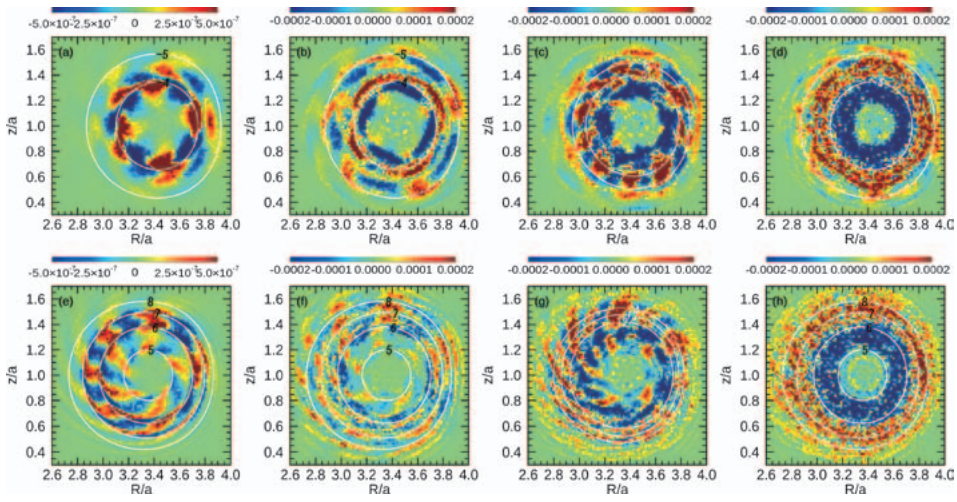

Fig. 1 Fast-ion distribution function perturbations in the evolution of multiple Alfvén eigenmodes (AEs) for (a, e) linear growth phase of the primary AE, (b, f) saturation phase of the primary AE, (c, g) nonlinear phase with the growth of the secondary AE, and (d, h) final phase for (a-d) co-going particles and (e-h) counter-going particles to the plasma current. In the final phase shown in (d) and (h), the distribution functions are globally flattened due to the transport by the multiple AEs.

(Y. Todo)

Simulation of Alfvén eigenmodes destabilized by energetic electrons in tokamak plasmas

Alfvén eigenmodes (AEs) driven by energetic electrons were investigated via hybrid simulations of an MHD fluid interacting with energetic electrons [2]. The investigation focused on AEs with the toroidal number $n=4$. Both energetic electrons with centrally peaked beta profile and off-axis peaked profile are considered. For the centrally peaked energetic electron beta profile case, a toroidal Alfvén eigenmode (TAE) propagating in the electron diamagnetic drift direction was found. Figure 2 shows the resonance condition between energetic electrons and the TAE. The TAE is mainly driven by deeply trapped energetic electrons. It is also found that a few passing energetic electrons spatially localized around rational surfaces can resonate with the mode. For the off-axis peaked energetic electron beta profile case, an AE propagating in the ion diamagnetic drift direction was found when a q-profile with weak magnetic shear is adopted. The destabilized mode has a frequency close to the second Alfvén gap and two main poloidal harmonics $m=6$ and $m=8$, which indicate that this mode is an ellipticity-induced Alfvén engenmode. Passing energetic electrons and barely trapped energetic electrons are responsible for the mode destabilization.

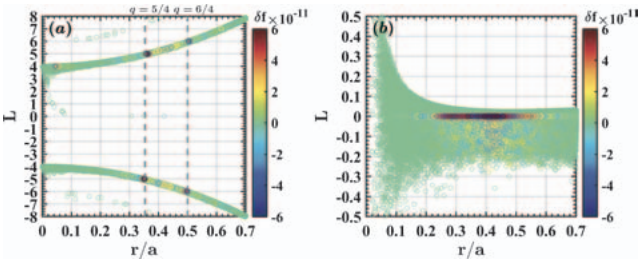

Fig. 2 (a) Resonance condition for (a) passing energetic electrons and (b) trapped energetic electrons along radial coordinate. Each marker in the figure represents one computational particle and all particles are included. Particle positions in the mid-plane during one bounce/transit period are stored and the average value of the stored positions is used as the particle location in the figure [2].

[2] Jialei Wang *et al.*, "Simulation of Alfvén eigenmodes destabilized by energetic electrons in tokamak plasmas", to appear in Nucl. Fusion **60** (2020).

(Jialei Wang)

Systematic investigation of energetic-particle-driven geodesic acoustic mode channeling

Energetic-particle-driven geodesic acoustic modes (EGAMs) channeling in the Large Helical Device (LHD) plasmas are systematically investigated for the first time using MEGA which is a hybrid simulation code for energetic particles interacting with a magnetohydrodynamic (MHD) fluid [3]. EGAM channeling behaviors are analyzed under different conditions. During the EGAM activities without frequency chirping, EGAM channeling occurs in the linear growth stage but terminates in the decay stage after the saturation. During the EGAM activities with frequency chirping, EGAM channeling occurs continuously. Also, lower frequency EGAM makes the energy transfer efficiency (E_{ion}/E_{EP}) higher, because the interactions between lower frequency mode and bulk ions are stronger. This is confirmed by changing the energetic particle pressure and energetic particle beam velocity, as shown in Fig. 3. Moreover, higher bulk ion temperature makes the energy transfer efficiency higher. In addition, under a certain condition, the energy transfer efficiency in the deuterium plasma is lower than that in the hydrogen plasma. Based on the simulations described above, suggestions are given for experiments. The higher neutral beam injection (NBI) power, the lower NBI velocity, the higher number of perpendicular injected particles, the higher bulk ion temperature, and the wider bulk ion temperature profile are probably applicable strategies for improving the observation of EGAM channeling.

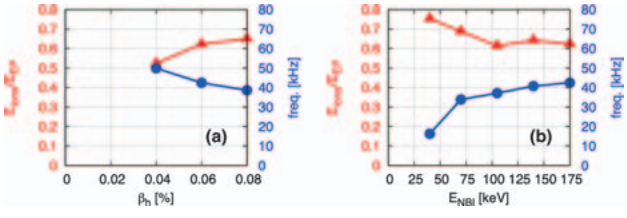

Fig. 3 The energy transfer efficiency (triangles) and EGAM frequency (circles) versus (a) the energetic particle pressure and (b) the beam energy.

[3] H. Wang *et al.*, "The systematic investigation of energetic-particle-driven geodesic acoustic mode channeling using MEGA code", to appear in Nucl. Fusion **60** (2020).

(Hao Wang)

Transport simulation for helical plasmas by use of gyrokinetic transport model

Highlight

The transport simulation results explain the experimental results for the temperature profiles, where the ion temperature gradient mode is unstable.

The transport simulation is performed in helical plasmas by use of two kinds of the reduced models [1] for the kinetic electron response (heat diffusivity and quasilinear flux models) for the turbulent transport. The neoclassical transport is included in the transport simulation. For the turbulent transport, the instability due to the ion temperature gradient (ITG) is studied. The additional modeling of the quantity related with the mixing length estimate and the zonal flow decay time in the diffusivity models is done. Electron heat diffusivity model is adopted to the transport simulation for the additional modeling by the normalized characteristic length for the ion temperature gradient. Furthermore, electron quasilinear flux model is installed to the transport simulation codes by the ratio of the electron quasilinear heat flux to the ion quasilinear heat flux, where the ion heat flux is evaluated by the heat diffusivity model. The ion heat diffusivity model is also installed into the integrated transport code for simulating evolutions of the plasma profiles in the LHD, when the additional modeling by the characteristic length for the ion temperature gradient is used.
The electron temperature profiles of the transport simulation results by the electron heat diffusivity model and the quasilinear flux model are compared with the experimental observation result in the LHD in figure 1 (a). The ion temperature profile of the dynamical transport simulation by use of the ion heat diffusivity model for the kinetic electron response is also compared with the LHD experimental result in figure 1 (b) [2].

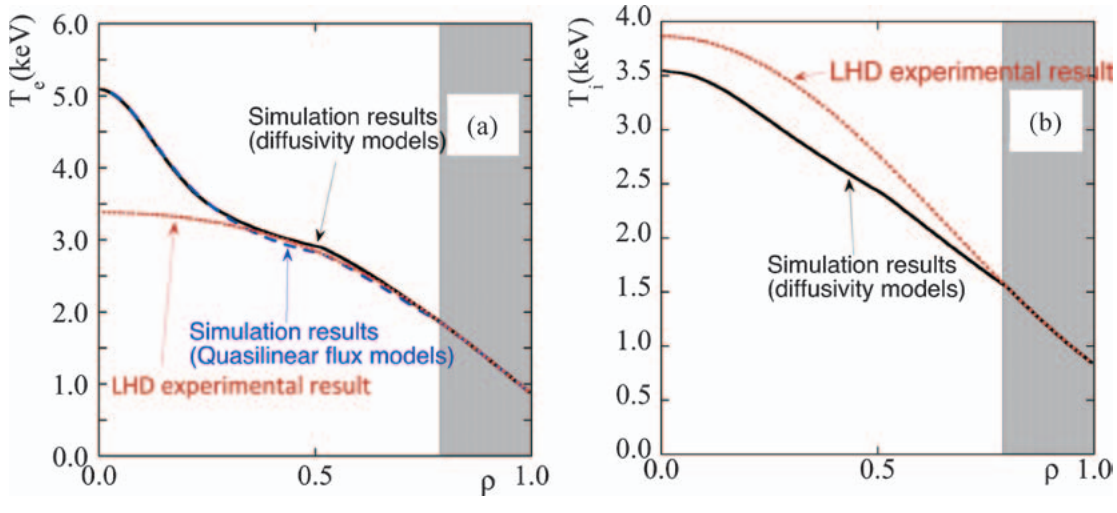

Fig. 1 The radial profiles of T_e are shown. The solid and dashed lines represent the electron temperature profiles for the simulation results, using the heat diffusivity model and the quasilinear flux model, respectively. The dotted line indicates the experimental results. (b) The T_i profiles are shown. The solid line represents the ion temperature for the simulation results. The dotted line indicates the experimental results at t=2.2s in the LHD.

[1] S. Toda *et al.*, Phys. Plasmas **26**, 012510 (2019).
[2] S. Toda *et al.*, Plasma Fusion Res. **14**, 3403061 (2019).

(S. Toda)

Gyrokinetic simulations for turbulent particle transport of multi-ion-species plasma with impurity hole structure in LHD system

The turbulent particle transport of multi-ion-species plasma with the impurity hole structure in the LHD system and their plasma profile sensitivities are investigated by the flux-tube gyrokinetic simulations [3]. In the plasma, the turbulent heat transport flux of each species has slightly different dependences on the radial gradients of the plasma temperatures and densities. On the other hand, while the particle transport is determined satisfying the ambi-polar condition between electrons and all ion species, the particle fluxes have quite different dependences for different species as shown in Fig. 2. In the LHD plasma having the hole density structure of the impurity carbon ions, it is found that the turbulent particle flux of the carbon ions is radially inward-directed robustly for the wide ranges of the radial gradient profiles of the temperatures and densities. Furthermore, we also found that there are clear balance relations in the turbulent particle fluxes between the pair of hydrogen and helium ions, and the pair of the electrons and carbon ions.

(M. Nunami)

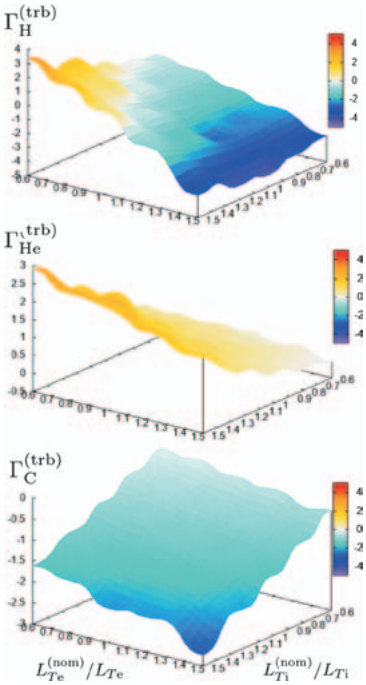

Fig. 2 Temperature gradient length dependences of turbulent particle fluxes for hydrogen $\Gamma_H^{(trb)}$, helium $\Gamma_{He}^{(trb)}$, and carbon $\Gamma_C^{(trb)}$ ions.

Development of global neoclassical transport simulation for multi-ion-species plasma

To study the impurity transport process and hydrogen isotope effect, neoclassical transport simulation code needs to be capable of handling the collisional diffusion process in multi-ion-species plasma. We developed a new linearized Landau collision operator, which is applicable to multi-ion-species plasma, and implemented to a global neoclassical δf-PIC code FORTEC-3D [4]. The new collision operator satisfies the conservation properties, self-adjointness, and H-theorem. As a verification, very good agreement in the dumping process of the mean flow and temperature fluctuation was demonstrated between FORTEC-3D and gyrokinetic code GKV as shown in Fig. 3. FORTEC-3D was applied to study the effect of potential variation on flux surface on impurity transport to study the impurity-hole phenomenon. It is revealed that the global simulation is essential for the evaluation of the impurity transport [5].

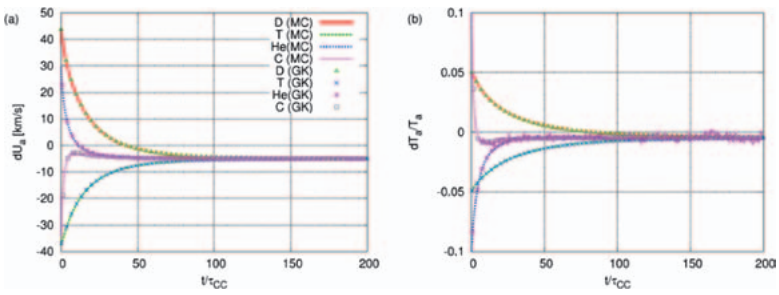

Fig. 3 Comparisons on the collisional damping process of the mean flow and temperature in 4 ion species plasma calculated by FORTEC-3D (curves) and GKV (points) [4].

[3] M. Nunami, M. Nakata, S. Toda, and H. Sugama, Phys. Plasmas **27**, 052501 (2020).
[4] S. Satake, M. Nakata, T. Pianpanit *et al.*, Comp. Phys. Comm. **255**, 107249 (2020).
[5] K. Fujita, S. Satake, R. Kanno *et al.*, J. Plasma Phys., *in press*.

(S. Satake)

Peripheral transport physics

Highlight

Nonlinear MHD simulation confirmed pellet injection drives edge MHD instability

The effect of pellets on the global magnetohydrodynamic (MHD) dynamics of the Large Helical Device (LHD) has been analyzed with the MIPS code [1], which is a nonlinear MHD simulation code [2]. A pellet ablation model based on the neutral gas shielding model has been implemented to the MIPS code. Excitation of MHD modes by the three-dimensionally localized pressure perturbation caused by the pellet injection has been observed. MHD instabilities depends on the pellet size.

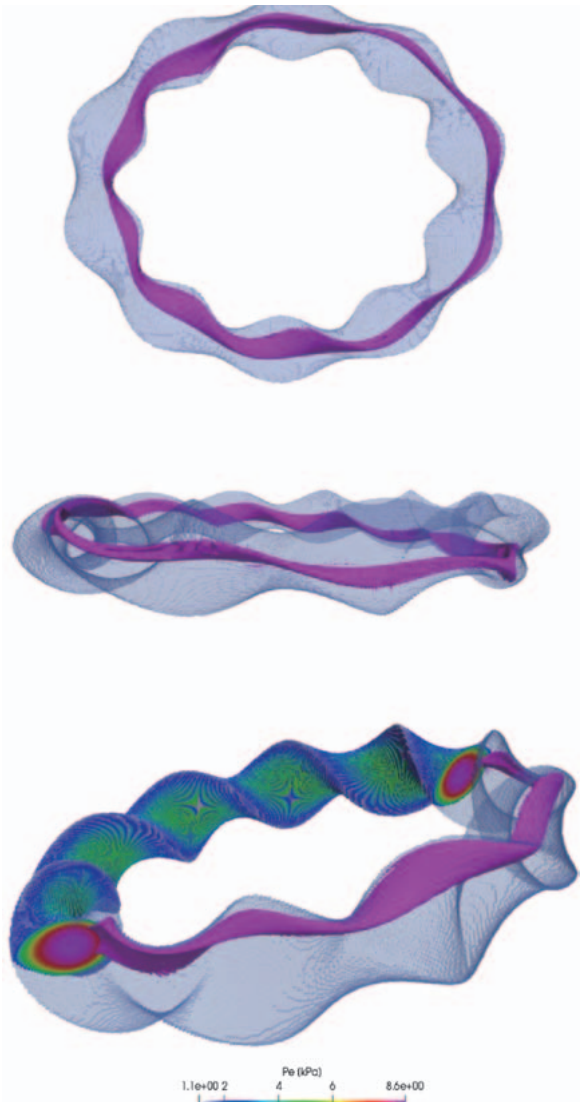

Fig. 1 The pellet cloud profile at the maximum ablation for the pellet size of 2.0×10^{21} particles/pellet.

Pellet injection is an experimentally proven method of plasma refueling in tokamak and stellarator plasmas. Pellet injection into the plasma is also used for plasma control, i.e. ELM (Edge Localized Mode) mitigation for tokamaks by means of the excitation of magnetohydrodynamic (MHD) activities. In stellarators, also ELM-like instabilities are frequently observed, and those instabilities must be controlled and mitigated. Besides the benefit of pellet injection in terms of the edge plasma instability control, plasma instabilities which are inimical phenomena via pellet injection are problems that have come into focus simultaneously. For considering those problems, the global MHD dynamics has been analyzed with the MIPS code, which solves the full MHD equations coupled with a pellet ablation model. The pellet ablation model, which is based on the neutral gas shielding (NGS) model, has been implemented in MIPS. There are two important features in our implementation of the model into the MIPS code. The first feature is that the pellet is modeled as a localized adiabatic time-varying density source. The pellet density source is toroidally and poloidally localized. The second feature is that the pellet moves at fixed speed and direction. An excitation of MHD modes by the three-dimensionally localized pressure perturbation originating from the pellet injection has been observed. Figure 2 shows the time evolution of the magnetic energies for the cases with no pellet and pellet sizes. If no pellets, the mode was not excited. The modes of m/n = 2/1, m/n = 2/2, m/n = 2/3 are plotted with solid lines, dashed lines and dotted lines, respectively. The amplitude of the excited MHD energies is proportional to the size of the injected pellet, larger pellets result in larger amplitudes of the excited MHD activity.

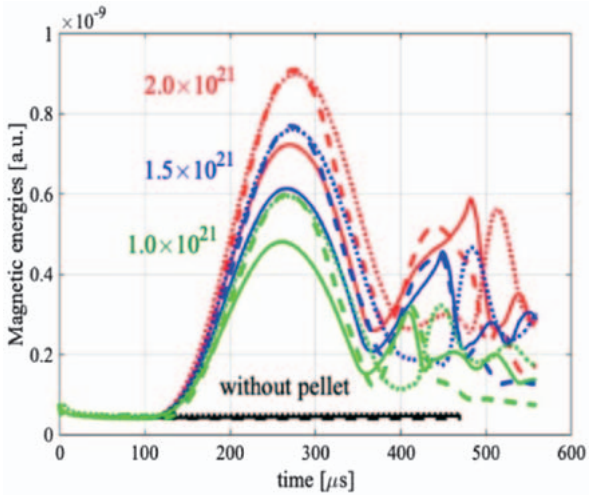

Fig. 2 Time evolution of the magnetic energies for the case of absence of the pellet, 1.0×10^{21} (green lines), 2.0×10^{21} (blue lines), 2.0×10^{21} (red lines). The pellet injection velocity is 1000 m s^{-1} for all cases. The modes of m/n = 2/1, m/n = 2/2, m/n = 2/3 are plotted in the solid lines, dashed lines and dotted lines, respectively.

Towards whole-volume kinetic modeling of helical fusion devices including the edge region

Highlight

Development of a global gyrokinetic particle-in-cell code utilizing unstructured meshes

It is crucial to evaluate plasma transport in the edge region near the divertor as well as in the core region with closed magnetic field lines. The edge plasma transport affects the durability of fusion devices through divertor heat load and also the plasma confinement through impurity contamination. While these two regions are not physically separated, conventional simulation studies focused on either of them because field line structures and plasma conditions are significantly different. We are developing a global gyrokinetic code toward whole-volume modeling of Helical fusion devices [1]. This code will enable us to perform kinetic simulations on edge plasma transport dynamically coupled with the plasma confinement in the core region. The simulation code originates from "X-point Gyrokinetic Code (XGC)" developed for Tokamaks with axi-symmetric geometries in Princeton Plasma Physics Laboratory. XGC utilizes particle-in-cell scheme with unstructured meshes potentially applicable outside the nested flux surfaces. We have extended XGC to non-axisymmetric geometries by implementing new mesh generation schemes, three-dimensional spline interpolation, and the VMEC equilibrium data interface. As the first step, we have successfully demonstrated fundamental plasma phenomena, such as neoclassical transport accompanied by a radial electric field and linear growth of ion temperature gradient mode in the core region of Large Helical Device (LHD). The novel simulation schemes and related benchmark tests were presented in the IAEA Fusion Energy Conference (FEC 2018) [2].

We are continuing to develop the code to include the edge region of LHD within the present simulation framework. A smooth magnetic field equilibrium with the edge region is obtained from the VMEC equilibrium through a virtual casing method in EXTENDER code. The unstructured mesh is constructed by numerical field line tracing in this equilibrium. We have tested elemental procedures in the time step cycles, such as particle orbit tracing and finite element field solver [2]. We will improve the field calculation and the mesh generation schemes to calculate the self-consistent time evolution of perturbed electrostatic fields in the edge region in the next step.

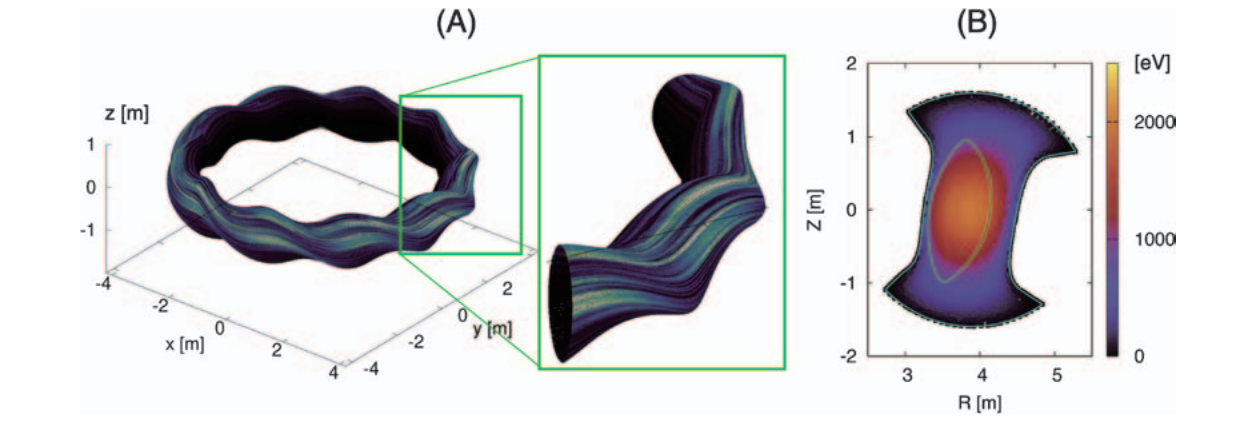

Fig. 1 Electrostatic potentials in Large Helical Device obtained from the developed code, XGC-S. (A) Electrostatic potential in linear ITG simulation for the core region. (B) Electrostatic potential generated from a uniform charge density in the entire region.

[1] T. Moritaka, R. Hager, M. Cole, S. Lazerson, C-S. Chang, S. Ku, S. Matsuoka, S. Satake and S. Ishiguro, Plasma **2**, 179–200 (2019).

[2] T. Moritaka, R. Hager, M. Cole, S. Laserzon, S. Satake, C-S. Chang, S. Ku, S. Matsuoka, S. Ishiguro, Proceedings of the 27th IAEA Fusion Energy Conference, 2018.

(T. Mortitaka)

Three-dimensional effect of particle motion on plasma filament dynamics

We have shown with the three-dimensional electrostatic particle-in-cell simulation that the particle motion influences plasma filament dynamics three-dimensionally. The intermittent filamentary plasma structure, which has been observed in the boundary layers of various magnetic confinement devices, is radially transported by the dipolar electrostatic potential structure formed in the filament cross-section. When the ion-to-electron temperature ratio T_i/T_e is higher, the ion gyro motion upsets the balance in the dipolar potential structure. Such an unbalanced potential structure induces the poloidal symmetry breaking in the filament propagation [3]. Furthermore, in the high T_i case, the pre-sheath potential drop on the hill side in the dipolar potential structure becomes larger than that on the well side. The large pre-sheath drop on the hill side induces the strong dependence of the perpendicular electric field in the filament on the toroidal position. As shown in Fig. 2, the filament dynamics in the high T_i case, in which the poloidal symmetry breaking occurs as mentioned above, are significantly influenced by such a three-dimensional structure of the electric field [4].

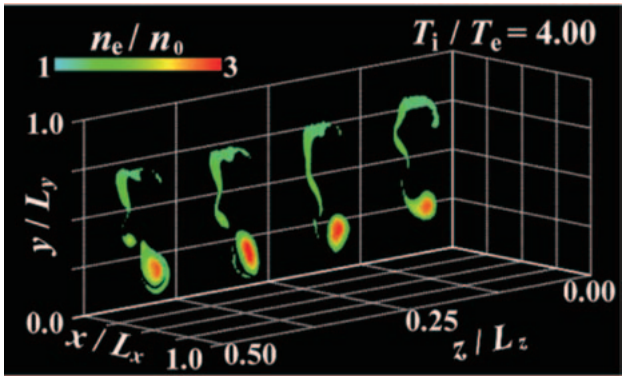

Fig. 2 Electron density distributions in the filament on four poloidal cross-sections at z/L_z = 0.125, 0.25, 0.375, and 0.5 for the high ion temperature (T_i/T_e = 4) case.

[3] H. Hasegawa and S. Ishiguro, Plasma **1**, 61 (2018).
[4] H. Hasegawa and S. Ishiguro, Phys. Plasmas **26**, 062104 (2019).

(H. Hasegawa)

Dependence of the ion heating on poloidal and toroidal fields in magnetic reconnection

By means of two-dimensional electromagnetic particle simulations, we have investigated ion heating mechanism in magnetic reconnection. In 2017, we reported that ring-shaped ion velocity distributions are formed in the downstream of reconnection and that ions are effectively heated [5].

We have further explored this effective heating process and then have found incomplete ring-shaped, i.e., circular-arc-shaped velocity distributions in some cases. It is noted that a ring is an arc with the central angle of 2π. According to our theory for the effective heating associated with the circular-arc-shaped structure of velocity distribution, the ion effective temperature depends on the radius and the central angle of an arc. Our particle simulations demonstrate two types of dependence of the ion heating [6]. Figure 3 (a) shows that (i) the ion heating energy is proportional to the square of the poloidal magnetic field. On the other hand, it is represented in Fig. 3 (b) that (ii) as the toroidal magnetic field is higher, the effective temperature is lower, but this dependence becomes small for very high toroidal field. The dependence (i) and (ii) are in good agreement with tendencies reported in STs such as TS-6, Univ. Tokyo.

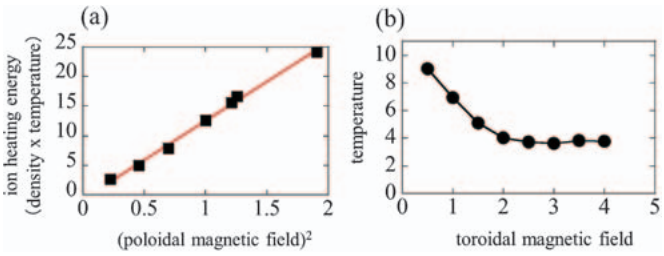

Fig. 3 Dependence of the ion effective heating on (a) the poloidal magnetic field and (b) the toroidal magnetic field. These tendencies are consistent with ones reported in ST experiments.

[5] S. Usami, R. Horiuchi, and H. Ohtani, Phys. Plasmas **24**, 092101 (2017).
[6] S. Usami, R. Horiuchi, H. Ohtani, Y. Ono, M. Inomoto, H. Tanabe, Phys. Plasmas **26**, 102103 (2019).

(S. Usami)

Visualization of the Plasma Shape in a Force Free Helical Reactor, FFHR

Highlight

A plasma shape is visualized by using the magnetic field lines calculated in the equilibrium plasma for optimization of a three-dimensional shape design of the component in the reactor.

FFHR generates twisted magnetic fields confining the plasma at the center of the vessel. To achieve a high usage of the energy generated from the nuclear fusion, the blankets are set closely to the plasma. At meanwhile, a gap between two blankets is arranged for the magnetic field lines to go through to the divertor for the online removal of impurities from the plasma. It should be noticed that these components need to be accurately designed as the energy for nuclear fusion will lost when the plasma is trend to attack the blankets.
Previously, a shape of the component in the reactor was designed considering a structure of the magnetic field line in two-dimensional cross section at the discrete toroidal angle, that is, the Poincare plots of the magnetic field lines. However, the magnetic field line has a three-dimensional (3D) structure and the plasma particle has a spread region of the Larmor radius around the magnetic field. Therefore, it is necessary to work three-dimensionally with the plasma for optimization of a 3D shape design of the component in the reactor. It will enable us to check interference between the plasma and the 3D design data of the components in the reactor.
Marching cubes algorithm is a sequential-traversal method commonly used in medical imaging technology for generating isosurface described by a scalar field [1]. Here, we have combined Marching cubes method with our approach and built a 3D model of the plasma shape.
Firstly, through applying MGTRC [2], the information of each magnetic field line is recorded. Secondly, we bring in the Larmor radius. Each magnetic field line is consisted of line segments. Further, a line segment is defined by two points. With these two points and their normal vectors calculated by the magnetic field, we can get two circular profiles representing the Larmor radius. By connecting averagely divided points on the two circles with straight lines. A tube-like structure is obtained. Figure 1 shows a magnetic field line with the other lines serving as Larmor radius. Subsequently, the position of all those lines can be transformed to the volume data.
To provide the volume data, the number of the magnetic field lines which go across each cube is recorded. A 3D digital differential analyzer [3] is applied for making sure that cubes between two relatively far points can be counted into the sum. After that, vertex values of a cube can be decided by averaging the recorded numbers belonging to its adjacent cubes. Recently, we reconsider the above method, proposing to calculate the distance between a vertex of a cube and the magnetic field line which goes across it. It is proved that the new method can provide a better visualization result. Figure 2 shows the model of the plasma shape.
Finally, we match the plasma model with the FFHR model for checking the interference.
This research has been organized into a paper and is about to be published in 'Journal of Advanced Simulation in Science and Engineering' [4]. In the future, we would like to improve our method according to the request from the domain expert in NIFS.

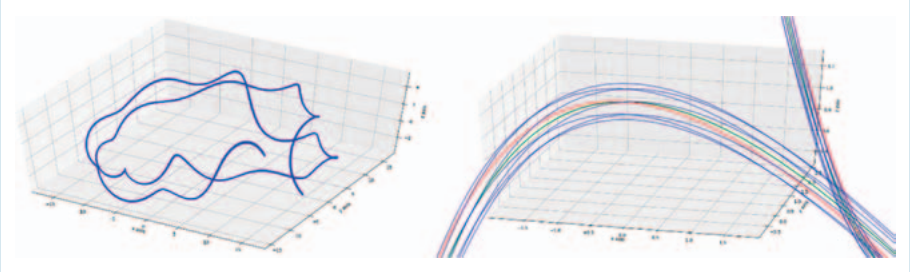

Fig. 1 On the left is a piece of magnetic field line. On the right is a part of the line after zooming in. In which, the green line refers to the original traced magnetic field line, the red and blue ones respectively are the starting line and those lines obtained by rotating the starting line, representing the Larmor radius.

Fig. 2 The 3D model of the plasma shape generated from specialized Marching cubes method.

[1] T. S. Newman, H. Yi, Computers & Graphics, **30**, 854 (2006).
[2] Project webpage. *https://github.com/yasuhiro-suzuki/MGTRC*.
[3] A.Y. Chang, Polytechnic University, Department of Computer and Information Science, (2001).
[4] H. Kunqi *et al.*, J. Adv. Sim. Sci. Eng., **7**, 151 (2020).

(K. Hu and K. Koyamada, Kyoto Univ., H. Ohtani)

Development of in-situ visualization library "VISMO"

We have been developing an in-situ visualization library VISMO [1], which is provided as a module of Fortran2003 and is easily combined with simulation codes. The simulation size becomes larger scale, and the simulation researchers can get fruitful results from the big data because of the rapidly advanced computer technology. However, it becomes difficult to deal with such large data by the traditional interactive visualization method on the PC due to the data size. In order to solve the problem, in-situ visualization method is investigated. In the in-situ visualization method, the visualization code is inserted into the simulation code, the visualization process is performed on the supercomputer the simulation code runs, and the visualized results are outputted as form of image instead of raw data.

We have added several visualization functions to the VISMO library: 1) Visualization of particle with sphere whose color and radius are changeable according to the physical value, such as velocity. 2) Coloring of isosurface whose color indicates the other scalar value. 3) Arrow presenting vector field. Arrows are scattered in whole calculation region or they are put only in the region the researcher focuses on. 4) Designation of background color. 5) Correspondence to single-precision real number. We have also optimized the library for Plasma Simulator with optimization of transfer function and have developed an interface module for implementation of the library to the simulation code to increase the convenience for users.

In order to visualize the objects from various viewpoints, VISMO has a function in which the visualized objects are outputted as forms of point clouds [2,3]. The special viewer of the point cloud data was installed to CompleXcope (Fig. 1). The viewer was also ported to the head-mount display system by using CLCL library [4].

This library was implemented to the simulation codes in other research fields, such as quantum turbulence system [4] and Hall MHD system [5]. The figure in Ref. [5] was selected as Kaleidoscope in Physical Review E. These facts prove that the VISMO library can generate a high-quality figure.

[1] N. Ohno and H. Ohtani, Plasma Fusion Res., **9**, 3401071 (2014).
[2] N. Ohno, H. Ohtani and W. Zhang, ITC26 (2017).
[3] N. Ohno and H. Ohtani, The 8th AICS International Symposium (2018).
[4] S. Kawahara and A. Kageyama, J. Adv. Sim. Sci. Eng., **6**, 234 (2019).
[5] K. Yoshida, H. Miura, Y. Tsuji, J. Low Temp. Phys., **196**, 211 (2019).
[6] H. Miura, J. Yang, T. Gotoh, Phys. Rev. E, **100**, 063207 (2019).

(N. Ohno of Hyogo Univ., H. Ohtani, H. Miura and A. Kageyama of Kobe Univ.)

Fig. 1 VISMO viewer in CompleXcope.

Current distribution optimization in electromagnet: Application to performance enhancement of superconducting linear acceleration system

As an alternative pellet injection system for a magnetic confinement fusion reactor, the Superconducting Linear Acceleration (SLA) system has been recently proposed. The SLA system is composed of an electromagnet and a pellet container to which a High-Temperature Superconducting (HTS) film is attached. The container is accelerated by the Lorentz force between the electromagnet and the HTS film. Therefore, in order to use the SLA system efficiently, it is indispensable to enhance the acceleration performance of a single electromagnet. To this end, by using the genetic algorithm [1], the current distribution in the electromagnet is optimized so as to maximize the acceleration performance. In the present study, the current distribution is represented by means of the on/off method [2], and the dynamic motion of the container is simulated by using the equivalent-circuit model [3].

According to the optimized result, the pellet velocity v is improved by a factor of 1.7 as compared with that for the homogeneous current distribution (see Fig. 1). Moreover, the cross section in which the electric current flows is reduced to 0.9. Therefore, the electric current should not be always applied to the entire electromagnet to achieve the enhancement of the acceleration performance.

[1] K. Deb *et al.*, *IEEE Trans. Evol. Comput.*, **6** (2), pp. 182–197 (2002).
[2] Y. Hidaka *et al.*, *IEEE Trans. Magn.*, **50** (2), 7015204 (2014).
[3] T. Yamaguchi *et al.*, *J. Adv. Simul. Sci. Eng.*, **4** (2), pp. 209–222 (2019).

(T. Yamaguchi, SOKENDAI, T. Takayama, Yamagata Univ., H. Ohtani, N. Yanagi and A. Kamitani, Yamagata Univ.)

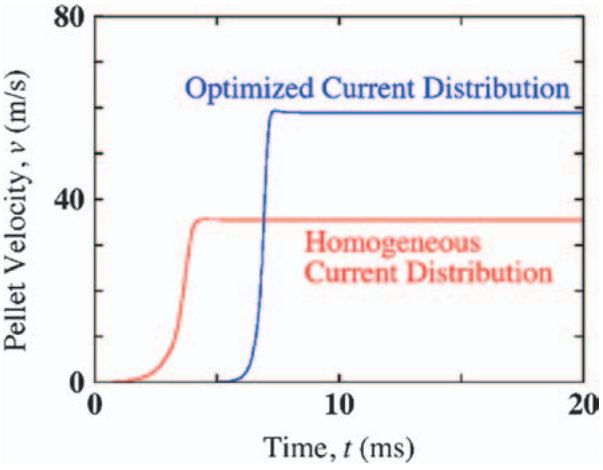

Fig. 1 Time dependences of the pellet velocity v. In this figure, the blue and red curves denote the values for the optimized current distribution and the homogeneous current distribution.

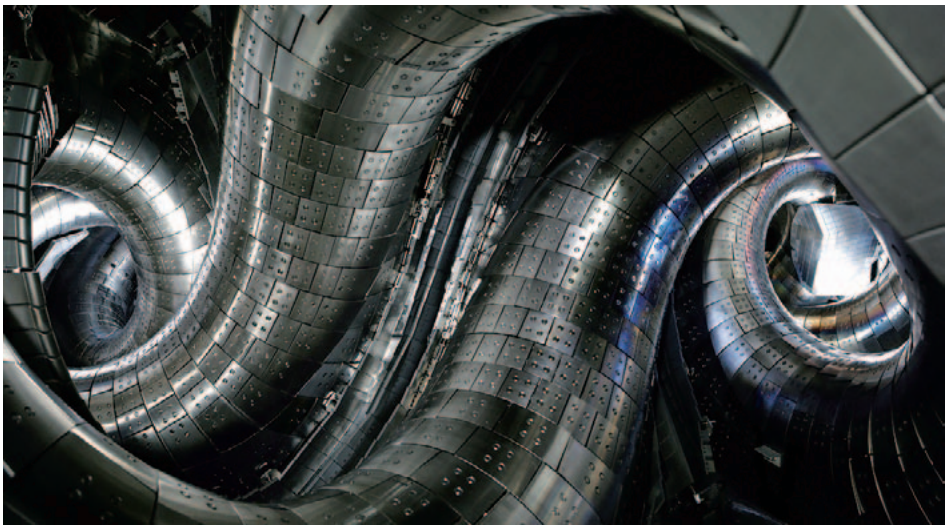

Task force for next research project

The task force for next research project has been established in late 2018 for prospecting for the next research projects beyond the LHD. The main tasks are (1) establishment of research strategies that reflect the view of the entire domestic research community in the field of plasma science and nuclear fusion research, and (2) investigation of the next research plan beyond the LHD.
With regard to the first task, the inter-university liaison conference in which the foremost research themes to be addressed by academia will be discussed is prepared in the framework of the NIFS general collaboration research. In the inter-university liaison conference, it will be also discussed the complementary role of the next research projects in the research community.
With regard to the second task, looking ahead to the future importance of the non-linearity and structure formation in magnetically confined plasmas, the plasma confinement experiment project based on the newly developed concept has been proposed. The goals of this project are creation and experimental verification of a new magnetically confined plasma in which various physical mechanisms including non-linearity and structure formation are controlled by three-dimensional magnetic field for the first time in the world. The outcome of the project will go a long way toward alleviating the engineering requirements for the realization of the fusion reactor by improving plasma confinement properties. Other important perspectives of the project are to provide a common platform for the plasma science and nuclear fusion research community, to advance the cultivation of human resources, and to enhance linkages and cooperation among different research areas such as inter-university research institute and international center of excellence.

In order to ensure the continuous and proper implementation of the next research projects, the following three preparative studies have been launched.

1. Research for creating a next generation magnetic configuration,
   - Creation of innovative magnetic configuration is addressed through the study of theoretical model, the exploration of new optimization factor, and development of the mathematical optimization techniques.
2. Development of high temperature superconducting (HTS) conductor,
   - HTS conductor development study is addressed in order to assess the technological feasibility.
3. Verification of new key concept and method using LHD.
   - The working hypotheses and outcomes of the preparative studies is verified by using LHD and contributes to the confinement improvement of LHD.

(R. Sakamoto)

Toward innovative plasma confinement

Creation research is accelerated to establish the next generation magnetic confinement with enhanced zonal flows and turbulence suppression, leading a new discovery of innovative confinement.

Turbulence and the related transport phenomena have widely been observed in magnetically confined plasmas. Clarifications and controls of turbulence are key issues in fusion plasma research, and many experimental and theoretical studies have been devoted so far. One of the most important findings is the turbulence suppression by spontaneously generated zonal flow, which is recognized as a key mechanism leading to improved confinement in Large Helical Device (LHD), etc. As a new activity, Next Generation Stellarator (NGS) creation research is extensively promoted. Significant progresses on the turbulence and zonal-flow modeling based on nonlinear gyrokinetic simulation studies are obtained, where the effects of nonlinearity, zonal-flow generation, and its geometric dependence in 3D magnetic field are incorporated into the modeling. Such an extended model for the turbulent transport enables us to explore novel helical plasmas with enhanced zonal flows and turbulence suppression, by utilizing mathematical optimization techniques. As exemplified in figure 1, the numerical exploration of 3D magnetic field geometry successfully found a helical plasma in which the turbulent transport is much reduced by enhanced zonal flows. Also, experimental studies in LHD in order to verify and extend the turbulence and zonal-flow modeling are being conducted.

(M. Nakata)

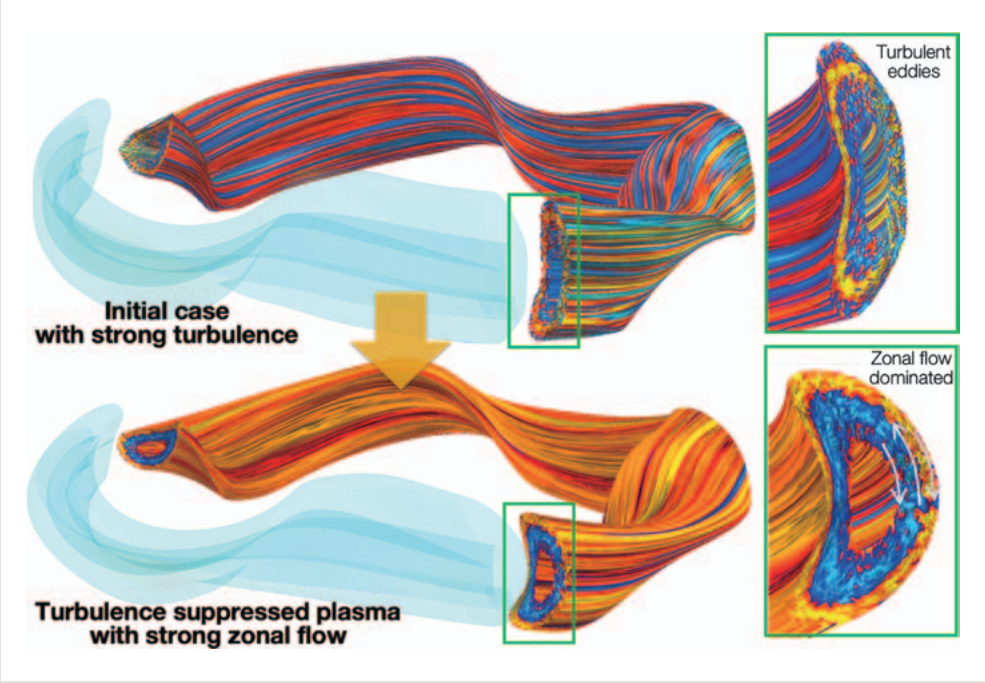

Fig. 1 An example of the numerical exploration for optimum 3D magnetic field structures. Enhanced zonal flows appear in the turbulence suppressed helical plasma (bottom).

Physics and engineering studies in NGS creation research activity

Toward a new discovery of innovative plasma confinement to accelerate the fusion plasma research, Next Generation Stellarator (NGS) creation research is extensively promoted. Combining and extending the current best knowledge from experimental and theoretical studies, a novel helical plasma, which has never been realized so far, is created. Here, the synchronized/integrated plasma confinement with the turbulence suppression by zonal flows, energetic particle confinement, and flexible peripheral structures is explored by fully utilizing the diversity of 3D magnetic field structures in helical systems. In addition to the physics studies, the engineering studies have been carried out as front-loading preparations for the feasible design of experimental devices, where some of the engineering constraints are provided to the physics studies as feedback.

The turbulence-related physics studies are presented as a highlighted result above. Here, another activities on the peripheral magnetic field structures such as the leg-type and island-type divertors are introduced. The main objective on this study is to establish flexible controls of several divertor magnetic field structures by keeping almost the same characteristics of the core plasma. To this end, numerical studies are conducted to find the optimum spatial configurations of external saddle-loop coils, where the distributions of connection-length and footprints on the vacuum vessel is systematically analyzed and compared. As shown in figure 2, the capabilities for both the leg-type and the island-type divertor structures are confirmed. More extended analyses utilizing mathematical optimizations will be addressed.

In order to explore wider possibilities of the 3D magnetic configurations and coil designs, the numerical codes for the mathematical optimization are also developed and extended, where both the modular coils and the continuously winding coils are incorporated. Such numerical tools are useful not only for the physics studies, but also for the optimization in the engineering studies. Using a trial configuration for the neoclassically optimized helical plasma, the modular coils, the support structures, and the heating/observation ports are designed, as shown in figure 2. In addition to the evaluation of engineering constraints/limits, systematic investigations are in progress for the improved designs based on the optimizations of modular coils in some additional constrains such as the curvature and the coil-coil distance. Furthermore, advanced measurement systems for the turbulent fluctuations and macroscopic flow patterns are being investigated.

(M. Nakata)

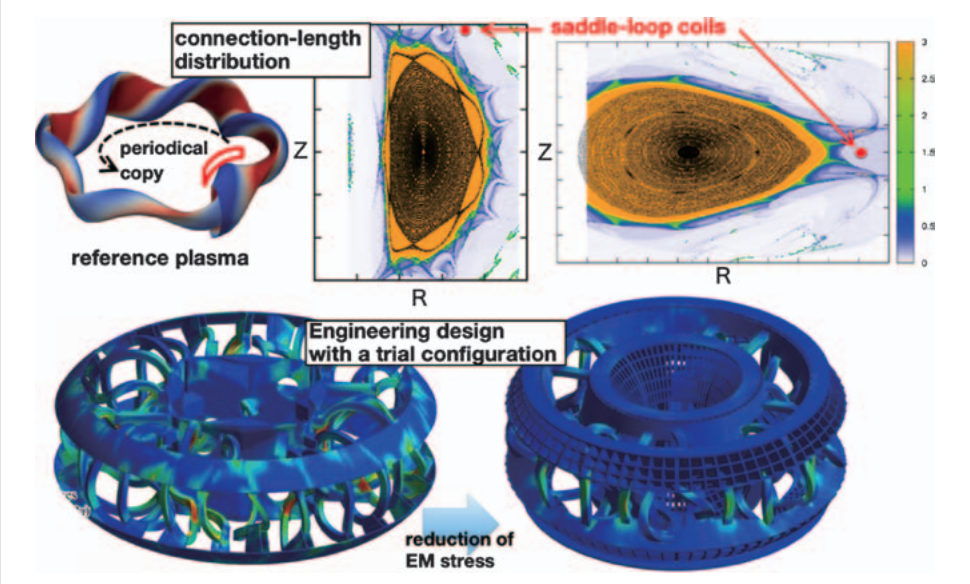

Fig. 2 Two different peripheral magnetic field structures produced by external coils (top), and an example of the stress distributions in coils and support structures. (bottom).

Development of High-Temperature Superconducting (HTS) Coils for Next Research Project

Application of a high-temperature superconducting (HTS) magnet to the next research project has been studied in continuation of its long development for the LHD-type heliotron fusion reactor FFHR [1], because the HTS can be operated at higher magnetic field than a conventional low-temperature superconducting (LTS) magnet and can enhance the confinement capability of a plasma experimental device. Moreover, the HTS coil can operate at higher temperatures than the LTS magnet and can have extremely high stability and low heat load by its nature.

In the first phase of the development, large-current capacity HTS conductors with REBCO (RE $Ba_2Cu_3O_7$, RE: rare earth) tapes have been developed with a goal of carrying 15 kA current at 20 K temperature and 10 T magnetic field. In addition, the large conductor should be able to bend with a radius of less than 1 m without damage.

At present, we have been developing three types of conductors and confirming their performances, such as a critical current, at 77 K (liquid nitrogen temperature). The conductors are named: (a) STARS (Stacked Tapes Assembled in Rigid Structure) [1, 2], (b) FAIR (Friction stir welding, an Aluminum alloy jacket, Indirect cooling, and REBCO tapes) [3], and (c) WISE (Wound and Impregnated Stacked Elastic tapes) [4]. Schematic diagrams are shown in figure 3. The common feature is that dozens of REBCO tapes are stacked in parallel in the conductor to increase the current capacity. Metals surrounding the tapes are different: copper and stainless steel for STARS; aluminum and aluminum alloy for FAIR; and low-melting-point metal for WISE.

Conductors that are confirmed to have predetermined performances will be tested in a magnetic field at 20 K. Eventually, a demonstration coil will be fabricated and tested.

[1] A. Sagara *et al.*, Fus. Eng. Des. **89**, (2014) 2114.
[2] N. Yanagi *et al.*, Nucl. Fusion **55**, (2015) 053021.
[3] T. Mito *et al.*, J. Phys. Commun., **4**, (2020) 035009.
[4] S. Matsunaga *et al.*, IEEE Trans. Appl. Supercond. **30**, (2020) 4601405.

(K. Takahata)

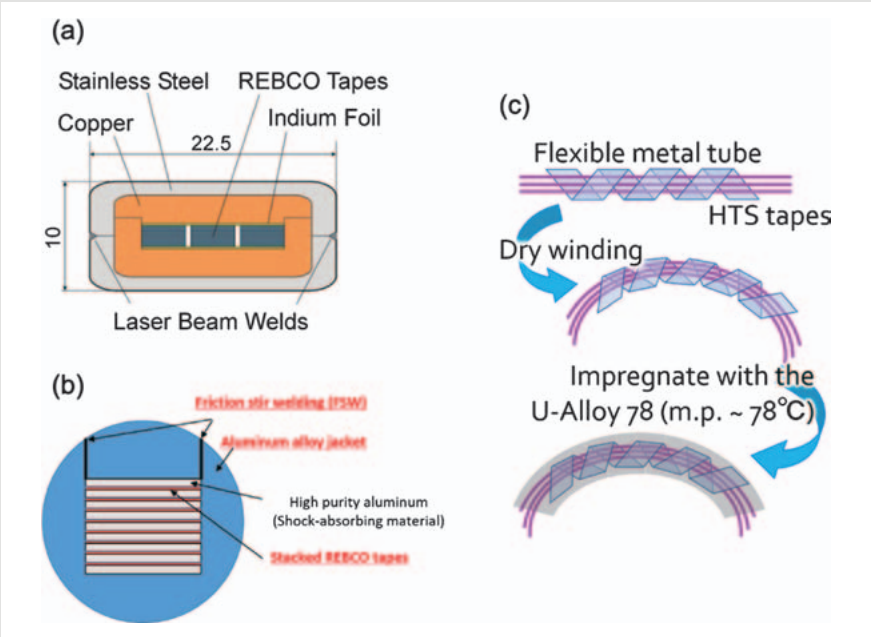

Fig. 3 Schematic diagrams of three conductors developed for the next research project: (a) STARS, (b) FAIR, and (c) WISE.

4. Basic, Applied, and Innovative Research

As an inter-university research institute, NIFS activates collaborations with researchers in universities as well as conducting world-wide top level researches. The collaboration programs in basic, applied, and innovative research support research projects motivated by collaboration researchers in universities. It is also important to establish the academic research base for various scientific fields related to fusion science and to maintain a powerful scientific community to support the research. Programmatic and financial support to researchers in universities who work for small projects are important.

For basic plasma science, NIFS operates several experimental devices and offers opportunities to utilize them in the collaboration program for university researchers. A middle-size plasma experimental device HYPER-I is prepared for basic plasma research. The compact electron beam ion trap (CoBIT) for spectroscopic study of highly charged ions, atmospheric-pressure plasma jet devices for basic study on plasma applications, and other equipment are operated for collaborations.

(I. Murakami)

Positive and negative ion reflections of low-energy ion beams from materials surface

We have studied the reflection of the positive and the negative hydrogen ions from the Highly oriented pyrolytic graphite (HOPG) and Mo surfaces on injection of several hundreds of eV to 1 keV of ion beams of H^+, H_2^+ and H_3^+ ions. The energy spectra of reflected ions were detected by a momentum analyzer, and both reflected positive and negative peaks were investigated [1]. The results showed clear difference between atomic and molecular ion injections. The intensity ratio of reflected negative to positive ions H^-/H^+ increased as the incident beam energy per nucleon decreased only when molecular ion beams are injected (Fig. 1). This implies that negative ions are more produced upon beam-surface interaction when molecules are injected. The incident energy dependence of the H^-/H^+ ratio was not observed for the H^+ ion injection. This could be explained by the difference in negative ion production processes between atomic and molecular ions. Both are neutralized once as they approach the surface. On the one hand, atomic ion requires tunneling effect for the electron capture to become a negative ion. The other hand, the molecular ion dissociates as an ion pair of H^+ and H^- via excitation to an anti-bonding state of molecule.

(N. Tanaka, Osaka University)

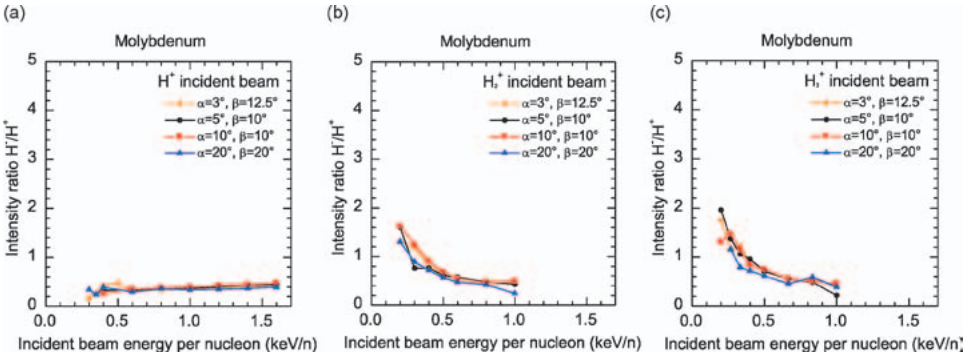

Fig. 1 Incident-beam energy dependence of the negative to positive ion intensity ratio for the incident beams of (a) H^+, (b) H_2^+, and (c) H_3^+ on the molybdenum target. [1]

Experimental turbulent transport study using electroconvection turbulence

Turbulent transport is a basic subject in a variety of research fields, such as fusion plasma, normal fluids, space/astrophysical plasmas, quantum fluids, and superfluid. An electroconvection (EC) turbulence, which can be driven by electric field in a liquid crystal, was newly applied to turbulent transport study. Due to the excellent controllability and easy flow pattern measurement (see Fig. 2), the diffusive nature of turbulent transport was clearly identified in an EC turbulence. The effective diffusion coefficient is observed to increase with Rayleigh number, which is consistent with normal fluid turbulence [2]. We also observed a variety of interesting phenomena such as rotational effects on turbulent transport, turbulence penetration toward convectively stable region, deviation of velocity distribution function of tracer particles in EC turbulence etc. The turbulence suppression effect due to flow shear which is a very important phenomenon in magnetically confined fusion plasma experiments will be also investigated in the future.

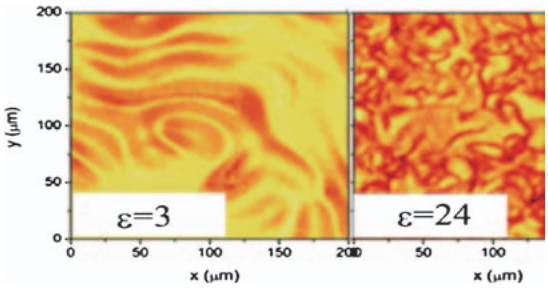

Fig. 2 Flow pattern of electroconvection turbulence with the normalized Rayleigh number of ε = 3 and ε = 24. The brightness indicates the parallel velocity to the line of sight.

(Y. Hidaka, Kyushu Univ., K. Nagaoka)

Multi-wavelength high-time resolution spectroscopy of atmospheric pressure plasma

Measurement of the electron temperature and density is one of the essential issues in atmospheric pressure plasma. Utilizing continuum emission due to bremsstrahlung of electron colliding with neutral particles is a promising method. On the other hand, high-time resolution is required because the plasma is usually produced in pulsed operation. Optimal color bands have been determined from a time-averaged spectrum of an atmospheric pressure plasma device in NIFS as shown in Fig. 3. The electron density $n_e = 3\times10^{19}$ m^{-3} and $T_e = 0.3$ eV is deduced from the bremsstrahlung curve fitting of the spectrum. Then, we have developed a two-color spectrometer with interference filters based on a grating spectrometer for high-time resolution spectroscopy [3]. Instantaneous emission in the 527 – 537 nm pass band measured with the spectrometer reaches about 3 μW/cm^2/sr, which is one order higher than that for the time-averaged spectrum. The result implies that high density plasma is ejected from the device in a short duration of about 0.1 ms.

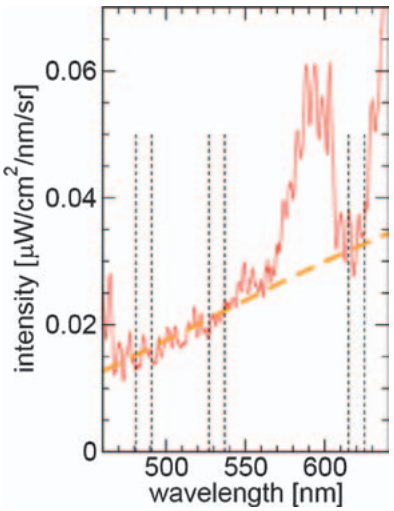

Fig. 3 Spectrum of atmospheric pressure plasma consists of bremsstrahlung continuum (fitted by thick broken curve) and band emission (560 – 600 nm). Dotted lines show candidates of filter pass band for high-time resolution spectroscopy.

[1] N. Tanaka *et al.*, Rev. Sci. Instrum. **91**, 013313 (2020).

[2] K. Nagaoka, S. Hotta, Y. Hidaka, T. Kobayashi, K. Terasaka, S. Yoshimura, High Energy Density Physics vol.31 79–82 (2019).

[3] A. Okamoto, *et al.*, Plasma Fusion Res. **14**, 1201165 (2014).

(A. Okamoto, Nagoya Univ.)

5. Network-Type Collaboration Research

The NIFS General Collaboration has been basically based on a one-to-one (especially, NIFS-to-University) collaborative system. Some collaborations, however, require the use of more than one experimental facility in different universities and institutes to achieve their objectives. In the network-type collaboration, this type of collaboration becomes practicable by admitting travel expenses for moving between universities, which have not been admitted as a rule in the general collaboration projects.

Since FY 2011, NIFS has employed this network-type collaboration. Three projects of the different fields were accepted in FY 2011 for the first time. Challenges in these collaborations spread over various fields. Before starting the collaborations, a collaboration plan for the year should be submitted. The plans include the items how the collaborations between research institutes are planned, that is, who goes when and where by what purpose.

In this fiscal year, seven proposals were accepted. The titles of the research items are listed below.

(1) "Effect of the resonant magnetic perturbation on MHD phenomena of toroidally magnetized plasmas" M. Okamoto (National Institute of Technology, Ishikawa College), and collaborators in NIFS, Kyoto Univ., Nagoya Univ., Kyoto Institute of Technology, Tokyo Institute of Technology, Kyushu Univ., Univ. of Hyogo, QST, National Institute of Technology (Gifu College and Yuge College), Hokkaido Univ., and Hosei Univ.

(2) "Hydrogen isotope retention of plasma facing materials damaged by neutron irradiation" N. Ohno (Nagoya University), and collaborators in NIFS, Univ. of Toyama, Shizuoka Univ., Hokkaido Univ., Kyushu Univ., Tohoku Univ., Ibaraki Univ., and Osaka Univ.

(3) "Interdisciplinary study of plasma heating at O-point and X-point using laboratory experiments, numerical simulations and solar observations" M. Ono (The University of Tokyo), and collaborators in NIFS, JAXA, Chiba Univ., NAOJ, NIST, Kyoto Univ., Nihon Univ., and AIST.

(4) "Comprehensive Understanding of Plasma Flow by Creation of a Basic Plasma Network" T. Kaneko (Tohoku University), and collaborators in NIFS, Kyushu Univ., Kyoto Institute of Technology, and Nagoya Univ.

(5) "Tritium, radon and radium concentrations in environmental water samples in Japan" M. Hosoda (Hirosaki University), and collaborators in NIFS, Univ. of the Ryukyus, Hokkaido Univ. of Science, Kobe Pharmaceutical Univ., Institute for Environmental Science, and QST.

(6) "Construction of gyrokinetic simulation research network" T. Watanabe (Nagoya University), and collaborators in NIFS, Kyoto Univ., Kyushu Univ., and QST.

(7) "Development of a plasma injector using high beta plasma sources for an active control of plasmas" N. Fukumoto (University of Hyogo), and collaborators in NIFS, the Univ. of Tokyo, Nihon Univ., Gunma Univ., AIST, and Kyushu Univ.

The items (1) to (6) are continuing items and (7) is a new item in FY2019. The items (1), (3) and (4) are related to the intercommunication of researchers and students, and are the comparative researches of the results

obtained in the different devices in universities, institutes, and NIFS.

The item (2) is related to the inspection of neutron-irradiated materials by utilizing the compact divertor plasma simulator (CDPS) installed at the Oarai Center of Tohoku Univ. The item (5) requires the movement of researchers and students over wide areas to collect samples in different places. The item (6) is related to construct a simulation research network to enhance the simulation research activities using gyrokinetic codes in Japan. The new item, (7) is related to plasma injector using compact toroids such as a Spheromak and a field-reversed configuration (FRC).

And all proposals take advantage of the merit of the network-type collaboration.

6. Fusion Science Archives (FSA)

The Fusion Science Archives was established in 2005 to learn lessons from the past fusion science archives preserved and to maintain collections of historical documents and materials that are related to fusion research in Japan. These activities are important from the viewpoint of the historical evaluation of fusion research, its social accountability and making references for seeking future directions.

Since then, historical materials on fusion research and/or organizations related to fusion research have been collected and preserved at FSA. They are stored in acid-free folders and boxes. The total number of registered items is now approximately 25,400. Most of those catalogues are available to the public through the internet in a hierarchical structure and can be accessed by the use of an electronic retrieval system.

The following collaborative works are performed this scal year along this line:

- **Studies on History of Activities of Researchers at the dawn stage of Fusion Research in Japan (NIFS17KVXV012)** T. Amemiya (CST, Nihon Univ.) *et al.*
  The History of Science Group of CST, Nihon University investigated the history of fusion research in Japan from the 1950s to the 1960s. In this collaborative work, the focus is placed on the individual researchers or the organizations that have led research in the dawn of fusion in Japan utilizing the historical documents in the NIFS FSA and the KEK archives office. The subjects specically investigated in this scal year are as follows: (i) On the detailed background and the decision process for the establishment of the Institute of Plasma Physics (IPP) under the Ministry of Education. (ii) On the discussions and decisions in the Science Council of Japan for establishing the IPP.
- **Making name authority data about persons, groups, and organizations appearing in FSAD, related to fusion science in Japan (NIFS17KVXV014)** H. Gotoh (The Kyoto University Museum) *et al.*
  FSA accepts various materials related to the fusion science history. It picks up essential information from materials, organizes it, and stores it in the database. The archives catalog created in such a way is provided to the users of interest. Researchers or research groups on fusion science and their mutual relations are not clear for the user only from the catalog. The purpose of this research is to clarify the method of accumulating and sorting the directories of those who have committed to fusion science. Issues found during last year and progress for resolving these issues during this year were the following: (1) Electrical database of the fusion science researcher is created by picking researchers up from the directories (as of 1961,1963 and 1971) of "KAKUYUGO (HANNOH) KONDANKAI" etc. and searched those of 1974, 1976, 1977 and 1982. (2) Those database are calibrated, modied by referring to the Overview of Japanese researcher and research subjects (1979, Kinokuniya) (3) Those database are also compared with the journal database of Nuclear Fusion and Physical Review Letters. (4) As one of the examples to identify the research group, the attributes of young researchers are searched from the directory of the Plasma Young Researcher's Group in 1970.
- **Archival Studies on Collaborations in Heliotron Studies at Kyoto University (NIFS17KVXV015)**
  T. Mizuuchi (Kyoto Univ.) *et al.*
  The activity of the archives of this scal year focused on the materials related to the development of the plasma experimental devices in contrast to the FSA activity in NIFS mainly on the fusion researchers and research organization. In this regard, the archives activity are promoted on the development of the series of Heliotron devices originated from Kyoto University. The range of objects of the archives is extended to the researchers, research group, and their activity which led the Heliotron development. In these years, digitizing the minutes of research meeting from the period of Heliotron-E is progressed more than half. Although relatively new minutes are produced using word processors or personal computers and exists as electrical files, but identifying the file is sometimes difficult and some are unreadable or figures are often missing in the file. Digitizing directly from printed out documents is more efficient and continuing the digitization even relatively new one. Reserved record media are sometimes unaccessible from present day computers and started to convert such media to accessible ones.
- **History of the early days of Nuclear Fusion Research Group in Japan (NIFS17KVXV017)**
  C. Namba (NIFS FSA) *et al.*
  The organization "Nuclear Fusion Research Group of Japan" (KAKUYUGO KONDANKAI, hereafter referred as KK) was established in 1958. Dr. H. Yukawa was the first president of this organization. This KK continued to perform an important role in the research and development in fusion science in Japan as a voluntary organization for researchers until it became "The Japan Society of Plasma Science and Nuclear Fusion Research" in 1983. The theme of this work is to clarify the establishment process of the KK and how organized researchers and how planned to promote the fusion development research. It is newly conrmed that the KK was established before November 1957 and was formed as a researcher's voluntary organization to promote plasma physics, but is different from "Assembly for Nuclear Fusion Reactions" (KAKUYUGO HANNOH KONDANKAI)

established under Science Technology Agency. After the establishment of the KAKUYUGO KONDANKAI, Advisory Committee on Nuclear Fusion (KAKUYUGO SENMONBUKAI) was organized in the Atomic Energy Commission of the Japanese Cabinet Office.

- **Collaborative Activities at NIFS Fusion Science Archives (NIFS FSA) (NIFS17KVXV018)**
  S. Kubo (NIFS, FSA) *et al.*
  The purpose of this collaboration is to arrange and promote the general archival activities under the NIFS collaboration framework. More than 50 researchers from universities and research institutions have joined this collaboration research. Nine collaboration programs were approved and performed as a NIFS general collaboration (NIFSKVXV012-022). One workshop type collaboration (NIFS19KKGV004) is approved and performed as a second Archives in Natural Science Workshop in December 2019 at NIFS. Beside those activities, the strengthening of the archive function is tried by increasing the racks for preserving the donated materials, introducing optical scanners, micro-film readers, etc.
- **Construction of Digital Library of Husimi Kodi Archives (NIFS18KVXV019)** H. Iguchi (NIFS, FSA) *et al.*
  Digitizing the historical documents left by Kodi Husimi, the first director of Institute of Plasma Physics (IPPJ), Nagoya University, is continued to be covered almost 12% among registered documents. All documents in the box number B401a and b are finished the digitization. Beside of these digitization, cataloging the historical materials donated from the bereaved family of Kenzo Yamamoto is completed. He lead the fusion energy development as a professor of Nagoya University and later as a Technical Advisor of JAERI and this catalogue will be useful for investigating the expanding period of the Japanese fusion energy research.
- **Archives of the Historical Material related to the Plasma Spectroscopy (NIFS19KVXV0020)**
  N. Yamaguchi (Comprehensive Research Organization for Science and Society (CROSS)) *et al.*
  Workshops called "Plasma Elementary Process workshop" or "Spectroscopy workshop" have been held as a collaboration research of Institute of Plasma Physics, Nagoya University (IPP) and NIFS from 1969 to the present. The editing work of the history of the these workshops is continued from last scal year. The agenda and reports of each workshop are piled up as an annex of the history.
- **Investigation and Analysis of Historical Materials on Startup and Development Phase of Fusion Technology Research in Japan (NIFS17KVXV021)** S. Matsuda (Tokyo Inst. Technology) *et al.*
  The startup and development phase of the fusion technology research in Japan was investigated from the view point of Japan Atomic Energy Research Institute (JAERI) and the Institute of Plasma Physics, Nagoya University (IPPJ) under the collaboration with FSA. Following the interview with Shigeru MORI last year about the origin and the background of the fusion reactor technology research in JAERI, he suggested that there had not been close relationship between those in JAERI and in IPPJ and universities. We have decided to summarize publish the historical flow of "Japanese Fusion Reactor Technology". General items to be described are, 1. The Dawn of Japanese Fusion Reactor Technology Started in JAERI., 2. Fusion Advisory Committee and Subcommittee., 3. Fusion Technology Development under Grants-in-Aid for Scientific Research., 4. Advances in the Fusion Reactor Material Development.
- **Establishment and Evolution of the Inter-University Research Institute Cooperation System (NIFS16KVXV022)** K. Matsuoka (NIFS, FSA) *et al.*
  Institute of Plasma Physics (IPPJ) of Nagoya University was established as a joint usage/research center and has functioned as a center of the plasma and fusion research in Japan, but has lost a leadership during the course of the future plan discussion in the Japanese Academic Council which began in 1982. Although the toroidal plasma connement experiments had started in 1970's, not many academic results which are useful in the fusion energy development were achieved and IPPJ could not propose an attractive future plan.
- **Comparative Studies of Practical Issues of Archiving and Utilization of Historical Records of Scientic Activities and Academic Policy Making (NIFS19KKGV004) (NIFS19KKGV004)**
  Y. Takaiwa (KEK, Archives Office) *et al.*
  Archives activities of NIFS has been performed for more than ten years collaborating with some institutes of Inter-University Research Institute Corporations, Sokendai and others. During this process, the importance of understanding conceptual and practical issues in managing the archives of scientic or academic research institutes is noticed, which is not necessarily well understood by most of practitioners of archive. In this sense, the information exchange among such archives and related audiences is also important. The workshops for this purpose have been held twice a year in recent days; in 2019, one, in Tsukuba (KEK and National Museum of Nature and Science) in August, and the other, at NIFS in December. Joint proceedings of the two workshops will be published as a NIFS-memo and KEK reports.

(S. Kubo)

7. Bilateral Collaboration Research Program

The purpose of the Bilateral Collaboration Research Program (BCRP) is to enforce the activities of nuclear fusion research in the universities by using their middle-size experimental facilities of the specific university research centers as the joint-use facilities for all university researchers in Japan. The current program involves 5 university research centers, as follows:

- Plasma Research Center, University of Tsukuba
- Laboratory of Complex Energy Process, Institute of Advanced Energy, Kyoto University
- Institute of Laser Engineering, Osaka University
- Advanced Fusion Research Center, Research Institute for Applied Mechanics, Kyushu University
- Hydrogen Isotope Research Center, University of Toyama

In BCRP, each research center can have its own collaboration programs using its main facility. Researchers at other universities can visit the research center and carry out their own collaboration research there, as if the facility belongs to NIFS. That is, all these activities are supported financially by NIFS as the research subjects in BCRP. The BCRP subjects are subscribed from all over Japan every year as one of the three frameworks of the NIFS collaboration program. The collaboration research committee, which is organized under the administrative board of NIFS, examines and selects the subjects.

(T. Morisaki)

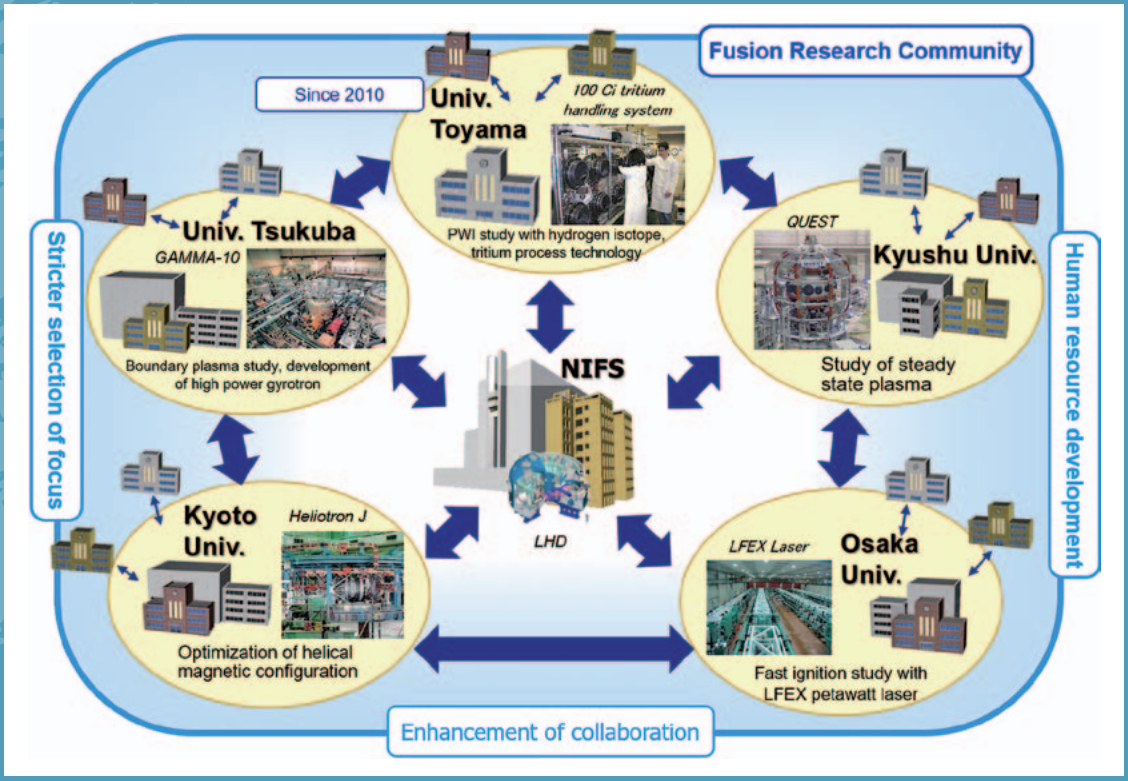
Fusion Research Community
Since 2010
Univ. Toyama
100 Ci tritium handling system
PWI study with hydrogen isotope, tritium process technology
Univ. Tsukuba
GAMMA-10
Boundary plasma study, development of high power gyrotron
QUEST
Kyushu Univ.
Study of steady state plasma
NIFS
LHD
Kyoto Univ.
Heliotron J
Optimization of helical magnetic configuration
LFEX Laser
Osaka Univ.
Fast ignition study with LFEX petawatt laser
Stricter selection of focus
Human resource development
Enhancement of collaboration

University of Tsukuba

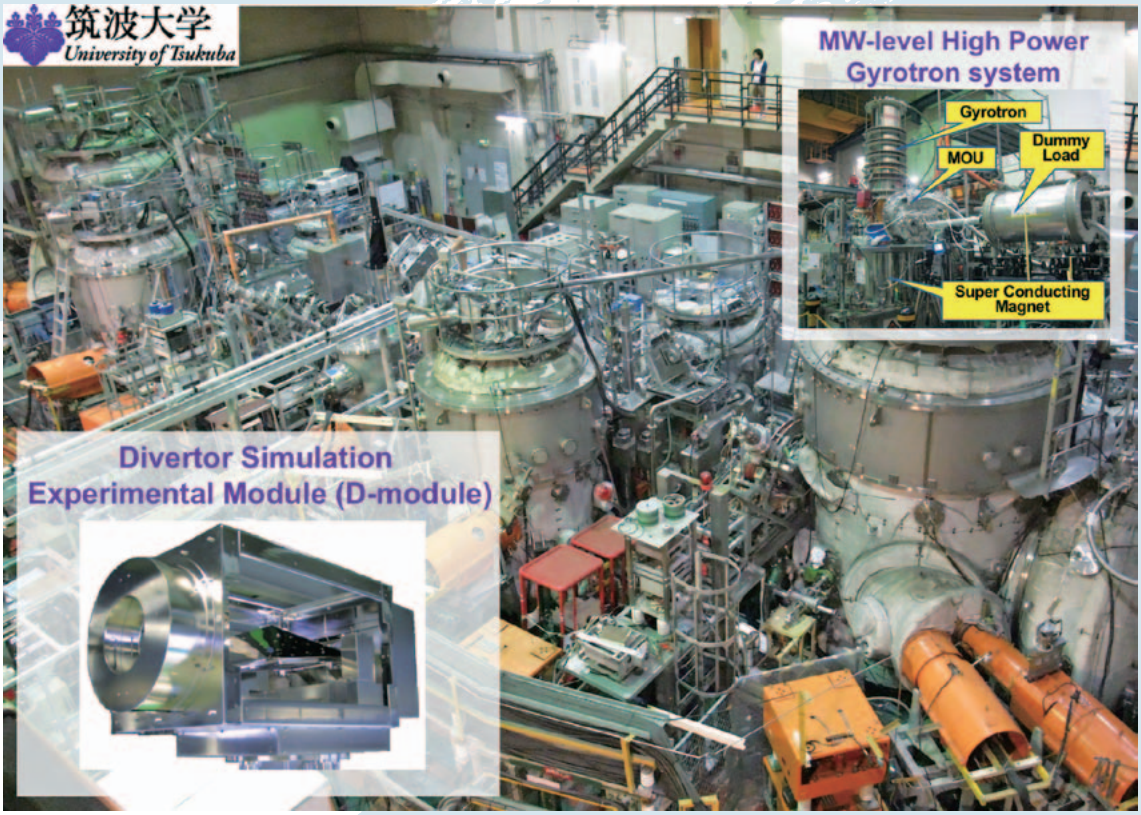

Fig. 1 Bird's eye view of GAMMA 10/PDX.

Highlight

Study of boundary plasmas by making use of open magnetic field configuration and development in high power gyrotrons toward the DEMO project

GAMMA 10/PDX (Fig.1) is the world's largest tandem mirror device and has many plasma production/heating devices with the same scale of present-day fusion devices. By using the controllability of end-loss plasma flow, divertor-simulation experiments at the end region have been performed with strong ICRF and ECH systems. By using divertor simulation experimental module (D-module) installed at the west end region of GAMMA 10/PDX, characterizations of detached plasmas have been performed. A physical mechanism of the effective plasma detachment by the additional N_2+H_2 gas injection into the D-module has been investigated. The effect of an angle of the V-shaped target on the plasma detachment has been studied. Gyrotrons with wide range of frequencies from 14 to 300 GHz have been developed. A test of a new 28/35 GHz dual-frequency gyrotron was carried out. A double disk window of sapphire has been developed for high power and long duration gyrotrons. The new linear plasma device with superconducting coils is designed and under construction to contribute to the DEMO divertor design.

In the Plasma Research Center, University of Tsukuba, studies of boundary plasma and development of high-power gyrotrons have been performed under the bilateral collaboration research program. In FY2019, 26 subjects including the base subject were accepted and were productive in a number of excellent results.

Effects of a divertor target angle and a combination of N_2 and H_2 puffing on the plasma detachment have been investigated. A divertor target angle is expected to affect plasma detachment through the change of hydrogen recycling processes. Experiments of different target angles have been conducted using a variable angle V-shaped target system in the D-module to study detailed physical mechanisms of dependence of the target angle on the plasma detachment. Figure 2 shows images for different target angles, which are obtained during the hydrogen discharge in the D-module using a high-speed camera with a bandpass filter of H_α. It is found that the intensity decreases near the corner of the V shaped target plate as the angle is decreased, even though no additional gas is injected. In the case of the smallest opening angle, ion fluxes near the corner of the target clearly decrease in spite of no additional gas seeding. Such a flux drop is possibly attributed in the local neutral pressure build-up near the corner of the target caused by hydrogen recycling processes. As for the experiments of a combination of N_2 and H_2 puffing into the D-module, a clear decrease of ion flux to the divertor target in the D-module has been observed. The observed spectrum emissions ratio of H_α and H_β decreased during the combination puffing, indicating that the importance of the plasma chemical processes involving N and N_2 related reactions indicate that N-MAR is? on the decrease in ion flux and plasma density.

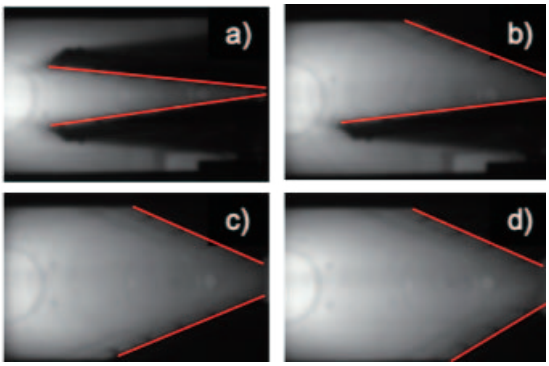

Fig. 2 High-speed camera images with H_α filter of different target angle (a) 16°, (b) 30°, (c) 45° and (d) 55°. Red lines show the position of target plate.

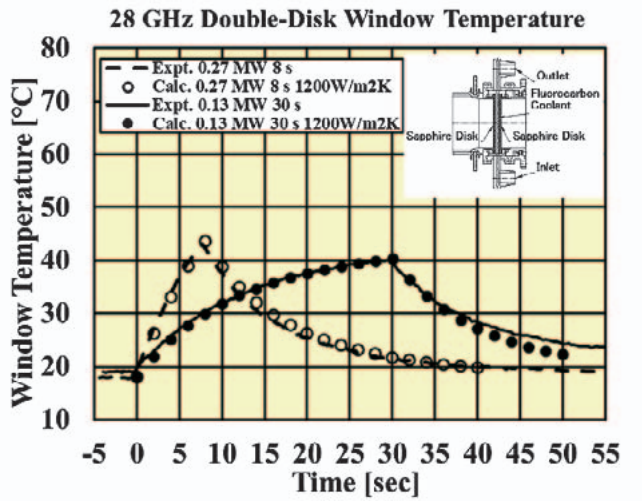

Fig. 3 Dependence of measured and calculated window temperatures on the gyrotron operation time. The insert shows a structural cross-section of the double disk sapphire window.

In the 2019 experimental test of a 28/35 GHz dual-frequency gyrotron (2 MW for 3 s and 0.4 MW CW at 28 GHz) for QUEST, NSTX-U, Heliotron J, and GAMMA 10/PDX, the cooling characteristics of a double-disk sapphire window were evaluated, because window cooling performance is a critical quantity limiting the CW power. The time evolutions of the measured and calculated window temperatures of the gyrotron with the 28 GHz operation are shown in Fig. 3. At the operation of 0.13 MW and 30 s, the measured window temperature increased during the operation period and tended to saturate at approximately 42 °C (solid curve). The heat transfer coefficient h from the sapphire disk to coolant is estimated to be 1200–1500 W/m^2 K by comparing calculated results and the experimental measurements. The calculated result for 0.13 MW and 30 s oscillation with 1200 W/m^2 K is plotted with closed circles. Further, the measured and calculated results with 1500 W/m^2 K for 0.27 MW and 8 s oscillation are plotted with a dashed curve and open circles, respectively. These results show that the operation of 0.4 MW with CW at 28 GHz is possible.

A dual-path YAG-Thomson scattering (TS) system has been constructed for measuring electron temperatures and densities both in the central and the end cells of GAMMA 10/PDX. The electron temperatures and densities both in the central and end cells have successfully been obtained in a single plasma shot. A multichannel (multi-frequency) Doppler reflectometer using a frequency comb generator has been developed to clarify the spatiotemporal structure of fluctuation flows. (M. Sakamoto)

Kyoto University

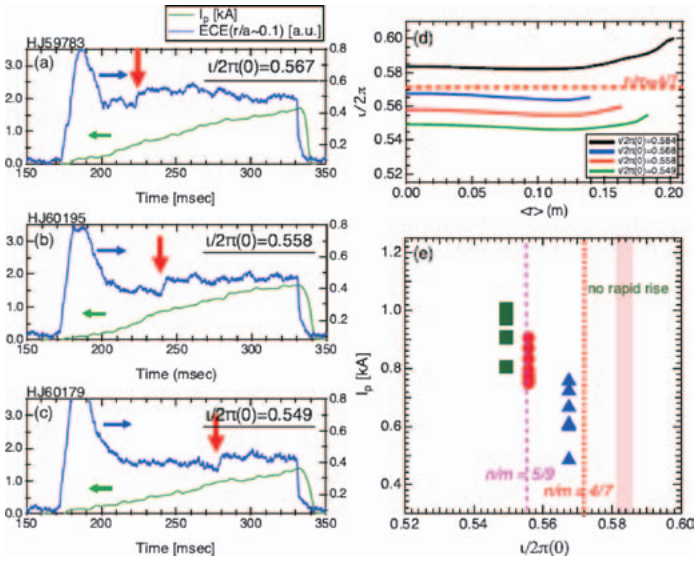

Fig. 1 ECE signals and plasma currents for different rotational transform profiles: (a) $\iota/2\pi(0)0=.549$, (b) $\iota/2\pi(0)0=.558$, and (c) $\iota/2\pi(0)0=.567$. (d) Vacuum rotational trans-form profiles and (e) current at the start of the expansion of eITB as a function of $\iota/2\pi(0)$ for the vacuum magnetic field.

Highlight

Reformation of the electron internal transport barrier (eITB) with the appearance of a magnetic island:

When realizing future fusion reactors, their stationary burning state must be maintained and the heat flux to the divertor must be reduced. These essentially require stationary internal transport barrier (ITB) plasma with a fast control system. However, the time scale for determining the position of the foot point of an ITB is not clearly understood even though its understanding is indispensable for fast profile control. To clarify the role of the rational surface and/or magnetic island in the structural formation, the eITB formations for other magnetic configurations with rotational transform values of $\iota/2\pi(0)$ = 0.549, 0.558, 0.567, and 0.584 were investigated. The profiles of the rotational trans-form are shown in Fig. 1 (d). In addition, the plasma with eITB was produced by a centrally focused 70 GHz ECH (P_{inj} ~ 270 W). Figure 1 (a–c) show the ECE signals and plasma currents for the different rotational transform profiles. The structural formation was delayed with the decrease in the rotational transform values. In contrast, no structure was formed for the magnetic configuration of $\iota/2\pi(0)$ = 0.584. Figure 1 (e) shows the current at the start of the expansion as a function of $\iota/2\pi(0)$ of the vacuum magnetic field. The required plasma current to the expansion decreased with the decrease in the rotational transform values except the rotational profile at $\iota/2\pi(0)$ = 0.584. The n/m = 4/7 rational surface is important because it is a candidate in which the magnetic island is produced owing to the n = 4 toroidal periodicity of the vacuum magnetic field of Heliotron J. The n/m = 4/7 is larger at $\iota/2\pi(0)$ = 0.567 and smaller at $\iota/2\pi(0)$ = 0.584. As the bootstrap current is driven in the direction of the rotational-transform increase, the 4/7th rational surface cannot be produced at $\iota/2\pi(0)$ = 0.584. Consequently, the small differences between the 4/7th rational surface and rotational transform values reduce the required plasma current for a structure formation, except at $\iota/2\pi(0)$ = 0.584. Although there exist other low-order rational surfaces (e.g., n/m = 5/9 ~ 0.556), at which the possibility of the formation of a magnetic island is low, around the n/m = 4/7 rational surface, the structural formation is only related to that particular rational surface. This result strongly suggests that the movement of the eITB foot point is affected by the existence of a magnetic island instead of a rational surface.

Research Topics from Bilateral Collaboration Program in Heliotron J

The common objectives of the researches in Heliotron J under this Bilateral Collaboration Program are to investigate experimentally/theoretically the transport and stability of fusion plasma in advanced helical-field, and to improve the plasma performance through advanced helical-field control. Picked up in FY2019 are the following seven key topics; (1) studies of plasma confinement improvement and related plasma self-organization through advanced helical magnetic field control, (2) study of plasma profile, plasma flow, and plasma current control for the confinement improvement, (3) study of fluctuation-structure formation and its control in plasma core region and peripheral region, (4) investigation of MHD instabilities of energetic particle modes and their control, (5) extension of high-density operation region, (6) optimization of particle supply and heating scenario, and (7) empirical research of new experimental methods and analysis methods.

Radial electric field during the formation of the electron internal transport barrier (eITB):
Radial electric field in plasmas of helical plasma confinement devices significantly contributes to the neo-classical transport. It is estimated using plasma flow velocity from the charge-exchange recombination spectroscopy (CX-RS) for Heliotron J plasmas. The radial electric field is investigated in NBI and/or ECH plasmas during eITB appearance. In an NBI plasma, negative radial electric field that means "ion root" is observed in whole plasma radial position. This electric field is almost explained by the neoclassical theory. Superimposing ECH in an NBI plasma, the electron temperature is increased and the density in the core region is decreased, then, the eITB appears in the core region. In this region, the radial electric field becomes positive, "electron root" in this region. In the region of the normalized radius larger than 0.4, the electric field is negative as the NBI case. The radial electric field in the core region changes from negative (ion root) to positive (electron root) during the formation of eITB. There are two solutions of radial electric field from 0.4 to 0.7 in normalized radius from the ambipolar condition of neoclassical theory, one is positive and the other is negative. The electric field beyond 0.4 in normalized radius is supposed to be ion root among two solutions.

Bumpiness dependence of electron confinement, and temperature and density distributions:
Magnetic field ripple in the toroidal direction (bumpiness) in Heliotron J magnetic configuration is one of key parameters to control neoclassical particle transport and high energy particle confinement. The global plasma confinement has been studied for ECH and/or NBI heating plasmas and its bumpiness dependence was clarified. For the next step, the electron temperature and density distributions, and kinetic stored energy are measured by using a Thomson scattering measurement system to investigate electron confinement properties in ECH plasmas under the condition of 270 kW in injection power. The line-averaged electron density is in the range from 0.5 to 1.5×10^{19} m^{-3}. The high and the medium bumpiness configurations are almost the same for the stored energy, while the stored energy is low in the low bumpiness configuration. The central electron temperature is also low in the low bumpiness case. The higher bumpiness case than already investigated cases, the stored energy becomes lower than that in the low bumpiness case. The anomalous transport is planned to study, since it is significant in the peripheral region in the plasma.

Proceeding research has been achieved with collaborative researchers under Bilateral Collaboration Program in Heliotron J project. The field configuration research including bumpiness dependence is advanced, and the fast local-fluctuation measurement is prepared by improvement of BES sensitivity. The 0.7-mmϕ pellet injector has been installed for the high-density operation. A laser blow-off system for the impurity transport measurement, and a multi-path Thomson scattering system for the high reliability measurement will be available soon. Making effort to extend the plasma operation region, comprehend plasma self-organization and control instabilities according to the confinement field optimization, we seek the way to the high-beta plasma research.

(K. Nagasaki)

Osaka University

Fast Ignition of Super High-Dense Plasmas

Laser-driven inertial confinement fusion by the Fast Ignition (FI) scheme has been intensively studied as the FIREX-1 project at the Institute of Laser Engineering, Osaka University. The researches consist of target fabrication, laser development, fundamental and integrated implosion experiments, simulation technology and reactor target design, and reactor technology development. In FY2019, the following progress was made through Bilateral Collaboration Research Program with NIFS and other collaborators from universities and institutes (NIFS12KUGK057 as the base project).

Fundamental and Integrated Plasma Experiments

The energy distribution of laser-accelerated electrons is one of the most important factors to determine plasma heating efficiency. We investigated experimentally and numerically the dependence of their energy distribution on the pulse duration. In the conventional model, their mean kinetic energy depends on the ponderomotive force of the incident laser light, namely $I_L\lambda_L^2$, here I_L and λ_L are laser intensity and wavelength, respectively. However, this understanding is not adaptable in the case in which the pulse duration exceeds 1 ps. Giant electric and magnetic fields grow very rapidly in the laser-plasma interaction zone after a few ps. The electrons are trapped in the zone, and experience acceleration by laser light multiple times. This is the loop-injected-direct-acceleration (LIDA) mechanism. We are now investigating how the pulse duration affects the plasma heating efficiency.

Target Fabrication

We fabricated disk-shaped resorcinol-formaldehyde (RF) target for laser plasma experiments. To make disk-shaped and polymerized targets at room temperature, a thin film holder was filled with deuterated resorcinol, formaldehyde, and heavy water. After polymerization, the heavy water was replaced with acetone, and the target was dried using the supercritical drying method. The fabricated target has a thickness of 100 μm and a density of ~ 100 mg/cm^3.

Theory and Simulation

The petapascal pressure achieved in the FIREX experiment was confirmed by two-dimensional particle-in-cell (2D PICLS) simulations. Figure 1 (a) shows the time evolution of the heated region indicated with contour lines of 1 keV from the heating laser peak time (t = 0) for the cases with the density profile at the maximum compression timing (t_{exp} = 0.72 ns). The heating laser is irradiated from the right side through the cone and it heats directly the front edge of the dense plasma core owing to the high contrast laser light. The electron temperature evolves temporally via the thermal heat transport to the core by diffusive heating. The heat wave propagates with velocity > 10 μm/ps even after the heating laser irradiation terminated, and then the core region (X < 40 μm) is heated over 1 keV electron temperature at t = 4.8 ps. Figure 1 (b) shows the two-dimensional pressure distribution at t = 4.8 ps. The pressure of the core region (X < 40 μm) starts from 2 PPa at the front edge to 0.5 PPa at the other side (X ≃ –10 μm). Figure 1 (c) shows the bulk electron temperature on the density distribution of the doped copper having the charge states $Z \geq 27$. The doped copper densities with $Z \geq 27$ indicate the position where Cu-He$_\alpha$ photons are coming from. We see that the doped copper ions inside the core region get $Z \geq 27$, namely, the large amount of He emissions are coming from the core. The core region at the maximum compression is heated to 1–2 keV, which is consistent with the experimental observation. The electron phase plots of the longitudinal momentum are shown in Figs. 1 (d) and 1 (e). The diffusive feature is seen from the heating surface (X ~ 70 μm). This PIC simulation reveals that diffusive heating is the heating process which can locally heat up the front region to the core region over petapascal pressure.

Improvement of GXII and LFEX laser system

Temporal waveform shaping has been demonstrated in both GXII and LFEX laser systems. Temporally multi-stepped implosion laser pulses are effective for compressing plasma target. In the GXII laser system, three-

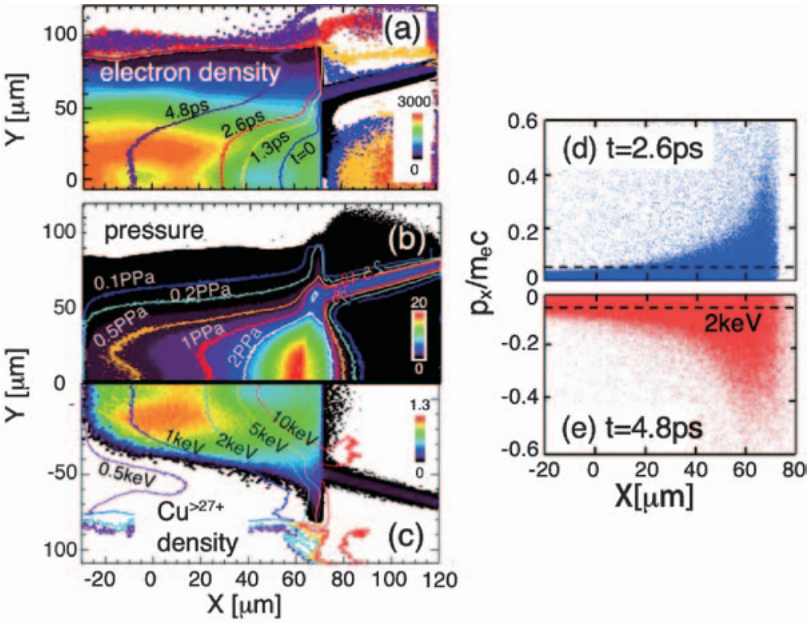

Fig. 1 PIC simulation at the maximum compression (t_{exp} = 0.72 ns): (a) The propagation of heat wave indicated by 1 keV contour lines on the electron density [n_c]. (b) Pressure distributions with the contour lines (petapascal). (c) Electron temperature distribution on the doped copper density [n_c] with charge state $Z \geq 27$, which indicates the position where the He_α emissions come from. The contours are plotted at t = 4.8 ps after the heating laser peak time. (c), (d) The electron phase plots, X – p_x/m_ec, at 2.6 ps (d) and 4.8 ps (e) from the peak time of LFEX. The phase plot is vertically symmetric, so that only the upper and lower halves are shown due to the space limitation.

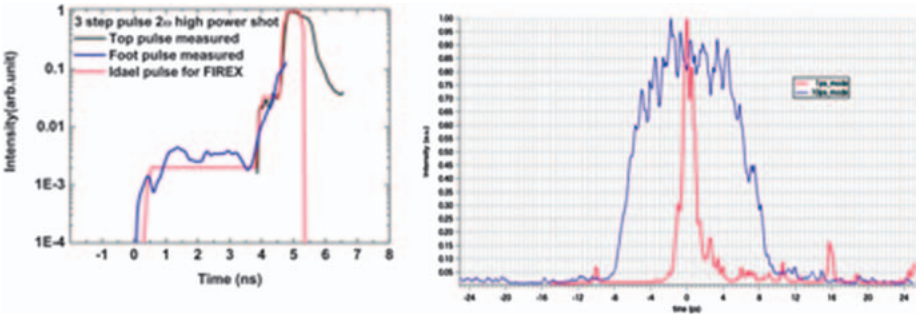

Fig. 2 The obtained three-stepped pulse shaping in GXII laser system (left), and flattop pulse demonstration after the pulse stretcher of the LFEX laser (right).

stepped pulse shaping of the amplified pulse has been demonstrated by adding a fiber wave-shaper after the fiber oscillator, as shown in Fig. 2 (left). The shaping is controllable with programming of the software to generate an arbitrary waveform.

On the other hand, a longer pulse duration than 1 ps which is still in use has been required for heating a high-density plasma. A 10-ps flattop pulse can be generated by putting a spectral phase modulator into the pulse stretcher, as shown in Fig. 2 (right).

Individual Collaborations

In parallel to the main base project, 16 other collaborations by individual researchers including two from abroad as described below have been performed. Those collaborations were on electron-driven fast ignition (7 collaborations), ion-driven fast ignition (1), alternative scheme of laser-driven inertial fusion (3), diagnostics of high-temperature and high-density plasmas (4), and reactor technology (1). 12 were projects continued from the previous year(s) and 4 were newly accepted in FY2018.

(R. Kodama, H. Shiraga, S. Fujioka, K. Yamanoi, Y. Sentoku and J. Kawanaka)

Kyushu University

Research activities on QUEST in FY2019

We will summarize the activities of the Advanced Fusion Research Center, Research Institute for Applied Mechanics in Kyushu University during April 2019 – March 2020. The QUEST experiments were executed during 9th April – 27th Sep. (2019 Spring/Summer; shot no. 38975–41263) and 8th Oct. – 14th Feb. (2019 Autumn/Winter; shot no. 41264–42538). Main topics of the QUEST experiments in FY2019 are listed below.

1) The highest plasma current discharge of more than 100kA in non-inductive current drive adding a bit of ohmic heating was obtained by 28 GHz microwave injection which was developed with Tsukuba University (Gyrotron) and NIFS (polarizer) (shot no. 40527). The control of refractive index parallel to the magnetic field, N// could give us the controllability of electron temperature up to 500 eV at N//~0. Superimposed Ohmic heating provided an 800 eV in electron temperature.
2) The water-cooling of the hot wall during plasma discharges were successfully executed and the plasma duration was extended. The sequence of plasma termination was the same in both with and without water cooling of the hot wall. The value of H^+ was gradually increasing around the mid-plane area where no hot wall was equipped, and then a bright area around the center stack in the ion drift direction was developed just before the plasma termination. This indicated that the unknown outgassing due to active recycling was made in the mid-plane area. It was found that the key issue to extending plasma duration is to reduce the unknown outgassing in the mid-plane area.
3) Experiments were conducted with 8.3 GHz RF heating for 600 sec pulse, where permeation probe data were obtained. Analysis of diffusion transport in the PdCu film shows that atomic flux of order of 10^15 atoms/m^2/s reaches the first wall during the discharge. Dynamics of the atomic flux with a time scale of ~ 100 sec is observed.
4) In order to increase ohmic plasma current upto two times, double swing of center solenoid current must be enabled. To alternate two mono-polar positive and negative thyristor power supplies, IGBT switches were installed. Analyzing the low-speed interlock sequence, high-speed interlock circuit was designed and installed. Due to the current monitor error, however, IGBT's were injured. Such an error will be taken into account in the interlock system.
5) The system of QUEST is networked and implemented as software to reduce the burden of human work. Examples are systems for monitoring the cooling water of the PF coil using a clamp-on type ultrasonic flow meter and for monitoring the coil temperature directly using a 3-wire Pt100, etc. These are composed of software and can be operated flexibly according to experiments, and information is transmitted to a distant central control system via a network.
6) Temperature dependence of retention of tritium ions (EDT+=0.5 keV) impinged into tungsten at higher temperatures has been examined, and an interesting tendency of tritium retention was observed and the minimum was 523 K. It was suggested from the present examinations that change in the tritium retention strongly depends on release rate of tritium molecules from the surface in comparison with diffusion rate into the bulk.
7) Asymmetric deposition/erosion has been observed on the first wall in QUEST. To understand the mechanism of the asymmetry formation, Mach probes which can measure a plasma flow are planned to be installed at the top and the bottom of an outer port. Directional material probes on which a direction of a deposition layer formation can be observed are also planned to be installed near Mach probes. They will be installed in experiments in 2020.
8) Divertor biasing using several electrodes arranged toroidally every 90 degrees was attempted for divertor heat load control. It showed noticeable expansion of particle flux to the upper divertor plate. The method also produced several SOL-current filaments, which can generate resonant magnetic perturbations (RMPs) for edge plasma control.

9) Electron Bernstein wave (EBW) heating/current drive is one of the key issues to attain a steady state tokamak configuration in the QUEST. The collective scattering system utilizing the 400 GHz gyrotron and quasi-optical system including transmission, antenna, and reflector gratings are under detailed design to detect EBW in the core of the QUEST. The 400 GHz gyrotron developed in the Univ. of Fukui was transferred to be installed on the QUEST during FY2019.
10) For vertical plasma position control to extend the operation regime, simultaneous equation with 6x6 consisting of four vacuum chamber currents, one pair of the horizontal coil, and the plasma current are solved with PD control prior to dividing into the many vacuum chamber currents. As the mass-less approximation behaves opposite, we have used the equation with the plasma mass.
11) Correlation between surface chemical state and hydrogen isotope retention for tungsten exposed to hydrogen plasma in 2019S/S and A/W campaign was studied by XPS and TDS. Additional D implantation was performed these samples to reveal the D trapping efficiency after hydrogen plasma exposure. In the present campaigns, the damage was not accumulated, which also reflects the lower D retention, suggesting that a stable plasma would reduce the plasma wall interaction.
12) We investigated the possibility of PFC surface thermometry using the rotational-temperature of H2 d-state, which was previously reported in TEXTOR and PICES. The temperature obtained on an edge viewing chord was approximately 500 K and close to the surface temperature of 473 K. We plan to study the effects of collisional processes and surface reactions on the obtained temperature.
13) To locate the fundamental resonance layer of 28 GHz electron cyclotron frequency in the QUEST vacuum vessel, twice the strength of toroidal field is requested, where the total current in the central stack is 1.6 MA. The use of high temperature super conducting wire made of REBCO material is proposed for the development of a new toroidal coil.
14) It is expected that the combination of current ramping up by CS and current sustainment by RF current drive is effective for stable divertor configurations. In order to verify the operation scenario, numerical simulations of QUEST plasma with coils and vacuum vessel were introduced.
15) The driving mechanism of the toroidal flow by ECH is investigated, assuming an essential role of $J \times B$ torque due to the radial diffusion of ECH supra-thermal electrons. The 3D magnetic ripples and the large orbit size of supra-thermal electrons enhance the radial diffusion in QUEST. The GNET code is prepared to evaluate the supra-thermal electron behaviors and radial current in the QUEST plasma.
16) A novel fast–electron measurement instrument has been designed to investigate a fast–electron dynamics and its role in a non–inductive ST plasma startup with ECH/CD on QUEST. Asynchronous counting of two thin scintillators mounted in a box with an appropriate hole gives a pure fast–electron energy distribution while eliminating the effects of X-rays.
17) Hydrogen retention processes occurring on the plasma-facing walls in QUEST and in-vessel material migration were investigated using a technique of a transmission electron microscopy and elastic recoil detection analysis. It was found that hydrogen would be trapped by the carbon-dominated mixed-material layer.

Kazuaki Hanada (Kyushu University) 1), 2)
Masahiro Kobayashi (NIFS) 3)
Kazuo Nakamura (Kyushu University) 4)
Makoto Hasegawa (Kyushu University) 5)
Masao Matsuyama (University of Toyama) 6)
Suguru Masuzaki (NIFS) 7)
Kazuo Toi (NIFS) 8)
Shin Kubo (NIFS) 9)
Osamu Mitarai (Institute for Advanced Fusion and Physics Education) 10)
Yasuhisa Oya (Shizuoka University) 11)
Taiichi Shikama (Kyoto University) 12)
Takumi Onchi (Kyushu University) 13)
Hiroaki Tsutsui (Tokyo Institute of Technology) 14)
Sadayoshi Murakami (Kyoto University) 15)
Ryuya Ikezoe (Kyushu University) 16)
Miyuki Yajima (NIFS) 17)

(K. Hanada)

University of Toyama

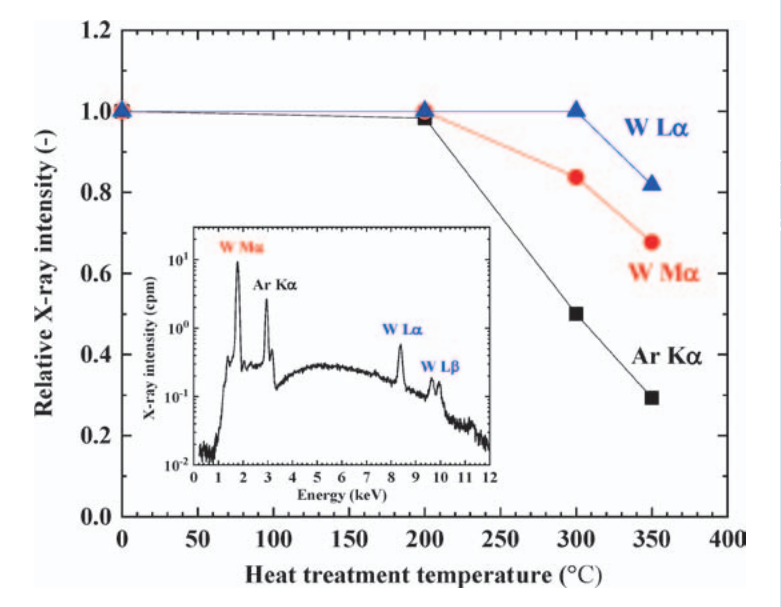

β-ray induced X-ray spectrum from tritium-charged Fe-ion irradiated W and change in intensity of characteristic X-rays by heat treatment

Highlight

Research Activities in Hydrogen Isotope Research Center, Organization for Promotion of Research, University of Toyama

Development of tritium (T) removal technique from plasma-facing materials (PFMs) used in a fusion reactor is important for safe and cost-effective disposal. Lattice defects induced by neutron irradiation in tungsten (W) act as traps against hydrogen isotopes. In this study, T release from a W sample irradiated with heavy ions and the non-irradiated sample were examined at 200–350 °C to evaluate the effects of irradiation defects on T removal. A plate of W irradiated with 6.4 MeV Fe ions to 0.5 displacement per atom was exposed to a mixture gas of deuterium (D) and T at 500 °C together with the non-irradiated sample. Then, the sample was heated one by one under Ar gas flow sequentially to 200, 300 and 350 °C. T retention in the irradiated sample was clearly higher than that in the non-irradiated sample due to trapping effects by radiation-induced defects. The heat treatment at 200–300 °C resulted in T release solely from non-irradiated sample and non-damaged zone of the irradiated sample. Clear T release from the damaged zone started at 350 °C and the rate of release was controlled by diffusion of T in the damaged zone. The majority of T was released as HTO.

[*Isotope effects on trapping and release of hydrogen isotopes in fusion reactor materials (Y. Hatano, U. Toyama)*]

Hydrogen isotope transport through plasma modified fusion reactor materials: Experiments were performed to study the effect of rhenium (Re) addition on hydrogen isotope transport and trapping in undamaged tungsten (W). In comparison to pure-W, W-Re alloy (3 wt.%) was observed to trap lower and higher amounts of T at 473 K and 673 K, respectively. The retention behavior was similar at 573 K. Self-consistent modeling of the TDS profiles constrained by the T depth profiles qualitatively indicates such temperature dependency is due to higher trapping energies (<0.5 eV) in W-Re. (H. T. Lee, Osaka U.)

High temperature and high flux irradiation effect on hydrogen isotope retention in damaged W: The effect of high temperature and high flux irradiation on the hydrogen isotope retention behavior in damaged tungsten was studied. It was found that the types of irradiation damage were not changed, but the amount of damages were reduced due to annealing at high temperature. In addition, the D retention behavior was affected by formation of blisters on the surface caused by high temperature and high flux plasma. (Y. Oya, Shizuoka U.)

Hydrogen isotope exchange in tungsten with irradiation damage: Successive exposure to tritium gas and deuterium gas was performed at elevated temperatures for W samples with irradiation defects created by helium (He) ion irradiation to investigate the effects of hydrogen isotope exchange on T removal. It was found that the heat treatment in deuterium gas was more effective for removal of T retained in a deep region of sample compared to the case of heating in a vacuum. (Y. Nobuta, Hokkaido U.)

Hydrogen isotope exchange on metaric plasma facing walls: Specimens for hydrogen isotopic exchanges by glow discharge cleanings on stainless steel were produced. Based on previous experiments in Univ. of Toyama, tungsten, which is a candidate material for the DEMO reactor, has a low sputtering rate by deuterium, and then it was not useful for the laboratory experiment due to limited experimental time. Remaining tritium on surfaces of stainless steel measured by ITP shows lower amounts to compare with that on tungsten, and it is also a preferable sample condition. Using the stainless steel, an evaluation of experimental conditions will be obtained.
(N. Ashikawa, NIFS)

Tritium retention on facing materials modified by plasma wall interactions: ITER specification W (SR-W) and its recrystallized W (RC-W) were irradiated by high energy electron beam. Before and after that, positron annihilation experiment and EBSD (Electron Back Scatter Diffraction Patterns) analyses were carried out to identify the radiation defect. Tritium exposure experiments on the specimens have been carried out using the tritium (T) exposure device. (K. Tokunaga, Kyushu U.)

Impact of bulk helium retention and damages introduction on hydrogen isotope retention behavior in tungsten: Effects of high energy He irradiation and damage introduction at high temperatures on hydrogen isotope retention in W were investigated. The results showed that weak trapping sites such as vacancies with higher concentration were produced during single energetic He^+ irradiation events. Fe^{3+}-He^+ simultaneous irradiation promoted the formation of He_xV_y complexes, which reduced the concentration of vacancy trapping sites. (F. Sun, Shizuoka U.)

The production of high purity deuterium-tritium water for laser fusion fuel: At Institute of Laser Engineering Osaka University (ILE-Osaka) a tritium-water doped target for inertial confinement fusion (ICF) has been developed. H_2O water (which is mimic of T_2O water) doping to a D_2O-filled with a real-size ICF target was firstly succeeded by using a testing system which was developed in this study. (Y. Arikawa, Osaka U.)

Gamma-ray irradiation effect on hydrogen isotopes at fusion material surfaces: The D retention in yttrium oxide, silicon carbide, and zirconium oxide coatings decreased after γ-ray irradiation in the dose rate of 2.43 Gy/s, while no clear change in the retention was observed at the lower dose rate. From these results, the γ-ray irradiation effect on deuterium retention would have a threshold dose rate. (T. Chikada, Shizuoka U.)

Evaluation of hydrogen isotope retention and release of SiC and SiC/SiC composite: The NITE SiC/SiC composites consist of β-SiC matrix and β-SiC fibers and carbon matrix/fiber interface. Basic inventory and release behaviors of hydrogen isotopes in SiC, and the effects of fibers and carbon interface in the SiC/SiC composites need to be revealed for the design of fusion components. In this research, α-SiC, β-SiC and NITE SiC/SiC composite plates were prepared. Observation of their surfaces by a scanning-electron microscope was followed by irradiation of 3 keV DT^+ ions at room temperature. T desorption tests will be performed.
(H. Kishimoto, Muroran Inst. Technol.)

Development of methodology and quantitative measurement on double-strand breaks of genome-sized DNA caused by beta-ray: We have developed an appreciation tool to detect an outline of giant DNA molecules in an aqueous solution and count number of double-strand breaks in real-time observation, adopting a canny method of Open CV. The tool has succeeded in detecting outline of DNA in a movie of DNA under Brownian motion. Based on the tool, we will establish a methodology of real-time observation on double-strand breaks of DNA in a quantitative manner. (T. Kenmotsu, Doshisha U.)

8. Activities of Rokkasho Research Center

At Rokkasho village in Aomori Prefecture, the International Fusion Energy Research Centre (IFERC) project and the International Fusion Materials Irradiation Facility/Engineering Validation and Engineering Design Activities (IFMIF/EVEDA) project have been conducted under the Broader Approach (BA) agreement between the EU and Japan from June 2007, in order to complement ITER and to contribute to an early realization of the DEMO reactor. The roles of the NIFS Rokkasho Research Center (RCE) established in May 2007 are to assist NIFS and universities to cooperate with those activities, and to prepare the environment for promoting various collaborative research including technology between activities at Rokkasho and at universities. As cooperation activities, the head of the NIFS RCE is undertaking tasks as the IFERC Project Leader (PL) from September 2010. Also, the head of the NIFS RCE is working as the leader of the general coordination group of the Joint Special Team for a Demonstration Fusion Reactor (DEMO) design, which is the organization set in May 2015 for establishing technological bases required for the development of DEMO as an all-Japan collaboration.

The activities of IFERC project in 2019 JFY were devoted to completing the planned activities and the EU/JA contributions to IFERC project in BA Phase I. Hereafter, the outline is described very briefly:

The joint activities of DEMO Design Activity (DDA) began in 2010. The DDA in 2019 FY concentrated on compiling the Final Report of DDA, and on the design activities in order to complete the Final Report. The Final Report describing common conclusions and different approaches on design options for key design issues was issued in February 2020 as a comprehensive summary of DDA in BA Phase I. Integrating critical requirements into reduced systems codes has led to a similarity in the design configurations identified by EU and JA. These activities are also presented in the IAEA Fusion Energy Conferences (IAEA FEC) and other international conferences such as Symposium on Fusion Technology (SOFT) and International Symposium on Fusion Nuclear Technology (ISFNT), and more than 550 peer reviewed papers are published in the major academic journals in this field such as “Fusion Engineering and Design” and “Nuclear Fusion”.

The results of the original DEMO R&D Activity composed of 5 generic task areas were reported in the Final Report of DEMO R&D Activity in December 2017. In the extension phase from June 2017 to March 2020, some activities such as Materials Properties Handbook of the structural materials of blanket and database of the functional materials of blanket were conducted with DDA, and their activities are reported in the Final Report of DDA. In parallel, the JET-ILW tile and dust analysis was conducted from 2014 to 2019, and the results were summarized in the Final Report of JET tile and dust analysis issued in December 2019. Besides implementing DEMO R&D activity, the peer review was held in 2012 and 2018 in order to assess the activity and accelerate the communication with DDA. These DEMO R&D activities are presented in IAEA FEC, SOFT and ISFNT as well as DDA, and more than 300 peer reviewed papers are published in the major academic journals in this field such as “Fusion Engineering and Design”, “Journal of Nuclear Materials” and “Nuclear Materials and Energy”.

After successfully implementing the operation of Helios supercomputer from 2012 to 2016 with a very high availability and a very high usage rate, which was reported in the Final Report of CSC issued in October 2017, IFERC HPC follow-up Working Group continues the activity in view of the CSC activity in BA Phase II. Based on the very recent re-investigation to PIs of Helios users, more than 640 peer reviewed papers are published in the academic journals of plasma and fusion research including reactor materials and technology such as “Physics of Plasmas”, “Nuclear Fusion”, “Plasma Physics and Controlled Fusion” and “Fusion Engineering and Design”. Also, about 20 papers are published in the journals with high impact factor such as “Physical Review Letters”, “Nature Communications” and “Physics Reports (Review Section of Physics Letters)”.

REC activity was implemented based on the Overall plan of REC created in October 2012 and approved by BA SC in November 2012. The overall activity is summarized in the Final Report of REC issued in December 2019, where the preparation, execution, and discussions and summary of Remote Participation with WEST experiment, which was successfully implemented in November 2018 with public visitors/audiences, are included as one of the significant results of REC activity. Also, REC activities are presented in the IAEA FEC, and 8 peer reviewed papers are published in the fusion related academic journals such as “Fusion Engineering and Design”.

As described above, all the planned activities of IFERC project and all the contributions by both EU and JA have been completely accomplished within BA Phase I from June 2007 to March 2020 (the almost final situation was reported in the symposium of the 36th Annual Meeting of the JSPF in November 2019), which leads to IFERC project in BA Phase II from April 2020 to March 2025.

The head of NIFS RCE is also undertaking the role of the leader of the general coordination group of the Joint Special Team for a DEMO design. Since the collaboration among many researchers from NIFS and other institutions and technicians from companies is indispensable for the conceptual design of DEMO reactor, the head of the NIFS RCE tries to work as a coordinator.

In summary, the NIFS RCE contributes widely not only to the success of ITER but also to the realization of fusion energy through the continuous efforts mentioned above.

Cover page of the presentation in the symposium of the 36th Annual Meeting of JSPF

(N. Nakajima)

Cover page of the presentation in the symposium of the 36th Annual Meeting of JSPF

9. Research Enhancement Strategy Office

The Research Enhancement Strategy Office (RESO) was founded in October 2013, and three University Research Administrators (URAs) were assigned. Under the Research Planning Task Group, the following four Task Groups were organized.

(1) IR(Institutional Research)/Evaluation Task Group
(2) Public Relations Enhancement Task Group
(3) Collaboration Research Enhancement Task Group
(4) Young Researchers Development Task Group

(1) The collaborative research activities

1) Enhancing international collaborative research in the stellarator-heliotron (S-H) plasma, and steady-state operation (SSO) toward a fusion reactor

Wendelstein 7-X (W7-X) of the Max Planck Institute of Plasma Physics (IPP) at Greifswald in Germany was upgrading for the water-cooled divertor from November 2018. In 2019, several scientists of NIFS visited IPP in order to install diagnostics devices and other instruments, such as the Charge Exchange Recombination Spectroscopy (CXRS) and the fast ion detectors. Especially, a joint research between NIFS and IPP was conducted intensively for the investigation of the re-deposition layer on the fast wall of W7-X.

Collaborative research was also enhanced with PPPL and the University of Wisconsin in the United States, CIEMAT in Spain, CEA in France, CONSORZIO RFX in Italy, Culham Centre in the United Kingdom, and Peking University and Southwest Jiaotong University (SWJTU) in China. New collaboration agreement with the University of Belgrade was signed in November 2019. First workshop on the plasma physics is planned at Belgrade in 2020.

2) International research network for integrated plasma physics

In addition to the individual MoUs with Princeton University and three Max-Planck institutes (IPP, MPA and MPS), a new MoU for starting the International Research Collaboration Center for Astro-fusion Plasma Physics (IRCC-AFP) in NINS was signed.

3) Promoting establishment of Agreements with Asian institutes to accelerate collaborative research

In order to enhance helical and stellarator research in Asian countries, the Chinese First Quasi-axisymmetric Stellarator (CFQS) project between NIFS and SWJTU and an international research collaboration between NIFS and Peking University has been promoted. In the CFQS project, test fabrication of the modular coil was successfully conducted. Substantial construction of the CFQS device will start soon. As the collaboration between NIFS and Peking University, Design of the Time-of-Flight neutron spectrometer (TOFED) is completed for LHD. The construction of TOFED is initiated in 2019.

(2) Supporting young researchers

In the activities for supporting young researchers, international collaboration activities of young researchers were encouraged, enhancing their basic research skills. RESO supported the international collaboration plans proposed by young researchers in NIFS. Applications were reviewed by the Young Researchers Development Task Group. One program was supported in FY2019 as follows.

1. Experimental study of the dynamical responses of the detached plasmas with abrupt impulses of ELM type heat pulses.

In addition, RESO supported the basic research plans of young scientists for the purpose of enhancing their fundamental scientific skills. Two programs were supported in FY2019 as follows.

1. Development of the direct construction of the heat deposition profile of ECH using optical vortex measurement.

2. Study of the heat transportation through micro channel using microscope under the ultra low temperature condition.

RESO also assisted with the applications of young scientists to the 'Grants-in-aid Scientific Research' program. About 70 application documents were reviewed and suggestions were given to the authors for improvement.

(3) Enhancing public relations

1) Dissemination of research achievements through EurekAlert!

Four topics were released: i) "Fusion scientists have developed *the nano-scale sculpture technique*: ~ This enables observation inside hard materials with an atomic-scale ~," ii) "Demonstration of alpha particle confinement capability in helical fusion plasmas," iii) "Simulations demonstrate ion heating by plasma oscillations for fusion energy," and iv) "Isotope movement holds the key to the power of fusion reactions". These topics were released to the media in Japan, too. Some topics attracted attention from the international media.

2) Information release about NIFS and fusion science

RESO participated in the AAAS annual meeting and introduced NIFS and our research results to meeting participants in collaboration with other Japanese institutes, 13-16 February 2020.

3) Outreach activities based on the fusion community

One of the outreach activities is to join the organization of the ITER/BA Projects annual report meeting. RESO exhibited panels showing NIFS research activities at the meeting. RESO also joined the discussion of the fusion science outreach headquarters and contributed to the start-up of the web page of nuclear fusion by the Ministry of Education, Culture, Sports, Science and Technology.

4) Others

RESO introduced interesting science topics to the public on the occasion of the science café at the Open Campus of NIFS shown in the Figure 1.

(4) IR/Evaluation activities

The task group for the IR (Institutional Research) and evaluation continued its role to make systematic analyses of the present research activities of the institute. The statistical data of the publications and the scientific reports were collected using the NIFS article information system (NAIS) with complementary data obtained through SCOPUS and WoS public research resource supplying companies. The outcome results of the collaboration activities were collected through the annual collaboration reports of NIFS. Six IR reports were submitted to the director general of NIFS describing the analyzed academic data and proposals to improve the research management of the Institute.

Fig. 1 The science café at the Open Campus of NIFS.

(T. Muroga, S. Okamura, H. Kasahara and K. Yaji)

10. The Division of Health and Safety Promotion

The Division of Health and Safety Promotion is devoted to preventing work-related accidents, to ensuring safe and sound operation of machinery and equipment, and to maintaining a safe and healthful environment for researchers, technical staff, co-researchers, and students. Each division cooperates with each other to ensure health and safety.

As a nationwide activity, we hold an information exchange meeting on health and safety each year, calling on those involved in the health and safety of university related organizations. This fiscal year's event was held on February 6-7 2020, with about 50 participants from 16 organizations.

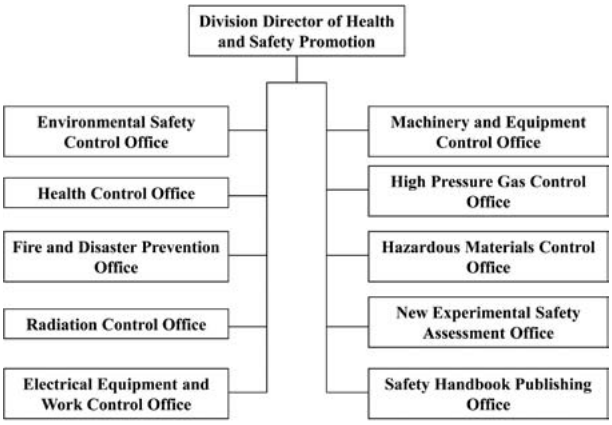

Fig. 1 Division of Health and Safety Promotion

1. Environmental Safety Control Office

This office has the responsibility to maintain a safe work space and environment. Although the other nine offices of the division of health and safety promotion cover most of the risks that exist in the institute, some problems fall wide of them. The role of this office is to cope with such problems. Therefore, this office has a broad range of tasks.

(i) Management to solve the problems pointed out by the safety and health committee.
(ii) Maintenance of the card-key system for the gateways of controlled areas.
(iii) Maintenance and management of the vehicle gate at the entrance of the experimental zone.
(iv) Maintenance of the fluorescent signs of the evacuation routes and the caution marks.

2. Health Control Office

The main role of this office is to keep the workers in the institute healthy, including co-researchers and students.

(i) Medical checkups both for general and special purposes and immunization for influenza.
(ii) Mental health care services and health consultation.
(iii) Accompany the inspections of the health administrator and the occupational physician.
(iv) Maintenance of AEDs.
(v) Alerts and response to the COVID-19.

Various lectures were held for physical and mental health. And an online stress-check was held in October.

3. Fire and Disaster Prevention Office

The main role of this office is to prevent or minimize damage caused by various disasters.

(i) Making self-defense plans for fires and disasters, and implementation of various training.
(ii) Promotion of first-aid workshops and the AED class.
(iii) Maintenance of fire-defense facilities and attending on-site inspections by a local fire department.
(iv) Review and update disaster prevention rules and disaster prevention manuals.

All workers must attend the disaster prevention training held every year.

4. Radiation Control Office

The main role of this office is to maintain radiation safety for researchers and the environment. Legal procedures for radiation safety and regular education for the radiation area workers are also important roles of this office

(i) Maintain radiation safety for the workers.
(ii) Registration and dose control of radiation area workers.
(iii) Observation of radiation in the radiation controlled area and the peripheral area.
(iv) Maintenance of the radiation monitor.
(v) Applications for radiation equipment to the national agencies and the local governments.
(vi) Revise official regulations and establish new rules.

One educational lecture was held on February 21, 2020 for the radiation area workers. The other planned lectures were changed to those using DVD viewing. Non-Japanese workers can be educated and trained in English.

5. Electrical Equipment and Work Control Office

The main role of this office is to maintain electrical safety for researchers, technical staff members and students.

(i) Check and control the electrical facilities according to the technical standards.
(ii) Safety lecture for researchers and workers.
(iii) Annual check of the electric equipment during a blackout.

The annual inspection of the academic zone was carried out on May 18, 2019, and that of the experimental zone was carried out on June 6 and June 7, 2019.

6. Machinery and Equipment Control Office

The main role of this office is to maintain the safe operation of cranes. The tasks of this office are as follows.

(i) Inspection and maintenance of cranes.
(ii) Management of the crane license holders and safety lectures for the crane users.
(iii) Schedule management of crane operations.

7. High Pressure Gas Control Office

This office has a very important role in NIFS, because the main experimental machine, LHD, is the super-conducting machine which requires cooling by liquid helium. Many other machines have cryogenic pumping systems, which also require cooling down. The tasks of this office are summarized as follows.

(i) Safety operation and maintenance of high pressure gas handling facilities in NIFS.
(ii) Daily operation, maintenance, system improvement, and safety education according to the law.
(iii) Safety lectures for researchers and workers.

8. Hazardous Materials Control Office

The main role of this office is the management of the safe treatment of hazardous materials and maintaining safety for researchers against hazardous events.

(i) Research the requests for hazardous materials and the storage status.
(ii) Management to ensure safe storage of the waste.
(iii) Monitoring of discharging water to prevent water pollution.
(iv) Implementation of chemical substance risk assessment.

9. New Experimental Safety Assessment Office

The main role of this office is to check the safety of experimental devices other than LHD. For this purpose, researchers who want to setup new experimental apparatus must apply for the safety review. Two reviewers are assigned from members of this office and other specialists. They check the safety of these devices.

(i) Examine new experiments for safety problems and advise on safety measures. (New experiments in LHD are reviewed by the LHD Experiment Group.)
(ii) Improve safety in each experiment and reinforce the safety culture at NIFS by annual reviews by NIFS employees.

10. Safety Handbook Publishing Office

The tasks of this office are publication of the Safety Handbook in Japanese and in English and to update them as necessary. The regular safety lectures were held on May 9, May 22, and May 24, 2019. All workers including the co-researchers and students must attend this safety lecture every year.

Detailed information is available on our web-site:
http://www.nifs.ac.jp/

(K. Nishimura)

11. Division of Deuterium Experiments Management

The deuterium experiment has been carried out on LHD since March 7, 2017. Objectives of the deuterium experiments are (1) to realize high-performance plasmas by confinement improvement and by the improved heating devices and other facilities, (2) to explore the isotope effect study, (3) to demonstrate the confinement capability of energetic particles (EPs) in helical system and to explore their confinement studies in toroidal plasmas, and (4) to proceed with the extended studies on Plasma-Material Interactions (PMI) with longer time scales.

The division of deuterium experiments management was founded to establish the safety management system and to consolidate experimental apparatus related to the deuterium experiments. After the start of the deuterium experiment on the LHD, the function of this division was shifted to the management of the safe and the reliable operation of the deuterium experiment. Under this division, a taskforce named 'Deuterium experiment management assistance taskforce' was established. The main jobs of the taskforce were (1) the establishment and improvement of manuals to operate LHD and peripheral devices safely during deuterium experiments, (2) check and improvement of the regulations related to proceeding with the deuterium experiments safely, (3) the upgrade of the LHD itself, its peripheral devices and the interlock systems for safe operation during the deuterium experiments, (4) upgrade and optimization of heating devices and diagnostic systems for the deuterium experiments, (5) remodeling the LHD building and related facilities, and so on. These jobs are proceeding with the cooperation with the LHD board meeting and the division of health and safety promotion. In addition, the necessary tasks related to the safety evaluation committee founded by NIFS and those related to the safety inspection committee for the National Institute for Fusion Science (NIFS) founded by local government bodies are proceeding in this division. The publication of an annual report for the radiation management of the LHD deuterium experiment is another important task of this division.

During the fiscal year of 2019, the safety evaluation committee meeting was held three times. The main topic of the committee is the evaluation of the annual report for the radiation management at the deuterium experiment and the evaluation of the safety operation of the deuterium experiment in the experiment campaign of 2019. In addition, the prospect for the next three years of the deuterium experiment was discussed.

The cooperation of the safety inspection committee for NIFS, which is organized by the local government bodies, such as Gifu-prefecture, Toki-city, Tajimi-city, and Mizunami-city, is an important task for the division of the deuterium experiments management. The environmental neutron dose monitoring at NIFS and the tritium concentration monitoring in the environmental water around NIFS has been performed by the committee since 2015. In 2019 FY, these monitoring activities were performed twice as scheduled under the cooperation with the division of the deuterium experiment management.

a)

b)

c)

d)

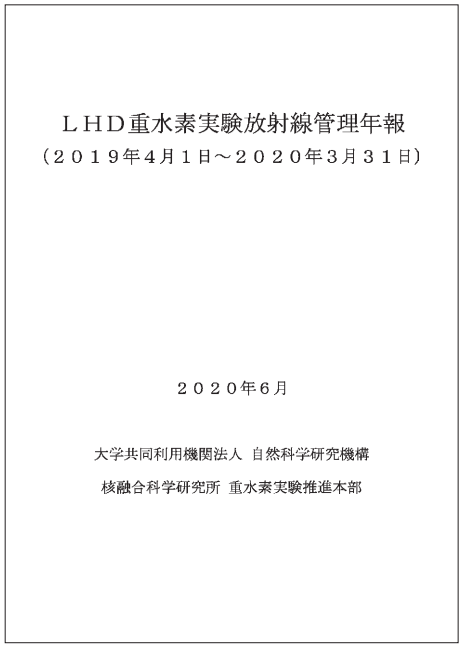

(a) The photographs at the environmental water sampling with the secretariat of the safety inspection committee. (b) The real-time radiation monitoring post where the cooperative environmental neutron monitoring is performed with the secretariat. (c) Additional neutron dosimeters placed by the secretariat of the safety inspection committee (left) and by the division of deuterium experiment management (right) near the radiation monitoring post at the cooperative environmental neutron monitoring with the secretariat. (d) The front cover of the annual report for the radiation management at the first LHD deuterium experiment (written in Japanese).

(M. Osakabe and M. Isobe)

12. Division of Information and Communication Systems

The Department of Information and Communication System (ICS) was founded in 2014 in order to develop and maintain the information and network systems of NIFS efficiently. All of the information system experts in NIFS belong to the ICS. There are five TASK groups which correspond to the job classifications in NIFS. The Network Operation task group manages and maintains the communication systems in NIFS, such as the E-mail system including security issues. The Experimental Data System task group performs operation and development of data acquisition systems for the LHD experiment. The Institutional Information Systems task group carries out the maintenance and development of the management systems for collaboration research and its output. The Atomic and Molecule Database task group maintains the atom and molecule database which is open to researchers around the world. The Integrated ID Management and Authentication System task group manages integrated ID and authentication systems.

The ICS works as follows: the request for the maintenance, improvement, and development of the information and communication system from each section is submitted to the ICS. The deputy division directors of ICS check all the requests, establish the priority among them, and assign them to the appropriate Task Group. Because all the experts belong to the Technical Service Section of ICS, each Task Group Leader asks the Section Leader to allot the required number of experts for a prescribed period of time so as to finish the job.

In NIFS, three research projects extend across the research divisions. It can be said that the ICS is another "project" which lies across all the divisions in the institute for keeping the information and communication systems stable, secure, and up-to-date.

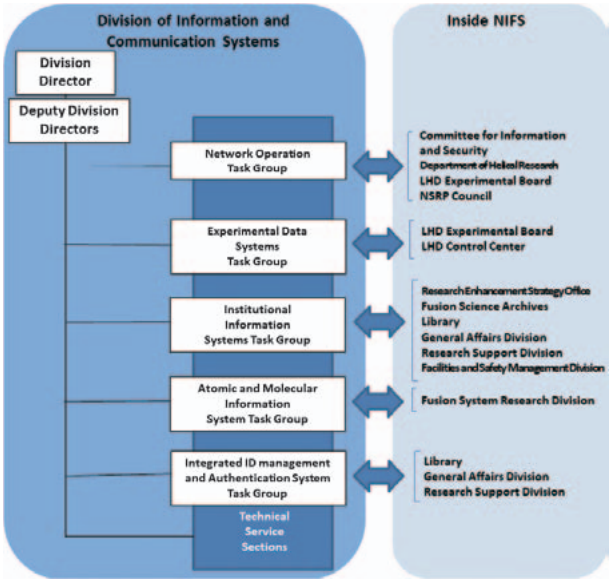

Fig. 1 Structure of Division for Information and Communication Systems.

Information Network Task Group

The information network is a foundation for research activity. The Information Network Task Group operates the advanced NIFS campus information network named "NIFS-LAN," which contributes to the development of fusion research, with strong security systems.

Notable activities in FY 2019 by the Information Network Task Group:

- The firewall system of Internet Connection Cluster has been upgraded. A throughput to the internet

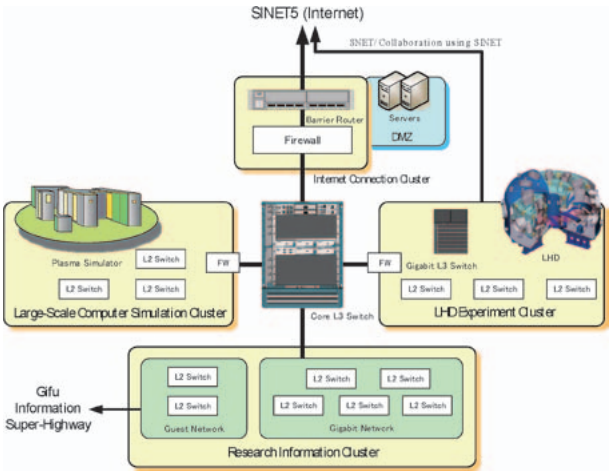

Fig. 2 Block diagram of the NIFS campus information network, which consists of three autonomous clusters that have their own purposes and usages.

has been improved by 10 GbE interfaces of the new firewall system. The interface boards of core L3 switch have also been upgraded.

- The firewall appliance of the LHD Experiment Cluster has been upgraded. Before the LHD experiment campaign, the security condition of each PC was checked in order to keep the safety network free of malware.
- Security incidents were treated with a malware detection appliance and the firewall. Lectures were held regarding the information network and its security. An informational system audit held by NINS was also accomplished.

Integrated ID Management and Authentication System Task Group

Many information technology (IT) systems require a user authentication and an authorization mechanism in order to keep their confidentiality. Because a traditional IT system has its own independent authentication mechanism, users of these systems are forced to manage many credentials such as a password for each IT system, and administrators of these systems are responsible for their ID management. Such a circumstance leads to a security risk and is a waste of human resources both for users and IT system administrators. Switching from one's own authentication mechanism to a shared authentication system is a possible solution for this issue.

The integrated ID management and authentication system task group (IDMAS-TG) investigates various technologies and protocols related to authentication and ID management to develop an integrated ID management and authentication system, which provides a shared user authentication service to IT systems in NIFS.

The IDMAS-TG has been developed and deployed for some services such as the following:

GakuNin

The GakuNin is the academic access management federation consisting of universities and academic institutes in Japan. NIFS joined the GakuNin in FY 2017. The current status of the GakuNin service in NIFS is still experimental.

Eduroam

The eduroam is a world-wide Wi-Fi roaming infrastructure. NIFS joined the eduroam in FY 2018. The Wi-Fi access points providing internet connection service for guests were gradually replaced to eduroam-ready devices in FY 2018-19. Further, the eduroam service covers each room in the accommodation facility (Helicon Club) in FY 2019.

Colid

An ID management system for collaborators of NIFS research collaboration program (Colid), which is based on SAML (security assertion markup language) under shibboleth IdP and LDAP (light-weight directory access protocol) similar to GakuNin, is utilized for information disclosure to collaborators via web sites.

(S. Ishiguro)

13. International Collaboraiton

Many research activities in NIFS are strongly linked with international collaborations with institutes and universities around the world. These collaborations are carried out in various frameworks, such as 1) coordination with foreign institutes, 2) bilateral coordination with intergovernmental agreements, and 3) multilateral coordination under the International Energy Agency (IEA).

The coordination with foreign institutes is important as a basis of collaborative research. From 1991, NIFS concluded 30 coordinations through FY2018. In FY2019, a new coordination was concluded between NIFS and Belgrade University (Serbia). In this collaboration, progress in research of plasma transport simulation and plasma-wall interactions are expected.

NIFS is the representative institute for the three bilateral coordination with intergovernmental agreements (J-US, J-Korea, and J-China), and for the four multilateral coordinations under the IEA (Plasma Wall Interactions (PWI), Stellarator-Heliotron concept, Spherical Tori, and Steady State Operation). For the three bilateral coordinations, and the multilateral coordination PWI Technology Collaboration Program (TCP), NIFS coordinates the collaborative research not only for NIFS researchers, but also for researchers in universities. The activities of the bilateral and the multilateral coordination activities are reported in the following subsections, respectively.

In 2019, the 28th International Toki Conference on Plasma and Fusion Research was held on 5 – 8 November in Toki, Japan, and NIFS hosted the meeting. More than 200 researchers from 11 countries participated.

(S. Masuzaki)

Academic Exchange Agreements

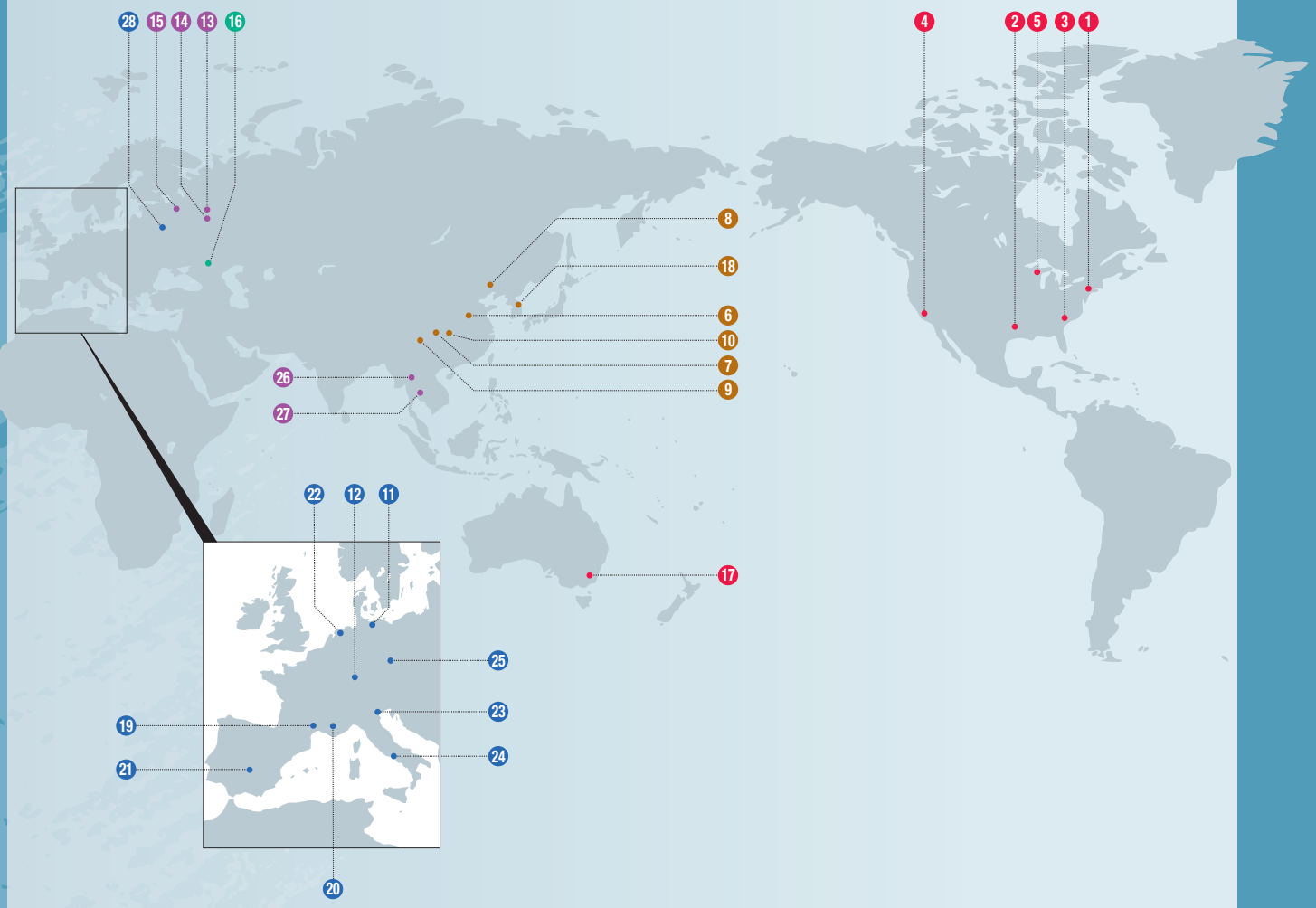

U.S.A. 1 Princeton Plasma Physics Labolatory (PPPL)
2 Institute for Studies, The University of Texas at Austin (IFS)
3 Oak Ridge National Laboratory (ORNL)
4 Center for Energy Science and Technology Advanced Research, University of California, Los Angelse (UCLA)
5 College of Engineering, University of Wisconsin, Madison

China 6 Institute of Plasma Physics, Chinese Academy of Sciences (ASIPP)
7 Southwestern Institute of Physics (SWIP)
8 Peking University
9 Southwest Jiaotong University (SWJTU)
10 Huazhong University of Science and Technology

Germany 11 Max Planck Institute for Plasma Physics (IPP)
12 Karlsruhe Institute of Technology (KIT)

Russia 13 Russian Research Center, Kurchatov Institute (KI)
14 A. M. Prokhorov General Physics Institute, Russian Academy of Sciences (GPI)
15 Peter the Great St. Petersburg Polytechnic University

Ukraine 16 National Science Center of the Ukraine Khar'kov Institute of Physics and Technology Institute of Plasma Physics (KIPT)

Australia 17 Australian National University (ANU)

South Korea 18 National Fusion Research Institute (NFRI)

France 19 Aix-Marseille University (AMU)
20 Commissariat à l'énergie atomique et aux énergies alternatives (CEA)

Spain 21 National Research Center for Energy, Environment and Technology (CIEMAT)

Netherlands 22 Dutch Institute for Fundamental Energy Reseearch (FOM)

Italy 23 CONSORZIO RFX
24 Institute of Lonized Gas (IGI)

Czech 25 HiLASE Center, Institute of Physics CAS (FZU)

Tailand 26 Chiang Mai University
27 Thailand Institute of Nuclear Technology (TINT)

Poland 28 Institute of Plasma Physics and Laser Microfusion (IPPLM)

The ITER International Fusion Energy Organization (ITER)

US – Japan (Universities) Fusion Cooperation Program

The US-Japan Joint Activity has been continued from 1977. The 40th CCFE (Coordinating Committee for Fusion Energy) meeting was held on March 6, 2020 via televideo conference system. The representatives from the MEXT, the DOE, Universities and Research Institutes from both Japan and the US participated. At the meeting, the current research status of both countries were reported together with bilateral technical highlights of the collaborations. The FY 2019 cooperative activities were reviewed, and the FY 2020 proposals were approved. It was noted that both sides have developed significant and mutually valuable collaborations involving a wide range of technical elements of nuclear fusion.

Fusion Physics Planning Committee (FPPC)

In the area of fusion physics, 4 workshops (1 from JA to US, 3 from US to JA) and 24 personnal exchanges (15 from JA to US, 9 from US to JA) were carried out. Compared to the initial plan, 2 workshops and 1 personnel exchange from the U.S. to JA were not executed due to the COVID-19 effect, and 2 more personnel exchanges from the U.S. to JA were not executed due to lack of funding or time scheduling.

The exchanges continue to be productive and beneficial to both sides. Among them, the research categories “MHD and High Beta”, and “Diagnostics” were rather active in 2019.

In the category of diagnostics, a new collaboration with Princeton Plasma Physics Laboratory has started in LHD. An impurity particle dropper (IPD) to inject impurity powders, e.g., Li, B, C, BN, etc., was installed in an upper port of LHD. The first experiment of boron (B) and boron- nitride (BN) powder dropping was performed on Dec. 3, 2019. After the B powder injection, substantial reduction of the oxygen emission was observed, together with the reduction of the electron density, which suggests the low wall recycling.

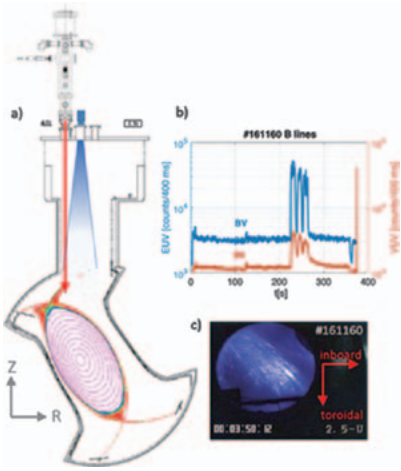

Fig. 1 (a) Experimental set-up, (b) BII and BV line intensities during long-pulse discharge, and (c) video image during B injection.

Joint Institute for Fusion Theory (JIFT)

Most of the activities in the two categories, workshops and personal exchanges, that had been scheduled for the 2019–2020 JIFT program were carried out. Three workshops were successfully held in addition to the JIFT Steering Committee meeting. In the workshops, “US-Japan collaborations on co-designs of fusion simulations for extreme scale computing,” “Theory and simulation on the high field and high energy density physics,” and “Progress on advanced optimization concept and modeling in stellarator-heliotrons” were discussed as main topics (Figure 2). In the category of personal exchanges, one Visiting Professor and nine Visiting Scientists made exchange visits for the purpose of collaborations on theoretical modeling and simulation of magnetic and inertial confinement fusion plasmas. One personal exchange

Fig. 2 Workshop on “US-Japan collaborations on co-designs of fusion simulations for extreme scale computing” which was held in Kobe during October 28–29, 2019.

program for a Visiting Professor was postponed to 2020–2021 due to the influence of COVID-19. At the JIFT Steering Committee meeting that was held using Zoom on December 6, 2019, the status of JIFT activities for 2019–2020 was reviewed and the recommendation plans for 2020–2021 were discussed. The JIFT discussion meeting was held at Toki on September 20, 2019, in the Plasma Simulator Symposium.

Fusion Technology Planning Committee (FTPC)

In this category of the US-Japan Collaboration, personal exchange programs were continued in six research fields, i.e., superconducting magnets, low-activation structural materials, plasma heating related technology, blanket engineering, in-vessel/high heat flux materials and components, and others (power plant studies and related technologies). One of the highlights in FY2019 was the joint research between Shimane University and University of California San Diego (UCSD) on the microstructural changes and deuterium retention properties of beryllides (intermetallic compounds of beryllium (Be) with other metals). Samples exposed to fusion relevant deuterium-helium mixture plasmas in the PISCES-B linear device at UCSD were analyzed at Shimane University. The beryllide samples exposed to deuterium (D) and helium mixture plasmas showed lower total retention of D than that of Be.

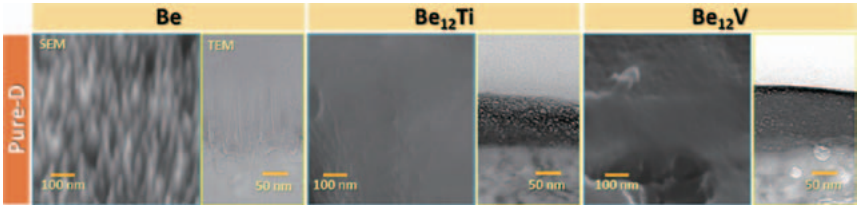

Fig. 3 Surface analysis of beryllide samples after exposure to mixed plasmas in PISCES-B. Formation of cone structures observed in beryllium was suppressed in beryllides.

US-Japan Joint Project: FRONTIER

The FRONTIER collaboration started in April 2019 to provide the scientific foundations for reaction dynamics in interfaces of plasma facing components for DEMO reactors.

The objectives of the task of Irradiation Effects on Reaction Dynamics at Plasma-Facing Material/Structural Material Interfaces (Task 1) are to understand neutron-induced microstructure modification and the consequent change in mechanical and heat transfer properties of the interfaces. Layered and joined materials were prepared, which will be irradiated with neutrons.

Task 2 (Tritium Transport through Interface and Reaction Dynamics in Accidental Conditions) examines the effects of neutron and helium irradiation on retention and permeation of hydrogen isotopes, and the oxidation of neutron-irradiated W materials. Oxidation of W-Re alloys was shown to be more moderate than that of pure W.

The objective of Task 3 (Corrosion Dynamics on Liquid-Solid Interface under Neutron Irradiation for Liquid Divertor Concepts) is to study the corrosion characteristics of liquid Sn for a divertor coolant with and without neutron irradiation. Screening tests showed that Al-rich steels have excellent compatibility with liquid Sn.

Task 4 (Engineering Modeling) aims to consolidate the results of each task.

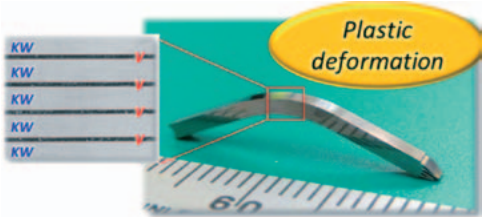

Fig. 4 Layered material of K-doped W (KW) and V-4Cr-4Ti alloy (V) developed by Tohoku U. and NIFS. In contrast to single phase W being brittle at room temperature, this material shows ductility. Effects of neutron irradiation will be examined in Task 1.

(T. Muroga, T. Morisaki, H. Sugama, N, Yanagi and Y. Hatano)

Plasma Wall Interaction (PWI) Collaboration

This collaboration is based on the IEA Technical Collaboration Programme (TCP) of the "Development and Research on Plasma Wall Interaction Facilities for Fusion Reactors" (in short, PWI TCP). The objective of this TCP is to advance physics and technologies of the plasma-wall interaction research by strengthening cooperation among plasma–wall interaction facilities (in particular, by using dedicated linear plasma devices), to enhance the research and development effort related to the first wall materials and components for fusion reactor. In this fiscal year, collaborations on PWI experiment such as effects of plasma exposure on ferritic steels, impacts of helium plasma exposure on tungsten erosion, mechanical examination of tungsten alloys, and plasma diagnostics were conducted. All the collaborations are listed in Table I. Highlight of each activity is described in this report.

Microstructure and Hydrogen Retention Property in Reduced-Activation Ferritic Steels Irradiated with High Density Plasma

Hydrogen retention behavior and the microstructure evolution for F82H samples irradiated with high density deuterium / helium (10%) mixture plasmas in the linear plasma device, PISCES-A in UCSD, were examined. Results of the examination show that bubbles and peculiar cone structures was formed at the near surface of samples exposed to the mixture plasma. Deuterium retention on the sample exposed to the mixture plasma was reduced to one-third of that on a sample exposed to a pure deuterium plasma exposure was observed.

Impact of plasma exposure on surface damage structure development and erosion in tungsten

Impact of the helium plasma exposure on the W surface damage structure development and erosion has been investigated by comparing impact of the hydrogen plasma exposure. The hydrogen and hydrogen / helium mixture plasma exposure experiments have been carried out in the linear device, PSI-2 in FJZ, with the typical flux and fluence of 0.6×10^{22} /m^2/s and 1×10^{26} /m^2, respectively. In the series of experiments over the past five years, the undulating surface structure which shows crystal orientation dependence is typically observed in the pure helium plasma exposure. However, it became clear that the undulating surface structure is not peculiar effect of the helium plasma exposure but common effect of the plasma exposure, because similar undulating surface structures are developed in pure hydrogen plasma and hydrogen/helium mixture plasma exposures.

Evaluation of High Temperature Impact Properties of Dispersion-strengthened Tungsten-Rhenium Alloys

To clarify the effects of grain refining, K-doping, dispersion strengthening by La_2O_3 particles, and alloying by Re on the ductile-brittle transition temperature (DBTT) of tungsten materials, high temperature Charpy impact tests were carried out at Karlsruhe Institute of Technology (KIT). K-doping and Re-addition could produce lower DBTT. Recrystallization was suppressed by K-doping, dispersion of La_2O_3 particles, and Re-addition. Based on these indexes, K-doped W-3%Re (H) plate could be a better solution. Although W-3%Re-1%La_2O_3 (L) and W-3%Re (L) could not show lower DBTT, this would be attributed to relatively lower deformation ratio in fabrication. Thus, the effect of dispersion of La_2O_3 particles on DBTT is not clear at present

Collaboration of plasma diagnostic study on Magnum-PSI

In the detachment plasma condition, which is a necessary condition for ITER and future fusion reactors, the strong density fluctuations are observed in the linear plasma devices. In this study, a 70 GHz frequency multiplied microwave interferometer (MIF) system which was constructed in GAMMA 10/PDX, was used as a reflectometer system for measuring the electron density fluctuations in the Magnum-PSI device in DIFFER. A low frequency fluctuation on the electron density was successfully observed. The fluctuation intensity changed according to the distance from the target plate. It is thought that the position of maximum fluctuation intensity shows the recombination front region in the detached plasma condition.

(S. Masuzaki)

Table I. List of collaborations

Subject	Participants	Term	Key persons
Microstructure and Hydrogen Retention Property in Reduced-Activation Ferritic Steels Irradiated with High Density Plasma	Yutaka Sugimoto (Shimane Univ.)	18 Aug. – 8 Sep. 2019	D. Nishijima (UCSD)
Impact of plasma exposure on surface damage structure development and erosion in tungsten	Ryuichi Sakamoto (NIFS)	1 – 9 Sep. 2019	A. Kreter (FZJ)
Evaluation of High Temperature Impact Properties of Dispersion-strengthened Tungsten-Rhenium Alloys	Shuhei Nogami (Tohoku Univ.)	8 – 20 Sep. 2019	M. Rieth (KIT)
Collaboration of plasma diagnostic study on Magnum-PSI	Masayuki Yoshikawa (Univ. Tsukuba)	21 – 29 Sep. 2019	H. V. Meiden (DIFFER)

IEA (International Energy Agency) Technology Collaboration Programme for Cooperation in Development of the Stellarator-Heliotron (SH) Concept ("IEA SH-TCP")

Highlight

IEA SH-TCP
Programmatic collaborations have been further extended in the next step of SH research

The SH TCP's objective is to improve the physics base of the Stellarator concept and to enhance the effectiveness and productivity of research by strengthening co-operation among member countries. All collaborative activities of the worldwide stellarator and heliotron research are combined under the umbrella of this programme, which promotes the exchange of information among the partners, the assignment of specialists to facilities and research groups of the contracting parties, joint planning and coordination of experimental programmes in selected areas, joint experiments, workshops, seminars and symposia, joint theoretical and design and system studies, and the exchange of computer codes. The joint-programming and research activities are organized via the Coordinated Working Group Meetings (CWGM), an interactive workshop to facilitate agreements on joint research actions, experiments, and publications under the auspices of the SH-TCP. The bi-annual "International Stellarator-Heliotron Workshop" (ISHW) serves as a forum for scientific exchange.

Fig. 1 The group photo at 22nd International Stellarator-Heliotron Workshop, Memorial Union, Madison, Wisconsin, September 2019, Courtesy of University of Wisconsin-Madison

Major achievements in 2019

In 2019, major achievements were the deuterium plasma campaign in the Large Helical Device (LHD) and the start of the first Island Divertor campaign of the Wendelstein 7-X (W7-X). Main highlights were reported in many presentations at the International Stellarator-Heliotron Workshop (ISHW) in Madison, WI. From LHD, the effects of isotope ratios (H vs. D) were investigated in detail, including diagnostic innovations to quantify the effects of isotope mixtures. Results from a variety of international conceptual design studies for next step stellarators were shown and advances in numerical methods to optimize these new experimental devices were discussed. W7-X demonstrated high performance plasmas with up to 1 MJ confined energy at 8 keV electron temperature and 3 keV ion temperature during pellet-fuelled high density plasmas. Also, full detachment of the island divertor for up to 30 s has been demonstrated.

22nd International Stellarator and Heliotron Workshop (ISHW)

The 22nd International Stellarator and Heliotron Workshop ISHW2019 was held at the University of Wisconsin - Madison, Wisconsin, USA from September 23–27, 2019. It was attended by 156 participants from ten countries. The workshop covered key stellarator topics from confinement and equilibrium, to plasma edge and divertor physics, reactor concepts, energetic particle confinement, and new numerical and computational methods for stellarator optimization.

48th S-H TCP executive committee meeting

The 48th Executive Committee meeting of the S-H TCP took place on September 24, 2019 during the 22nd International Stellarator and Heliotron Workshop. The meeting was attended by representatives from all six contracting parties and observers from Costa Rica (I. Vargas) and China (Y. Xu).

19th Coordinated Working Group Meeting (CWGM)

The 19th CWGM was held in Berlin, Germany from March 12–14, 2018. On-site and remotely, fifty participants provided reports on collaborations grouped into seven topics. In an informal workshop format, the participants discussed proposals for joint actions and experiments, taking advantage of comparative studies in different devices. The CWGM effectively tracked the progress in the most active research fields and initiated a series of new Coordinated Working Group Actions (CWGA) for joint activities. A session on the program planning of the main contributors served to enable the exchange of information, and the community was invited to provide feed-back to programmatic considerations. China's rapidly developing stellarator program has a sound balance of sustainable build-up of know-how and scientifically interesting new concepts. In particular, the outline of a quasi-axially symmetric device attracted great interest.

(Y. Takeiri, T. Morisaki and Y. Suzuki)

Japan-China Collaboration for Fusion Research (Post-CUP Collaboration)

I. Post-CUP collaboration

The post-Core University Program (Post-CUP) collaboration is motivated by collaboration on fusion research with institutes and universities in China including Institute of Plasma Physics Chinese Academy of Science (ASIPP), Southwestern Institute of Physics (SWIP), Peking University, Southwestern Jiaotong University (SWJTU), Huazhong University of Science and Technology (HUST) and other universities both in Japan and China. The Post-CUP collaboration is carried out for both studies on plasma physics and fusion engineering. Based on the following implementation system, the Post-CUP collaboration is executed.

Table 1. Implementation system of Japan-China collaboration for fusion research

Category	① Plasma experiment				② Theory and simulation	③ Fusion engineering research
Subcategory	①-1	①-2	①-3	①-4	—	—
Operator	A. Shimizu	S. Kubo	M. Isobe	T. Oishi	Y. Suzuki	T. Tanaka

①-1 : Configuration optimization, transport, and magnetohydrodynamics, ①-2 : Plasma heating and steady state physics, ①-3 : Energetic particles and plasma diagnostics, ①-4 : Edge plasma and divertor physics, and atomic process

II. Primary research activities of collaboration in FY 2019

2019 Post-CUP Workshop & JSPS-CAS Bilateral Joint Research Projects Workshop was held at Nagoya International Center, Japan from 24th to 26th, July, 2019, to continue and enhance close collaborations in fusion research between Japan and China, as shown in Fig. 1. Over 30 researchers and Ph.D. students from both parties attended this workshop. Key physics issues specific to high-performance plasmas through joint experiments on advanced fully superconducting fusion devices, i.e., LHD in Japan and EAST in China, and other magnetic confinement devices were discussed to carry out multi-faceted and complementary physics researches [1].

Fig. 1 2019 Post-CUP Workshop & JSPS-CAS Bilateral Joint Research Projects Workshop at Nagoya International Center, Japan.

In the category ①, the 2nd steering committee meeting for the NIFS-SWJTU joint project for CFQS quasi-axisymmetric stellarator, was held on May 29, 2019 at SWJTU in Chengdu, China, as shown in Fig. 2. Progress of engineering design and status of the construction of modular coil mockup were reviewed [2]. Also, construction site of CFQS building was discussed.

In the research of energetic particles, NIFS and ASIPP discussed to conduct collaborative research for understanding triton confinement characteristics in EAST deuterium plasmas and comparison with results from LHD deuterium plasmas. To predict 1 MeV triton confinement/loss and investigate the possible scenario for triton burnup experiment in EAST, 1 MeV triton orbit analysis was performed using Lorentz orbit codes for EAST plasmas with various plasma current conditions [3]. We found that relatively high plasma current is required to perform triton burnup experiment in EAST plasmas.

In the research of the edge and divertor plasmas, JSPS-CAS Bilateral Joint Research Projects, “Control of

wall recycling on metallic plasma facing materials in fusion reactor“ (FY2019–FY2021) was started. Figure 3 is a group photo of the kickoff meeting of the project which was held in May 2019 in ASIPP. For understandings of spatial profiles of deuterium atoms, deuterium Balmer series was measured around divertor targets in EAST, which was operated under our own experimental time by our proposal [4]. A collaborative study on the extreme-ultraviolet spectroscopy had also continued progress, especially in a quantitative evaluation on the tungsten impurity concentration in LHD, EAST, and HL-2A [5].

Fig. 2 The 2nd steering committee meeting of NIFS-SWJTU joint project for CFQS.

In the category ②, An EMC3-EIRENE modeling work on effects of neon injection positions on the toroidally symmetric/asymmetric heat flux on the EAST divertor was presented at the 2019 Post-CUP workshop in Nagoya, and its paper was published [6]. As for J-TEXT, 3D MHD analyses using 3D equilibrium calculation code, HINT, is progressing. This result was presented as an oral contribution at the 12th Asia Plasma and Fusion Association Conference, Dec. 11–13, 2019 in Shenzhen, China. Also, the special campaign for the international collaboration was organized in J-TEXT. From Japan, there topics, which are the heat transport, the disruption, and the 3D helical core formation, were accepted and conducted experiments in that campaign.

In the category ③, tritium release kinetics for core-shell Li_2TiO_3-Li_4SiO_4 tritium breeders was studied by tritium-TDS method. There were two main release peaks for mixed biphasic pebbles, whose activation energies were obtained as 0.92 eV and 1.78 eV. While, only one release peak can be found for single phase breeder. The tritium migration of core-shell Li_2TiO_3-Li_4SiO_4 breeders was mainly controlled by the decomposition of O-T bonds or recovery of irradiation defects with higher activation energy. FLiNaBe is a promising tritium breeding material for a fusion blanket system. The solid-state sample of FLiNaBe was irradiated by thermal neutrons at Kyoto University Research Reactor, and tritium release behavior from the free surface of FLiNaBe by heating in Ar flow was observed in Kyushu University. The release ratio of each chemical form was approximately TF: HT: HTO = 30:64:6. Most of the tritium was released as HT (or T_2). This result indicates that corrosion of metals by TF occurred in tritium release process.

Fig. 3 Kickoff meeting of the JSPS-CAS Bilateral Joint Research Projects which was held in May 2019 in ASIPP.

[1] Corrected papers at the 2019 Post-CUP Workshop & JSPS-CAS Bilateral Joint Research Projects Workshop, 24th–26th July, 2019, Nagoya, Japan. NIFS-PROC-116, 2019.
[2] CFQS TEAM, “NIFS-SWJTU JOINT PROJECT FOR CFQS - PHYSICS AND ENGINEERING DESIGN VER. 2.1.” NIFS-PROC-115, 2019.
[3] K. Ogawa, G. Zhong *et al.*, Plasma Fusion Res. **15** (2020) 2402022.
[4] K. Nojiri and N. Ashikawa, “Collaboration Works of JSPS Bilateral Joint Research Projects (Japan (NIFS)-China (ASIPP))”, Journal of Plasma and Fusion Research **96** (2020) 149.
[5] S. Morita, C.F. Dong *et al.*, Journal of Physics: Conf. Series **1289** (2019) 012005.
[6] B. Liu, S.Y. Dai, G. Kawamura *et al.*, Plasma Physics and Controlled Fusion **62** (2020) 035003.

(M. Isobe, T. Oishi, Y. Suzuki and T. Tanaka)

Japan-Korea Fusion Collaboration Programs

Closer and deeper cooperation in the areas of plasma heating systems, diagnostic systems, and SC toroidal device experiments were essential for physics research. Another important aspect of this collaboration is human resource development for future fusion research.

I. KSTAR collaboration

1 Plasma Heating Systems

Both Parties had information exchanges on the upgrade of ion sources and the development of advanced neutral beam technology in the 6th China-Japan-Korea (CJK) workshop.

1.1 Radio Frequency Systems

Both Parties continued the collaboration and exchange of technical knowledge for development of radio frequency technologies in fusion plasmas.

2 Diagnostic Systems

2.1 Bolometer Systems[1)]

Joint work was done by Japanese and Korean researchers from NIFS and NFRI on the design and the proposal of a future upgrade of the IRVB for disruption mitigation experiments in KSTAR. Discussions were continued regarding the reinstallation of the resistive bolometers on KSTAR as part of the KSTAR upgrade planned for 2021.

2.2 Edge Thomson Scattering System[2,3)]

Collaboration regarding high repetition rate sampling (5 GS/s) DAQ system has been carried out. For this collaboration, a Japanese expert from NIFS visited NFRI and a Korean expert from NFRI visited NIFS.

2.3 Electron Cyclotron Emission (ECE) and Imaging (ECEI) System

The KSTAR ECE diagnostic system with W-band and D-band heterodyne radiometers has been routinely operated for electron temperature profile measurements in both low and high field sides. However, because the W-band H-plane Tee was simply used as a beam splitting tool for both radiometers, the beam power into each radiometer was not controllable. In particular, it has led to poor measurements with a D-band radiometer. For solving this problem, the wire-grid beam splitter was adopted with a wire-grid polarizer and a linear polarization rotator. As a result of optimization by rotating the linear polarization, both radiometers successfully contributed to better ECE measurements.

2.4 Fast RF spectrometer system

Based on the systems developed on KSTAR and LHD, a new RF radiation measurement system in VEST spherical tokamak device in Korea. Consideration of the alignment of the measurement system at QUEST, LHD, and KSTAR is ongoing.

2.5 Charge Exchange Recombination Spectroscopy

Charge exchange spectroscopy is one of the active spectroscopy using neutral beam to measure ion temperature, plasma rotation velocity, and impurity density. Korean and Japanese researchers continued the collaboration on the three types of CES spectrometers for the advanced KSTAR physics research.

2.6 Neutron and Energetic-ion Diagnostics[4,5,6,7)]

Japanese and Korean researchers cooperated together to enhance temporal resolution of the Fast-ion Loss Detector (FILD) system utilizing fast electronics and digitizers. In addition, collaborative works on the Lorentz-Orbit (LORBIT) and/or Orbit Following Monte Carlo (OFMC) simulation were continued to understand energetic-ion transport in KSTAR.

2.7 Soft X-ray CCD Camera (SXCCD)

A researcher from NIFS visited NFRI to accelerate the progress of the installation of the SXCCD camera system, using the same support structure shared with the VUV telescope system. Both parties agreed that one NFRI researcher will newly join this project. The shipment of the remaining necessary items (a cooling water chiller and an in-vacuum neutron shield) of the SXCCD camera system was completed by March.

2.8 VUV Telescope System

Japanese and Korean researchers cooperated together to develop the interface of the VUV telescope system

to the KSTAR device. A Japanese researcher from NIFS visited twice to NFRI to discuss the interface. Japanese and Korean experts are continuing the collaboration on the VUV telescope for edge MHD activities and RMP physics studies.

2.9 EMA Post Data Analysis System[8,9)]
Japanese researchers visited NFRI, and updated the AutoAna (Automatic Analysis) system and myView2. These modifications were reflected to the AutoAna systems working for the LHD project in NIFS. Also, Japanese and Korean r researchers have developed analysis programs run by the AutoAna for the diagnostics devices for KSTAR projects.

2.10 The 10th Japan-Korea Seminar on Advanced Diagnostics
The 10th Korea-Japan Seminar on Advanced Diagnostics will be hosted in 2020 in Korea by Seoul National University. Detailed arrangements are currently being made.

2.11 SC Toroidal Device Experiments
Japanese researchers participated in the KSTAR experiment to study rotation transport dynamics under the non-axisymmetric magnetic perturbation field.

II. Human Resource Development

The total number of researchers that were exchanged between Japan and Korea in JFY 2019 were 29 from Japan to Korea and 53 from Korea to Japan. Eight Workshops in various fields were held in each country (4 in Japan and 4 in Korea).

- Workshop on Physics validation and control of turbulent transport and MHD in fusion plasmas, Busan, Korea, Apr. 21–24, 2019.
- Modeling and Simulation of Magnetic Fusion Plasmas, Kyushu U., Japan, Jun. 27–28, 2019.
- 15th JCM, Nagoya, Japan, Jul. 2–3, 2019.
- Physics of fine plasma particles, NFRI, Daejeon, Korea, Aug. 7–9, 2019.
- Evaluation of Tritium behavior for reactor design in fusion, Okinawa, Japan, Oct. 7–8, 2019.
- Workshop on ITER tritium system, Okinawa, Japan, Oct. 7–8, 2019.
- 13th Workshop on ITER Diagnostics, NFRI, Daejeon, Korea, Jan. 15–16, 2020.
- Korea-Japan Blanket Workshop, NFRI, Daejeon, Korea, Jan. 30, 2020.

1) Seungtae Oh, Juhyeok Jang, Byron J Peterson, "Radiation profile reconstruction of Infra-Red imaging Video Bolometer (IRVB) data using Machine Learning (ML) algorithm", Plasma Phys. Control. Fusion 62 (2020) in press.
2) Ichihiro Yamada, Hisamichi Funaba, Jong-ha Lee, Yuan Huang, and Chunhua Liu, "Influence of neutron irradiation on LHD Thomson scattering system", 28th International Toki Conference, Japan (2019).
3) H. Funaba *et al.*, "Fast-signal processing for Thomson scattering measurement and effects on evaluation of electron temperature on LHD", LAPD2019, USA, 2019.
4) E. Takada, T. Amitani, A. Fujisaki, K. Ogawa, T. Nishitani, M. Isobe, J. Jo, S. Matsuyama, M. Miwa, and I. Murata, "Design Optimization of a Fast-Neutron Detector with Scintillating Fibers for Triton Burnup Experiments at Fusion Experimental Devices", Review of Scientific Instruments 90 (2019) 043503.
5) Eiji Takada, Tatsuki Amitani, Kunihiro Ogawa, Takeo Nishitani, Mitsutaka Isobe, Jungmin Jo, Shigeo Matsuyama, Misako Miwa, Isao Murata, "Design optimization of a fast-neutron detector with scintillating fibers for triton burnup experiments at fusion experimental devices", 16th IAEA Technical Meeting on Energetic Particles in Magnetic Confinement Systems – Theory of Plasma Instabilities, 3–6 September 2019, Shizuoka City, Japan, P-15.
6) Mitsutaka Isobe, Kunihiro Ogawa, Eiji Takada, Tieshuan Fan, Jungmin Jo, Jan Paul Koschinsky, Sachiko Yoshihashi, Makoto Kobayashi, Shuji Kamio, Yutaka Fujiwara, Hideo Nuga, Ryosuke Seki, Takeo Nishitani, Masaki Osakabe, "The LHD Neutron Diagnostics", 16th IAEA Technical Meeting on Energetic Particles in Magnetic Confinement Systems – Theory of Plasma Instabilities, 3–6 September 2019, Shizuoka City, Japan, P-18.
7) Jungmin Jo, MunSeong Cheon, Junghee Kim, Jisung Kang, Tongnyeol Rhee, Mitsutaka Isobe, Kunihiro Ogawa, Takeo Nishitani, Tatsuki Amitani, Eiji Takada, Kyoung-Jae Chung, Yong-Seok Hwang, "1 MeV triton confinement study on KSTAR", 16th IAEA Technical Meeting on Energetic Particles in Magnetic Confinement Systems – Theory of Plasma Instabilities, 3–6 September 2019, Shizuoka City, Japan, P-101.
8) Masahiko Emoto, Katsumi Ida, Mikirou Yoshinuma, Won-Ha Ko, Jekil Lee, "Application of LHD Post Data Analysis Systems to the KSTAR Project" Fusion Engineering and Design 155 (2020) 111665.
9) Masahiko Emoto, Katsumi Ida, Mikirou Yoshinuma, Won-Ha Ko and Jekil Lee "Application of LHD Post Data Analysis Systems to the KSTAR Project" 12th IAEA Technical Meeting on Control, Data Acquisition and Remote Participation for Fusion Research, 13–17 May 2019, Daejeon, Korea Plenary Oral / 503.

(K. Ida)

14. Division of External Affairs

The Division of External Affairs, as a core organization responsible for public relations and outreach activities, promotes “dialogue” with society including the local area through a variety of activities. The organization has undergone a review in 2019 and now consists of five offices: Society Cooperation Office, Content Production Office, Event Planning Office, Public Relations and Tour Guide Office, and Outreach Promotion Office. A summary of the offices is depicted in Fig. 1. Many of the NIFS staff are active as members of the department. The main activities are: holding public explanatory meetings (Fig. 2), holding academic lectures for local residents (Fig. 3), providing tours of the NIFS facilities (Fig. 4), and science classroom activities (Fig. 5).

Fig. 1 Organization chart of Division of External Affairs

Activities held in 2019 include the following.

- Public explanatory meetings held at 23 places; 259 people participated
- Tours of the NIFS facilities (any time) held 281 times; more than 2,947 people participated
- Open academic lectures for the public held in Tajimi-city; 660 people participated
- Science classroom activities held 37 times
- Release of information through Web pages, mailing lists, and SNS (Twitter and Facebook)
- Publication of NIFS official pamphlet (in Japanese and in English)
- Publication of public relations magazine: NIFS News (6 issues) (Fig. 6)
- Publication of public relations magazine: Letters from Plasma-kun (6 issues)

Fig. 2 Public explanatory meeting in Toki-city

Fig. 3 Academic lectures in Tajimi-city

Fig. 4 Tour of the NIFS facilities

Fig. 5 Science classroom

Fig. 6 Public relations magazine: NIFS News

(K. Takahata)

15. Department of Engineering and Technical Services

The Department of Engineering and Technical Services covers a wide range of work in the design, fabrication, construction, and operation of experimental devices in the fields of software and hardware.

The department consists of the following five divisions. The Fabrication Technology Division oversees the construction of small devices and the quality control of parts for all divisions. The Device Technology Division works on the Large Helical Device (LHD) and its peripheral devices except for heating devices and diagnostic devices. The Plasma Heating Technology Division supports the ECH system, the ICRF system, and the NBI system. This year, a pair of FAIT antennas were installed to LHD for the ICH system. The Diagnostic Technology Division supports plasma diagnostic devices and radiation measurement devices, and oversees radiation control. Finally, the Control Technology Division concentrates on the central control system, the cryogenic system, the current control system, and the NIFS network.

The engineering department welcomed one new member in April. The total number of staff is now 59 (2019). We have carried out the development, the operation, and the maintenance of the LHD and those peripheral devices together with approximately 57 operators.

1. Fabrication Technology Division

In this division, the main work is the fabrication of experimental equipment. And, supplies of experimental parts and technical consultations are provided for many researchers. In addition, the administrative procedures are managed for the department.

The detailed activities of this division follow below.

(1) Fabrication of Corrugated Resonators

A cylindrical cavity wall with periodical corrugation, which excites a cylindrical Bloch wave at the frequency of 100 GHz or 200 GHz, was fabricated for the collaboration with Niigata University (Fig. 1).

The cylindrical cavity has 80 corrugations. The parameters of the rectangular corrugation for the frequency of 100 GHz are a width of 0.3 mm, a depth of 0.6 mm, and a periodic length of 0.5 mm. Also, the parameters of the other rectangular corrugation are a width of 0.15 mm, a depth of 0.3 mm, and a periodic length of 0.25 mm.

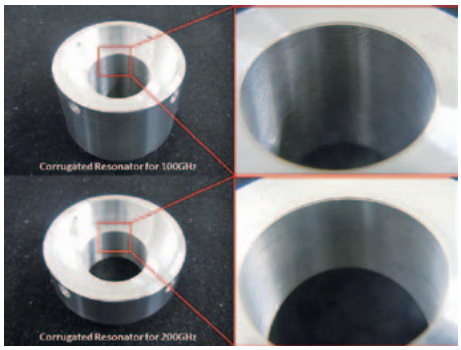

Fig. 1 Corrugated Resonator

(2) Fabrication of 77GHz notch filter

A 77GHz notch filter was fabricated for the Collective Thomson Scattering (Fig. 2). It consists of 24 cavities and waveguides in the internal space.

The cavity has a cylindrical shape with a diameter of 6.3mm, and each depth of cavity is adjusted with a

screw. The parameters of rectangular waveguide are a length of 5.69mm, and a width of 2.845mm.

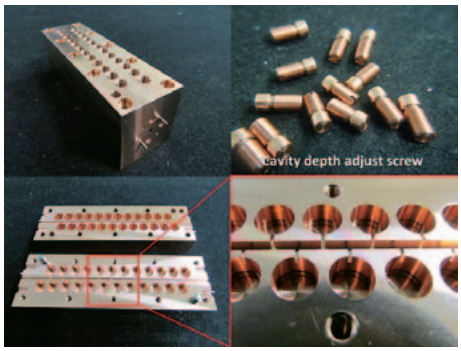

Fig. 2　2 77 GHz notch filter

(3) Fabrication of high gain filter amplifier

A high gain filter amplifier is used for a real-time measuring of the superconducting critical current (Fig. 3). This circuit has the following specifications. The voltage gain is 100dB, the frequency bandwidth is DC to 2 kHz, the band elimination frequency is 50 dB from 60 Hz to harmonics of until order 5, and the voltage of input referred noise is 0.6 μV.

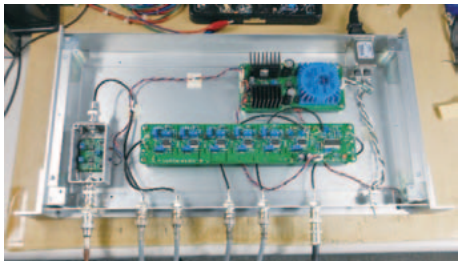

Fig. 3　High gain filter amplifier

(4) Fabrication of controller for 2.45GHz solid-state power amplifier

An introduced amplifier is a 2.45GHz 200W solid-state power amplifier (SSPA). The model number is TME-201B00. The manufactured controller for the SSPA is shown in Fig. 4. It has a graphic display module (TG12864B-02WWBV) and a rotary encoder inside the front panel. This controller is operated by pushing or rotating the encoder. Then the display shows the set and output voltage. The monitoring of rotary encoder value and the output voltage control is enabled by an Arduino Mega 2560.

Fig. 4　The controller for SSPA

2. Device Technology Division

This Division supports the operation, the improvement, and the maintenance of LHD.

(1) Operation of LHD

We started pumping of the cryostat vessel for cryogenic components on August 15, 2019 and pumping of the plasma vacuum vessel on August 16. Subsequently, we checked air leaking from the flanges on the plasma vacuum vessel. The number of checked flanges were 37. As a result, we found leaks at 3 devices and repaired those devices.

The pressure of the cryostat vessel reached the adiabatic condition ($< 2\times10^{-2}$ Pa) on August 16 and the pressure of the plasma vacuum vessel reached below 1×10^{-5} Pa on August 25.

The LHD experiment of the 21st experimental campaign began on October 3, 2019 and was implemented continuously until February 6, 2020. The number of days of the plasma experiment was 52 in total. Due to trouble with the divertor plates in the plasma vacuum vessel, the experimental days were reduced from 61 to 52 days.

During this experimental campaign, the vacuum pumping systems could eliminate air from both vessels without trouble. In addition, no major trouble was reported with the utilities (the compressed air system, the water-cooling system, the GN2-supply system, etc.) of the LHD, and the exhaust detritiation system. The LHD operation was completed on February 28, 2020.

(2) Design of CFQS baking heater

The world's first quasi-axisymmetric stellarator CFQS is under construction as a joint project between NIFS and SWJTU (South West Jiaotong University). We have finished the fabrication of the mockup coil, and conducted various performance tests, such as the heat run test and the breakdown test. Now, we are working on detailed designs for the actual coil. In addition, the construction of the vacuum vessel is also ongoing.

As a part of the design work of the vacuum vessel, we are considering specification of baking heater. Fig. 1 shows a moment where strings are wound directly on a 3D printer model to estimate the heater length. Based on this result, the voltage and the capacity were determined as well. We will continue the design work to finish the detailed analysis.

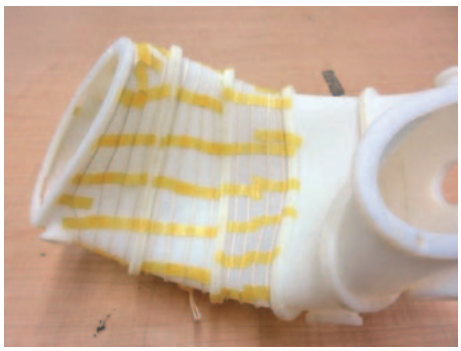

Fig. 1 Estimation of heater length using a 3D model of vacuum vessel.

(3) Upgrading of voltage waveform output systems

The fuel gas of a fusion plasma is injected via a piezo valve. Both the piezo valve and the amount of gas are controlled by a voltage waveform output system.

The voltage waveform output system comprises a graphical user interface (GUI) and an analog output unit as shown in Fig. 2(a) and Fig. 2(b), respectively. The GUI creates the control voltage waveform, while the analog output unit delivers voltage in the range from 0 to 5 V. The driving voltage of the piezo valve ranges from 0 to 150 V.

After the voltage waveform output system delivers the voltage, it is amplified 30 times by a piezo driver.

The conventional system sometimes stops running. Therefore, to avoid this problem, a new system that operates safely is required.

In the new system, the GUI was developed with LabVIEW and the hardware is built with CompactRIO, a product of National Instruments.

The new system has operated safely without stopping in the 21st experiment. Previously, the feedback control for the gas amount was carried out by an electronic circuit. It adopts an FPGA, so that the device size could be reduced.

In the future, we will expand the function of the system and improve the accuracy of the feedback control.

Fig. 2 Voltage waveform output system:
(a) GUI and (b) hardware (CompactRIO, product of National Instruments).

(4) Inspection and repair of an LHD vacuum vessel after the 21st experimental campaign

After the 21st experimental campaign, a damage analysis for the in-vessel equipment was conducted. The main damages were 1) damage of the tiles for the part B of NBI#1 (NBI 1-B) armor (Fig. 3(a)), 2) melting and deformation of vacuum vessel (VV) protection plates, and 3) impurity deposition on diverter tiles and melting of fixing bolts.

The NBI 1-B armor tiles had cracks caused by the thermal shock force as shown in Fig. 3(b). Therefore, the tile material (isotropic graphite) was replaced with carbon fiber composite, which could withstand thermal shock. Furthermore, we redesigned the tile structure such that the shear stress did not concentrate at locations that have been subjected to thermal shock. In the second case, the NBI beam was deflected due to the mirror effect, and the VV protection plates were heated. Thus, the material of the protective plate (SUS316 and copper) was changed to molybdenum, which is a high-melting-point material, and five protective plates were replaced. In the third case, in addition to the deposition of impurities such as iron and carbon on divertor tiles, sublimation and cracks on the heat-receiving surface were confirmed. Thus, the tiles that were severely damaged were replaced, and the SUS bolts that had melted and were damaged were replaced with molybdenum bolts.

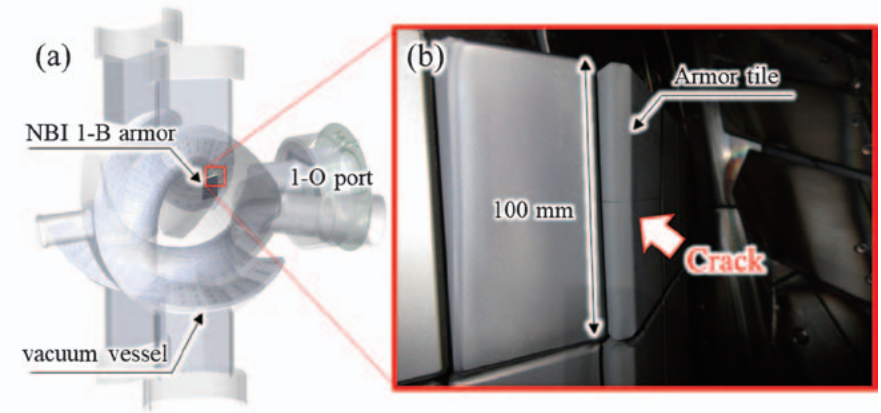

Fig. 3 Damage on NBI 1-B armor: (a) Bird's eye view of NBI 1-B armor and vacuum vessel of the LHD; (b) crack on the NBI 1-B armor tile.

(5) Replacement of power supply for glow discharge cleaning system in LHD

A DC power supply for a glow discharge cleaning system required a replacement because one of the parts was broken. The unit is composed of two programmable DC power supplies, an interlock system with indicators and circuit breakers. Specifications of the selected DC power supply are the output voltage of 1500 V, the output current of 30A, and the output capacity of 15kW. These DC power supplies have to be connected to the LHD central control unit via the interlock system for safe operation of the glow discharge cleaning system. The interlock system was newly designed to send status signals of DC power supplies and receive signals of LHD operating permission from the LHD central control unit. In addition, the system indicates status and warnings of DC power supplies on a front panel as shown in the photograph, which is also designed for the new system only, and can shut off circuit breakers in an emergency, such as over current.

Fig. 4 New power supply for glow discharge cleaning system in LHD

3. Plasma Heating Technology Division

The main tasks of this division are the operation and the maintenance of three individual different types of plasma heating devices and their common facilities. We have also performed technical support for improving, developing, and newly installing these devices. In this fiscal year, we mainly carried out device improvement and

modification for a deuterium plasma experiment. The details of these activities are as follows.

(1) ECH

During the 21st experimental campaign, we injected the heating power up to 4 MW to assist plasma experiments. That contributed to accomplishing the plasma with both 6.8 keV high ion temperature and 13 keV electron temperature simultaneously. And long pulse discharge by low power ECH helped to clean the wall of the vacuum vessel so to achieve the high potential plasma. Some trouble occurred, but all of the ECH technical staff of the LHD experimental group have contributed to the various plasma experiments.

(2) ICH

In the 21st experimental campaign, ICRF heating was carried out using the FAIT (Field-Aligned Impedance-Transforming) antenna installed at the 4.5U&L ports of the LHD for the first time in the deuterium experimental period.

We used two RF transmitters with fixed wave frequency (38.47 MHz) in the experiments. The #6A transmitter was connected to the 4.5U antenna and the #6B transmitter was connected to the 4.5L antenna.

The total injection power with the two antennas into the plasma reached 2.3 MW in the short pulse of 3.5 seconds.

(3) NBI

(a) The operation and maintenance of NBI in the 21st campaign of the LHD experiments

In the 21st experimental campaign, approximately 8,000 shots of beams were injected into the LHD plasmas with three negative-NBIs (BL1, BL2, and BL3). The injection history of the total injection power for the negative-NBIs is shown in Fig. 1. The maximum injection power in this campaign was 11.5 MW. As for the positive-NBIs (BL4 and BL5), about 4,500 shots of beams were injected into the LHD plasmas. The maximum total injection power of positive-NBI was 12 MW by hydrogen beam and 18 MW by deuterium beam.

NBIs had no troubles that led to serious problems in the plasma experiments.

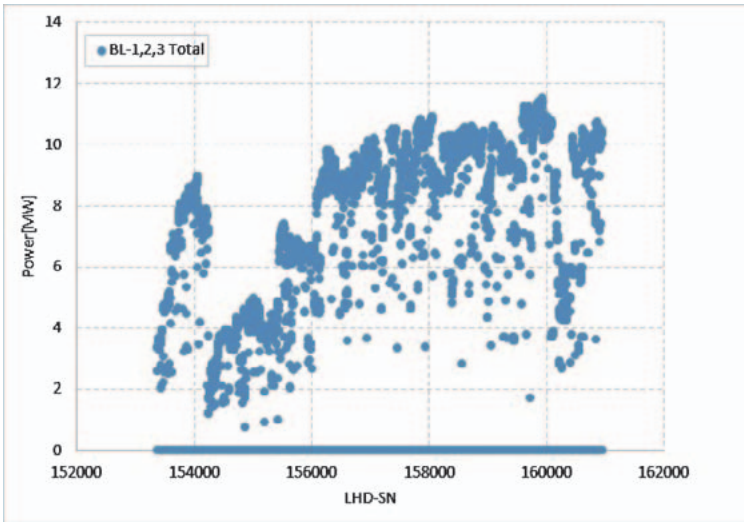

Fig. 1 History of the total injection power for the negative-NBIs

(b) Maintenance of ion sources for NBIs

Six negative ion sources and eight positive ion sources were maintained at the maintenance work room only for activated materials for the next experimental campaign. The main maintenance content was as follows: wiping off cesium from plasma-grid and arc chamber, polishing the extraction-grids and acceleration-grids, changing the tungsten filament, and helium leak test of ion sources, etc. Fig. 2 shows the work of wiping off the plasma-grids. We have continued an effort to acquire the maintenance technology for ion sources.

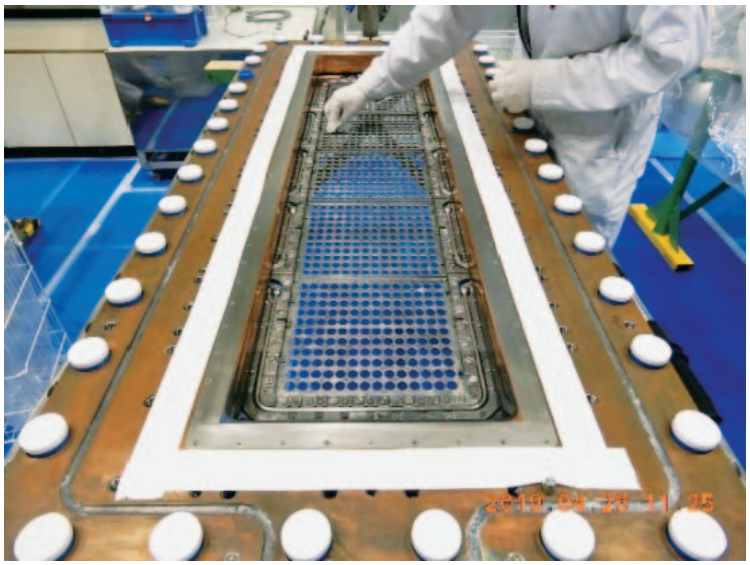

Fig. 2 Wiping off cesium from plasma-grid

(4) Motor-Generator (MG)

The MG is used to supply the pulsed power to the NBI and the ECH in the LHD plasma experiment. The MG has supplied power for 17,070 shots in the last fiscal year and power for 653,733 shots since its construction. The operation time was 928 hours. The control terminals were updated after the 21st experimental campaign.

4. Diagnostics Technology Division

This division mainly supports the development, the operation, and the maintenance for plasma diagnostic devices and radiation measurement devices for LHD. In addition, we also have taken charge of radiation control.

(1) Plasma diagnostic device

Some plasma diagnostics devices have functioned for more than 20 years and thus require maintenance. For the Nd:YAG Thomson scattering system, we replaced two high-performance type noise cut transformers for the data acquisition system power supplies with new ones, as shown in Fig. 1. We also augmented a standard-performance type transformer and outlets for the data acquisition system.

Modification of neutron energy spectra as requested using the neutron spectrum shaping assembly (NSSA) is important owing to enhancing joint research using neutron. We modified one of the irradiation ends of the neutron activation system from the 2.5-L port to the 10-O port for finding a space to construct NSSA. Subsequently, we built a new base in order to support NSSA on A-stage in the torus hall (Fig. 2).

The LHD DAQ system acquired the diagnostics data of 7797 plasma shots in the 21st experimental campaign.

The system worked also in the situation of long-pulse shots, and the size of the stored data was about 100.7TB in total after compression.

Fig. 1 Two noise cut transformers for Thomson scattering system

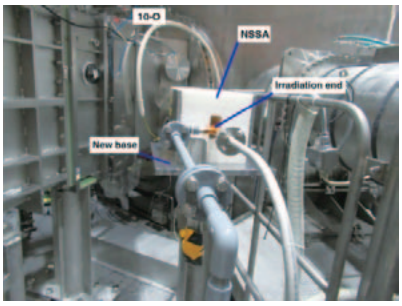

Fig. 2 Neutron spectrum shaping chamber installed at the front of 10-O port.

(2) Radiation measurement and radiation control

In order to control the safety of radioactivity, we carried out the operation and the maintenance for three high-purity germanium (HPGe) detectors, seven liquid scintillation counters, three stack tritium monitoring systems, two gas monitoring systems, two dust monitoring systems, and the drain water monitoring system. Especially, the smear test in the measurement of surface contamination has used a 2π gas-flow counter and an auto well gamma system. We carried out the smear test about 200 times. We also checked the work environmental radiation for the safety of workers using HPGe detector every month.

The tritium monitoring system of the stack monitors the tritium concentration of exhaust gas in the stack by using a tritium sampler every week. Two gas and dust monitor systems require constant measuring of radiation concentration in the stack and the LHD torus hole, respectively.

For the integrating radiation monitoring system, it is important to manage and to search the history of the event signals and the operations from the radiation measurement equipment. We developed a program which works continuously and indicates the history. It is also possible to search for the specific history with this program.

We manage the radiation worker registration. To save labor for manual data entry in the application procedure for registration of radiation workers, we developed a web-based application system and a card-reader system (Fig. 3) that obtains registration information from a NIFS staff card at the radiation education reception. And we have started to register and update the radiation worker information with these systems.

Fig. 3 Application to obtain registration information from a NIFS staff card (in Japanese)

5. Control Technology Division

The Control Technology Division is in charge of the important engineering tasks in the LHD project, such as operation, management, and development, which are mainly targeted to the central control system, the cryogenic system, coil power supply, and super-conducting coils.

We are also responsible for the IT infrastructures, for example, the LHD experiment network, NIFS campus information network and internet servers in every phase of the project including requirements analysis, design, implementation, operation, and user support.

The essential topics of the activities for the last fiscal year are described below.

(1) LHD cryogenic system and power supply system for superconducting coils

The cooling operation in the 21st experimental campaign was conducted without significant accidents. In the power supply system, the logging system as shown in Fig. 1 for collecting each superconducting coil energization signal was partially broken before the beginning of the 21st campaign. Unfortunately, the production of the old model (WE7000) has already been stopped. Therefore, we needed to find the substitute model with almost the same specifications.

To fulfill the requirements for the logging system, two sampling frequencies (1Hz sampling mode and at least 5 kHz sampling mode) and isolated 48 recording channels, we finally adopted EDX-200A which is more compact than WE7000 and has good cost performance.

The new loggers could collect all signals with no severe troubles in the 21st experimental campaign. Before the 22nd campaign, we will implement the logging program with automatic logging start/stop function developed by LabVIEW.

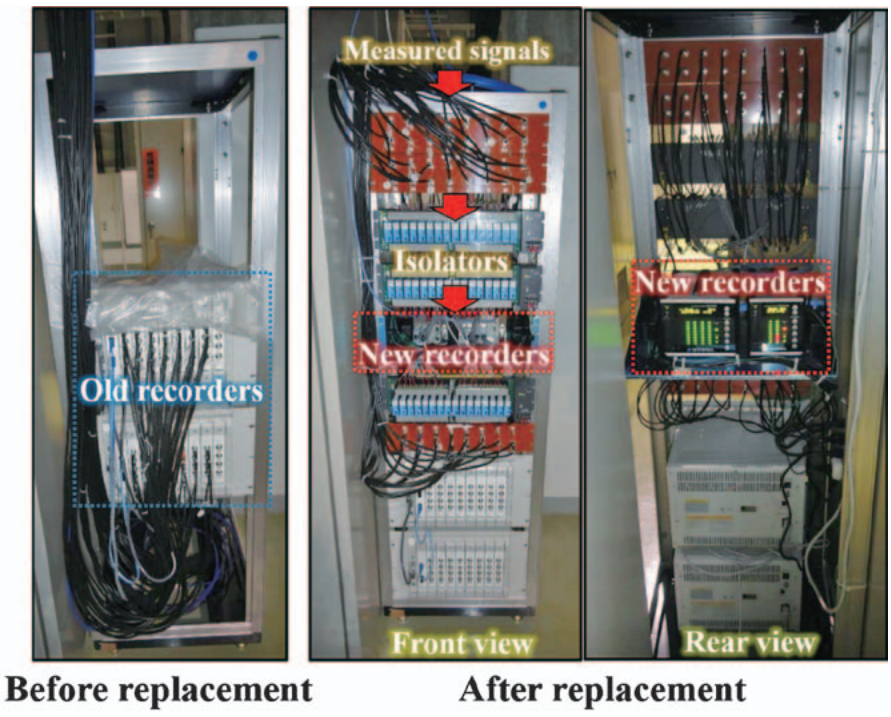

Fig. 1 Replacement results of the logging system.

(2) Development of pulse generator for NBI test stand

The research using a test stand for Neutral Beam Injection (NBI), which is an extremely important device in the LHD experiment, is conducted to improve the device performance.

In the actual experiment, a pulse generator which outputs simulated signals through the LHD Central Control System is used for the operation. However, it is obsolete and has bugs. Thus we have developed another pulse generator using FPGA board called MicroZed, a product of Xilinx, Inc. (Fig. 2). It is able to generate a maximum of 20 x arbitrary length pulses with 1 μs accuracy at arbitrary timing. Users can also select burst mode, which transforms the pulse wave from square to clock signal with selected frequency. These operations are performed through Web-based GUIs.

In the future, we are planning to add a function to demodulate external signals for more ideal operation.

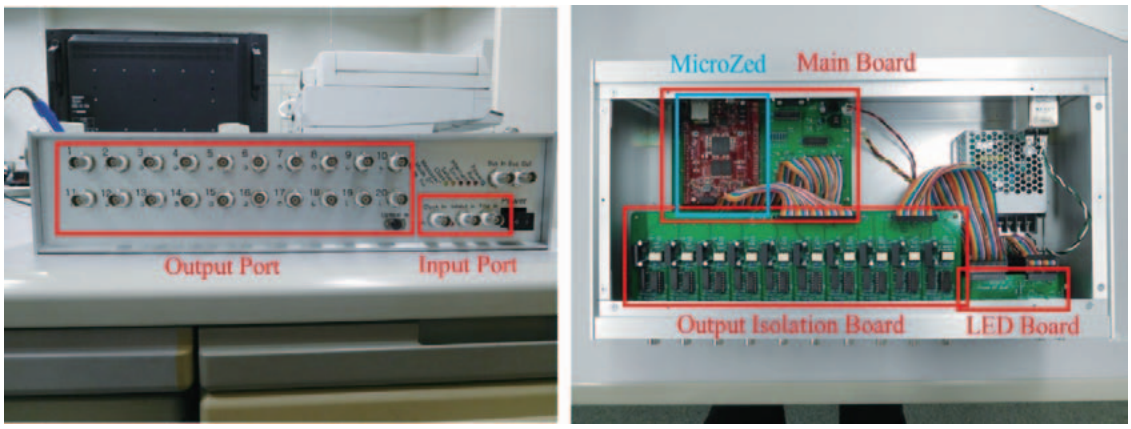

Fig. 2 External and internal view of pulse generator.

(3) Network management

The NIFS campus information networks consist of several clusters, for example, managed Research Information Cluster (NIFS-LAN) and LHD Experiment Cluster (LHD-LAN).

The achievements in FY 2019 are as follows:

(a) Upgrade of the NIFS-LAN core switch module

A 48 ports Ethernet module for the NIFS-LAN core switch has been upgraded.

(b) Renewing security servers

A quarantine server and log management server for the PC authentication system has been upgraded

(c) Update of LHD-LAN firewall

Updating from SSG550 (Juniper Networks) to SRX345 (Juniper Networks) was conducted (Fig. 3)/The maximum number of simultaneous sessions has been increased from 256,000 to 375,000.

Also, the connection between the uplink and the LHD-LAN was replaced to LAG (Link Aggregation) connection to improve reliability.

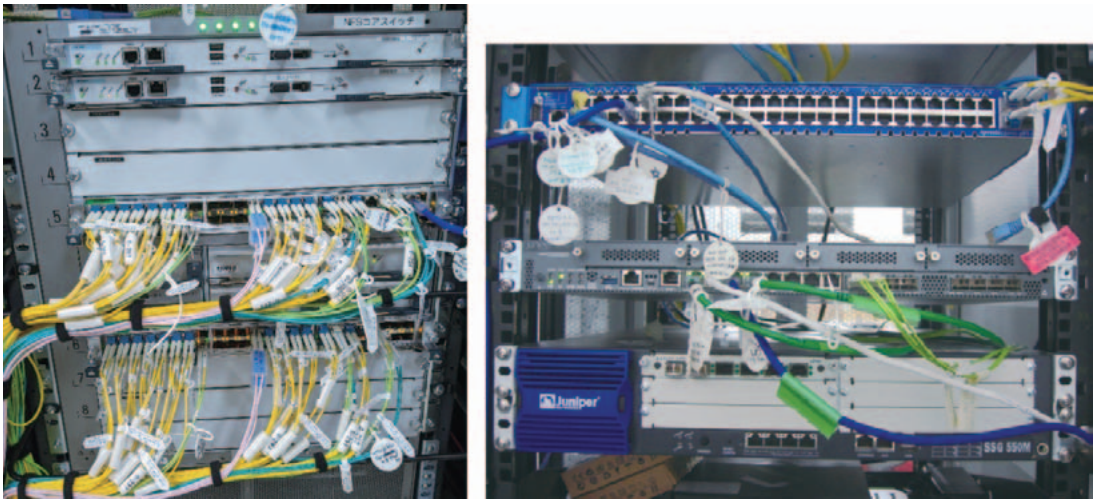

Fig. 3 Upgraded core switch and firewall.

6. Technical exchange and cooperation activities

(1) Third technical exchange meeting: "Structural analysis technology using finite element method"

On February 21, 2020, we held a technical exchange meeting on structural analysis technology based on the finite element method (FEM) as shown in Fig. 1. This was the third meeting. There were 7 presenters and 27 participants, including those who joined remotely with a Web conference application (ZOOM).

In this meeting, four outside presenters presented the comparisons between electromagnetic (EM) analysis software (ANSYS HFSS) and multi-physics analysis software (COMSOL), the analysis of growing polycrystalline silicon for solar cells using a developed FEM cord, and the development of a new electron spectroscopic device using FEM and substitute charge method. Three presenters within NIFS presented EM shield performance evaluation including numerical and shielding analyses, analysis and fabrication of microwave notch filter using ANSYS HFSS, structural analysis on quasi-axisymmetric stellarator CFQS, and EM analysis of magnetic shield performance using ANSYS Emag. We had engaging discussions related to all presentations.

Fig. 1 Technical exchange meeting.

(2) Technical cooperation program: “Analysis of electromagnetic force in the fusion experimental device RELAX”

As part of the technical cooperation program, the EM analysis of the fusion experimental device, RELAX, at the Kyoto Institute of Technology was conducted. At RELAX, in addition to the conventional reverse pinch-type magnetic field, there is a plan to make a modification to enable the tokamak-type magnetic field configuration that is planned to be used for core plasma confinement of the first-generation fusion reactor. To enable the tokamak configuration, the soundness of the magnetic field generation coil needs to be verified.

During March 9–13, 2020, a fourth-year undergraduate student pursuing electronic system engineering at the Plasma Basic Engineering Laboratory of the Kyoto Institute of Technology stayed in NIFS. He investigated the magnetic field generated by the coils and the EM force generated between the coils using ANSYS together with technical staffs in NIFS. First, a 3D analysis model as shown in Fig. 2(a) was created based on the 2D drawings of RELAX using 3D-CAD software (SolidWorks). We then created an appropriate calculation mesh and set boundary conditions that matched the actual phenomenon. The magnetic field distribution, as depicted in Fig. 2(b), in the total analysis region and the EM force generated by the magnetic field generation coils were calculated. Based on the results, we plan to study the modification of the magnetic field generation coils in the next step (Fig. 2(c)).

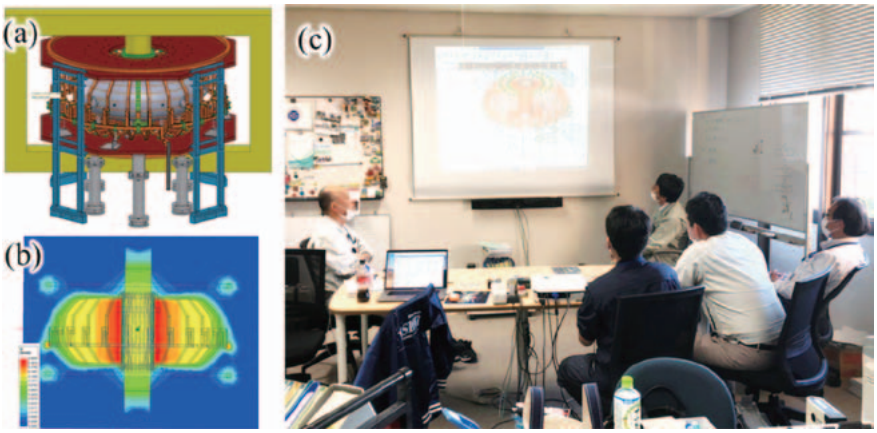

Fig. 2 Technical cooperation program: (a) 3D-CAD model of RELAX; (b) distribution of magnetic field in a vertical section; (c) technical discussion regarding the modification of magnetic field coils.

16. Department of Administration

The Department of Administration handles planning and external affairs, general affairs, accounting, research support, and facility management work.

The major operations of this department are to support the promotion of the Institute's regular research and the development of the collaborative research.

The department consists of the following four divisions, namely, the General Affairs Division, the Financial Affairs Division, the Research Support Division, and the Facilities and Safety Management Division. Details of these divisions are described below.

General Affairs Division

The General Affairs Division handles administrative work and serves as the contact point with the outside. This Division consists of four sections. The General Affairs Section is in charge of secretarial work for the Director General and the Deputy Director General, support for the Advisory Committee meetings, and enacting rules and regulations. The Planning and Evaluation Section is in support for assessment of the institution's performance including scientific achievement and management efficiency. The Personnel and Payroll Section is in charge of general personnel affairs, salary, and public welfare. And the Communications and Public Affairs Section focuses on outreach and publicity activities.

Number of Staff Members (※ This list was compiled as of March 31, 2020.)

Director General	1
Professors	33
Associate Professors	41
Assistant Professors	51
Administrative Staff	45
Technical and Engineering Staff	44
Employee on Annual Salary System	15
Center of Excellence Researcher	3
Research Administrator Staff	3
Visiting Scientists	10
Total	246

Financial Affairs Division

The Financial Affairs Division consists of six sections: The Audit Section, the Financial Planning Section, the Accounts and Properties Administration Section, the Contracts Section, the Procurement Section, and the Purchase Validation Section.

The major responsibilities of the division are to manage and execute the budget, to manage corporate property, revenue/expenditure, and traveling expenses of staff, and to purchase supplies and receive articles.

(JFY 2019)

Settlement (in million of Yen)

Salaried Wages	2,097
Operating Costs	7,054
Equipment	0
Site and Buildings	150
Grant-in-Aid for Scientific Research	149
Total	9,450

Research Support Division

The Research Support Division consists of four sections and one center. These are the Graduate Student Affairs Section, the Academic Information Section which includes the Library at NIFS (since Feb. 2014), the Research Support Section and the International Collaboration Section, which is in charge of inter-university coordination and arranging international cooperation. The Visitor Center assists collaborating researchers and visitors.

Collaboration Research Programs (JFY 2019)

	Applications Applied	Applications Accepted	Researchers Accepted
LHD Project Collaboration Research	25	24	296
Joint Research	249	247	1,854
Joint Research Using Computers	134	132	373
Workshops	31	31	643
Bilateral Collaboration Research	101	101	1,304
Total	540	535	4,470

Number of Graduate School Students
(SOKENDAI: The Graduate University for Advanced Studies) (As of March 31, 2020)

Doctoral Course					
Grade 1	Grade 2	Grade 3	Grade 4	Grade 5	Total
1	2	4	3	4	14

(The Joint Program of Graduate Education)

Graduate course education is given in NIFS apart from SOKENDAI in joint programs with the Department of Energy Science and Engineering of the Graduate School at Nagoya University, Division of Particle and Astrophysical Science of the Graduate School of Science at Nagoya University, Division of Quantum Science of the Graduate School of Engineering at Hokkaido University, Department of Energy Science of the Graduate School of Science and Engineering at University of Toyama, Interdisciplinary Graduate School of Engineering Science in Kyushu University and the Graduate School of Engineering at Tohoku University. In total, 19graduate students are involved in the programs as of March 31, 2019.

The Special Research Collaboration Program for Education (As of March 31, 2020)

Degree / Affiliation	Master's Course	Doctoral Course	Total
National Graduate School	27	6	33
Public Graduate School	1	0	1
Private Graduate School	1	0	1
Total	29	6	35

Foreign Researchers to NIFS (JFY 2019)

P.R. China	Rep. of Korea	Philippines	U.S.A.	Germany	Thailand	Italy	Spain	Others	Total
76	37	19	18	16	16	4	4	25	215

NIFS Researchers to Foreign Countries (JFY 2019)

U.S.A.	P.R. China	Rep. of Korea	Germany	France	Italy	Taiwan	Czech Rep.	Spain	Others	Total
62	54	41	37	18	16	15	15	11	45	314

Books and Journals (JFY 2019)

Books in Japanese	19,320
Books in Other Languages	50,354
Total (volumes)	69,674
Journals in Japanese	272
Journals in Other Languages	816
Total (titles)	1,088

Facilities and Safety Management Division

The Facilities and Safety Management Division consists of three sections: The Safety and Health Management Section, the Facilities Planning Section, and the Facilities Maintenance Section. They are in charge of planning, designing, making contracts, supervising the construction and maintenance of all facilities at NIFS, such as buildings, campus roads, electricity, telephone, power station, air conditioning, water service, gas service, elevators, and cranes. The Facilities and Safety Management Division submits a budget request and administers the budget for those facilities.

The Safety and Health Management Section also arranges medical examination and disaster drills. These three sections promote facilities' environment better for all staff.

Site and Buildings (JFY 2019)

Toki	
Site	464,445 m^2
Buildings	
Total Building Area	39,557 m^2
Total Floor Space	71,830 m^2

APPENDIX

APPENDIX 1. Organization of the Institute

NATIONAL INSTITUTE for FUSION SCIENCE

Organization

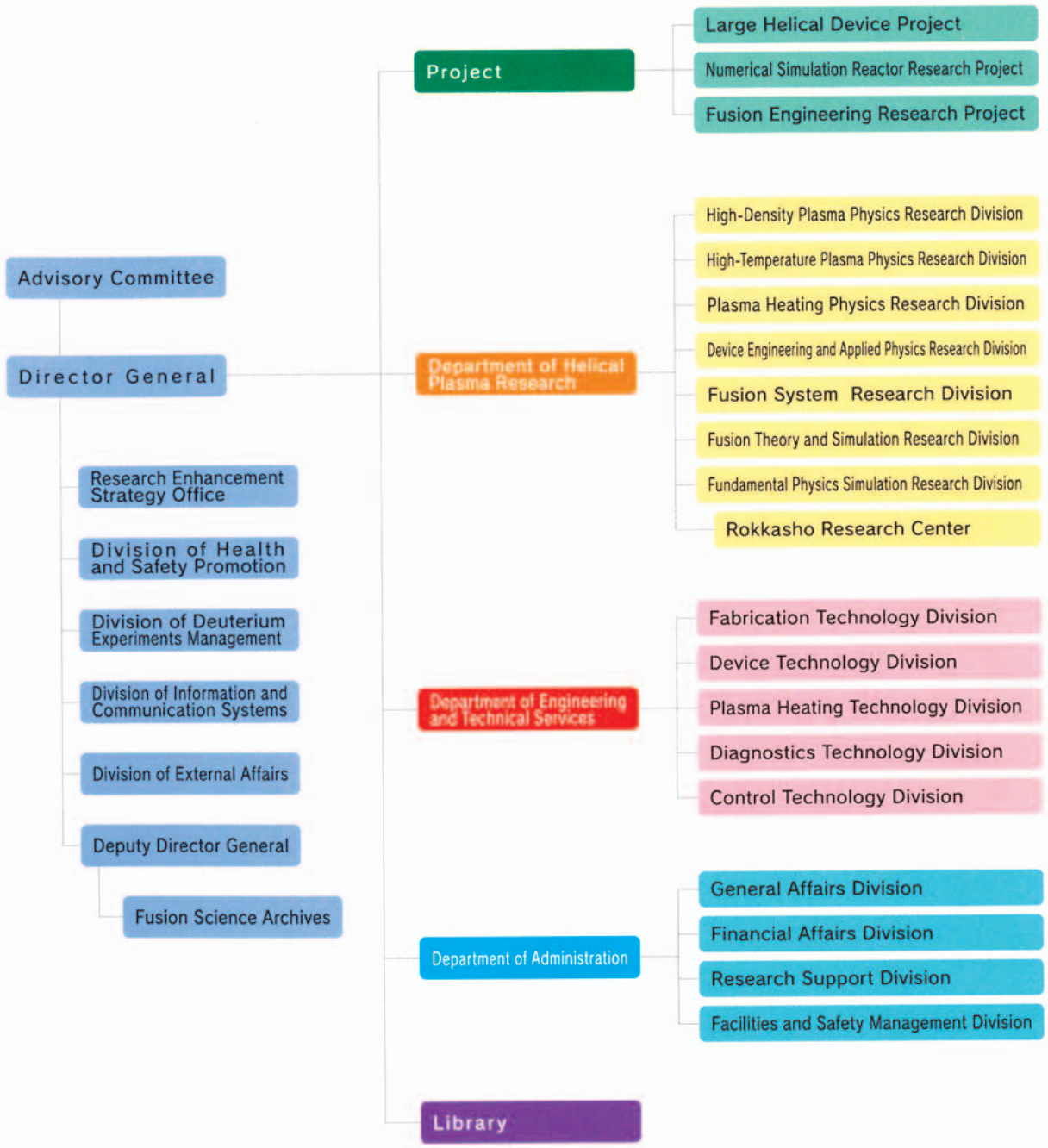

APPENDIX 2. Members of Committees

Advisory Committee

ANDO, Akira	Professor, Graduate School of Engineering, Tohoku University
USHIGUSA, Kenkichi	Managing Director, Fusion Energy Research and Deveropment Directorate, National Institutes for Quantum and Radiological Science and Technology
OHNO, Noriyasu	Director, Graduate School of Engineering, Nagoya University
OGAWA, Yuichi	Professor, Graduate School of Frontier Science, The University of Tokyo
KODAMA, Ryousuke	Director, Institute of Laser Engineering, Osaka University
NAGASAKI, Kazunobu	Professor, Institute of Advanced Energy, Kyoto University
NAKASHIMA, Yousuke	Director, Plasma Research Center, University of Tsukuba
HANADA, Kazuaki	Director, Resarch Institute for Applied Mechanics, Kyushu University
WATANABE, Tomohiko	Professor, Depaertment of Physics , Nagoya University
WADA, Motoi	Professor, Faculty of Science and Engineering, Doshisha University
MUROGA, Takeo	Deputy Director General, NIFS and Executive Director of Fusion Engineering Research Project, NIFS
MORISAKI, Tomohiro	Executive Director of Large Helical Device Project (on Science), NIFS
OSAKABE, Masaki	Executive Director of Large Helical Device Project (on Device), NIFS
SUGAMA, Hideo	Executive Director of Numerical Simulation Research Project, NIFS
YANAGI, Nagato	Executive Director of Fusion Engineering Research Project, NIFS
KUBO, Shin	Director of Plasma Heating Research Division, NIFS
MITO, Toshiyuki	Director of Device Engineering and Applied Physics Research Division, NIFS
MURAKAMI, Izumi	Director of Fusion Systems Research Division, NIFS
TODO, Yasushi	Director of Fusion Theory and Simulation Research Division, NIFS
ISHIGURO, Seiji	Director of Fundamental Physics Simulation Research Division, NIFS
NISHIMURA, Kiyohiko	Division Director for Health and Safety Promotion, NIFS

※ This list was compiled as of March 31, 2021

APPENDIX 3. Advisors, Fellows, and Professors Emeritus

Advisors

Michael Tendler	Professor Royal Institute of Technology Alfvèn Laboratory

Fellows

YAMADA, Hiroshi

Professors Emeritus

ICHIKAWA, Yoshihiko (1993)
MIZUNO, Yukio (1994)
FUJITA, Junji (1996)
KURODA, Tsutomu (1997)
AMANO, Tsuneo (1998)
MOMOTA, Hiromu (1998)
IIYOSHI, Atsuo (1999)
HATORI, Tadatsugu (1999)
TANAHASHI, Shugo (2000)
KAWAMURA, Takaichi (2000)
SATO, Tetsuya (2001)
FUJIWARA, Masami (2002)
TODOROKI, Jiro (2003)
KAMIMURA, Tetsuo (2003)
OHKUBO, Kunizo (2005)
HAMADA, Yasuji (2007)
KATO, Takako (2007)
NODA, Nobuaki (2008)
WATARI, Tetsuo (2008)
MOTOJIMA, Osamu (2009)
SATOH, Kohnosuke (2010)
OHYABU, Nobuyoshi (2010)
MATSUOKA, Keisuke (2010)
TOI, Kazuo (2012)
NARIHARA, Kazumichi (2012)
KUMAZAWA, Ryuhei (2012)
UDA, Tatsuhiko (2012)
SATO, Motoyasu (2012)
YAMAZAKI, Kozo (2013)
KAWAHATA, Kazuo (2013)
OKAMURA, Shoichi (2014)
KOMORI, Akio (2015)
SUDO, Shigeru (2015)
SKORIC, Milos (2015)
MUTO, Takashi (2016)
NAGAYAMA, Yoshio (2017)
NAKAMURA, Yukio (2017)
SAGARA, Akio (2017)
ITOH, Kimitaka (2017)
HORIUCHI, Ritoku(2017)
HIROOKA, Yoshihiko (2018)
MORITA, Shigeru (2019)
NISHIMURA, Arata (2019)

※ This list was compiled as of March 31, 2021

APPENDIX 4. List of Staff

Director General

TAKEIRI, Yasuhiko

Deputy Director General

MUROGA, Takeo

Department of Helical Plasma Research

Prof. MUROGA, Takeo (Director)

High-Density Plasma Physics Research Division

Prof. MORISAKI, Tomohiro (Director)
Prof. WATANABE, Kiyomasa
Prof. SAKAMOTO, Ryuichi
Assoc. Prof. YOSHIMURA, Shinji
Assoc. Prof. OHDACHI, Satoshi
Assoc. Prof. SHOJI, Mamoru
Assoc. Prof. TOKUZAWA, Tokihiko
Assoc. Prof. KOBAYASHI, Masahiro
Assoc. Prof. MOTOJIMA, Gen
Asst. Prof. NARUSHIMA,Yoshiro
Asst. Prof. TAKEMURA, Yuki
Asst. Prof. TSUCHIYA, Hayato
Asst. Prof. OISHI, Tetsutaro
Asst. Prof. NISHIMURA, Shin
Asst. Prof. HAYASHI, Yuki
Asst. KAWAMOTO, Yasuko
Specially Asst. Prof. OHTSUBO, Yohko

High-Temperature Plasma Physics Research Division

Prof. SAKAKIBARA, Satoru (Director)
Prof. TANAKA, Kenji
Prof. ISOBE, Mitsutaka
Prof. IDA, Katsumi
Prof. PETERSON, Byron Jay
Assoc. Prof. GOTO, Motoshi
Assoc. Prof. TAMURA, Naoki
Assoc. Prof. YAMADA, Ichihiro
Assoc. Prof. YASUHARA, Ryo
Assoc. Prof. OZAKI, Tetsuo
Assoc. Prof. NAKANISHI, Hideya
Asst. Prof. OGAWA, Kunihiro
Asst. Prof. KOBAYASHI, Tatsuya
Asst. Prof. MUTO, Sadatsugu
Asst. Prof. FUNABA, Hisamichi
Asst. Prof. YOSHINUMA, Mikirou
Asst. Prof. SUZUKI, Chihiro
Asst. Prof. SHIMIZU, Akihiro
Asst. Prof. EMOTO, Masahiko
Asst. Prof. MUKAI, Kiyofumi
Asst. Prof. UEHARA, Hiyori
Specially Appointed Prof. NISHITANI, Takeo

Plasma Heating Physics Research Division

Prof. KUBO, Shin (Director)
Prof. SIMOZUMA, Takashi
Prof. OSAKABE, Masaki
Prof. TSUMORI, Katsuyoshi
Assoc. Prof. YOSHIMURA, Yasuo
Assoc. Prof. NISHIURA, Masaki
Assoc. Prof. IGAMI, Hiroe
Assoc. Prof. TAKAHASHI, Hiromi
Assoc. Prof. SAITO, Kenji
Assoc. Prof. SEKI, Tetsuo
Prof. NAGAOKA, Kenichi
Asst. Prof. TSUJIMURA, Toru
Asst. Prof. NAKANO, Haruhisa
Asst. Prof. KAMIO, Shuji
Asst. Prof. IKEDA, Katsunori
Asst. Prof. KISAKI, Masashi
Asst. Prof. SEKI, Ryosuke
Asst. Prof. FUJIWARA, Yutaka
Asst. Prof. NUGA, Hideo
Asst. Prof. YANAI, Ryohma

Device Engineering and Applied Physics Research Division

Prof. MITO, Toshiyuki (Director)
Prof. TAKAHATA, Kazuya
Prof. IMAGAWA, Shinsaku
Prof. YANAGI, Nagato
Prof. NISHIMURA, Kiyohiko
Prof. HIRANO, Naoki
Assoc. Prof. IWAMOTO, Akifumi
Assoc. Prof. HAMAGUCHI, Shinji
Assoc. Prof. CHIKARAISHI, Hirotaka
Assoc. Prof. TAKAYAMA, Sadatsugu
Assoc. Prof. TANAKA, Masahiro
Assoc. Prof. SAZE, Takuya
Asst. Prof. TAKADA, Suguru
Asst. Prof. OBANA, Tetsuhiro
Asst. Prof. KOBAYASHI, Makoto
Asst. Prof. ONODERA, Yuta

Fusion Systems Research Division

Prof. MURAKAMI, Izumi (Director)
Prof. MUROGA, Takeo
Prof. MIYAZAWA, Junichi
Prof. NISHIMURA, Arata
Prof. MASUZAKI, Suguru
Assoc. Prof. TANAKA, Teruya
Assoc. Prof. TAMURA, Hitoshi
Assoc. Prof. NAGASAKA, Takuya
Assoc. Prof. HISHINUMA, Yoshimitsu
Assoc. Prof. KATO, Daiji
Assoc. Prof. TOKITANI, Masayuki
Asst. Prof. GOTO, Takuya
Asst. Prof. ASHIKAWA, Naoko
Asst. Prof. NOTO, Hiroyuki
Asst. Prof. SAKAUE, Hiroyuki
Asst. Prof. HAMAJI, Yukinori
Asst. Prof. YAJIMA, Miyuki

Fusion Theory and Simulation Research Division

Prof. TODO, Yasushi (Director)
Prof. SUGAMA, Hideo
Prof. ICHIGUCHI, Katsuji
Prof. YOKOYAMA, Masayuki
Assoc. Prof. MIZUGUCHI, Naoki
Assoc. Prof. TODA, Shinichiro
Assoc. Prof. SATAKE, Shinsuke
Assoc. Prof. KANNO, Ryutaro
Assoc. Prof. SUZUKI, Yasuhiro
Assoc. Prof. NUNAMI, Masanori
Asst. Prof. YAMAGISHI, Osamu
Asst. Prof. ISHIZAKI, Ryuichi
Asst. Prof. NAKATA, Motoki
Asst. Prof. WANG, Hao
Asst. Prof. KAWAMURA, Gakushi
Asst. Prof. SATO, Masahiko
Asst. Prof. YAMAGUCHI, Hiroyuki
Asst. Prof. MATSUOKA, Seikichi

Fundamental Physics Simulation Research Division

Prof. ISHIGURO, Seiji (Director)
Prof. MIURA, Hideaki
Prof. NAKAMURA, Hiroaki
Prof. SAKAGAMI, Hitoshi
Assoc. Prof. USAMI, Shunsuke
Assoc. Prof. OHTANI, Hiroaki
Assoc. Prof. ITO, Atsushi M.
Assoc. Prof. TOIDA, Mieko
Assoc. Prof. YAMAMOTO, Takashi
Asst. Prof. HASEGAWA, Hiroki
Asst. Prof. MORITAKA, Toseo
Asst. Prof. ITO, Atsushi
Asst. Prof. TAKAYAMA, Arimichi

Rokkasho Research Center

Prof. NAKAJIMA, Noriyoshi
Asst. Prof. SATO, Masahiko (Additional Post)

Project

Large Helical Device Project

Prof. MORISAKI, Tomohiro
Prof. OSAKABE, Masaki

Numerical Simulation Reactor Research Project

Prof. SUGAMA, Hideo

Fusion Engineering Research Project

Prof. MUROGA, Takeo
Prof. YANAGI, Nagato

Research Enhancement Strategy Office

Prof. MUROGA, Takeo (Director)
Specially Appointed Prof. OKAMURA, Shoichi
Specially Appointed Prof. ROBINSON, Kenneth
Specially Appointed Prof. YAJI Kentaro
Assoc. Prof. KASAHARA.Hiroshi

Division of Health and Safety Promotion

Prof. NISHIMURA, Kiyohiko (Division Director)

Division for Deuterium Experiments Management

Prof. OSAKABE, Masaki (Division Director)

Division of Information and Communication Systems

Prof. ISHIGURO, Seiji (Division Director)

Division of External Affairs

Prof. TAKAHATA, Kazuya (Division Director)

Fusion Science Archives

Prof. KUBO, Shin (Director)

Library

Prof. MURAKAMI, Izumi (Director)

※ This list was compiled as of March 31, 2021

Guest Professor

Prof. WANG, Weixing	Princeton Plasma Physics Lab	Mar. 22, 2019 – Apr. 21, 2019

COE Research Fellows

SIMON Partric
SHIN Shogeth
JACOBO Varela Rodriguz
MALIK Idouakass
CHEN Hengjiun
ISLAM Md. Shahinul

Research Fellow (Science research)

(None)

Research Fellow (Industrial-Academic coordination)

(None)

JSPS Research Fellow

(None)

Depertment of Administration

NISHIYAMA, Kazunori	Department Director

General Affairs Division

NISHIO, Naoaki	Director
ICHIOKA, Akihiro	Senior Advisor
ARAI, Masanori	Chief/General Affairs Section
SHIMIZU, Kazuma	Chief/Planning and Evaluation Section
MAEDA, Yoshikazu	Chief/Employee Section
SUGIMOTO, Michiho	Chief/Personnel and Payroll Section
MATSUBARA, Tomohisa	Chief/Communications and Public Affairs Section

Financial Affairs Division

SHIMIZU, Naomi	Director
TSUDA, Makoto	Deputy Director
KAWAI, Sanae	Chief/Financial Planning Section
Iwashima, Itsuki	Chief/Accounts and Properties Administration Section
FUJII, Kazuki	Chief/Audit Section
FUKUOKA, Miwa	Chief/Contracts Section
HIBINO, Atsushi	Chief/Procurement Section
HIBINO, Atsushi	Leader/Purchase Validation Section

Research Support Division

FUJITA, Hirotada	Director
TERUMOTO, Naoki	Deputy Director
SUZUKI, Takayuki	Chief/Research Support Section
SOGA, Shihoko	Chief/International Collaboration Section
URUSHIHARA, Satona	Chief/Graduate Student Affairs Section
OHTA, Masako	Chief/Academic Information Section
TERUMOTO, Naoki	Leader/Visitor Center (Additional Post)
KONDO, Takahiko	Chief/Visitor Center

Facilities and Safety Management Division

SHIRAHIGE, Tamio	Director
NITTA, Haruki	Senior Specialist.
NITTA, Haruki	Chief/Facilities Section (Additional Post)
MIYATA, Kazuaki	Chief/Equipment Section

※ This list was compiled as of March 31, 2021

APPENDIX 5. List of Publications I (NIFS Reports)

NIFS-PROC-114 The 7th Japan-China-Korea Joint Seminar on Atomic and Molecular Processes in Plasma (AMPP2018)
May 10, 2019

NIFS-PROC-115 IFS-SWJTU JOINT PROJECT FOR CFQS -.PHYSICS AND ENGINEERING DESIGN- VER. 2.1 2019. SEP
Nov. 08, 2019

NIFS-PROC-116 Collected papers at the 2019 Post-CUP Workshop & JSPS-CAS Bilateral Joint Research Projects Workshop, 24th–26th July, 2019, Nagoya, Japan
Feb. 21, 2021

NIFS-MEMO-86 Report on Administrative Work for Radiation Safety
From April 2018 to March 2019 (in Japanese)
Jan. 14, 2020

NIFS-MEMO-87 Proposal of the CHS-qa expriment
CHS-qa design team
July 22, 2020

※ This list was compiled as of March 31, 2021

APPENDIX 6. List of Publications II (Journals, etc.)

1 Akaslompolo S., Drewelow P., Gao Y., Ali A., Biedermann C., Bozhenkov S., Dhard C., Endler M., Fellinger J., Ford O., Geiger B., Geiger J., Harder N., Hartmann D., Hathiramani D., Isobe M., Jakubowski M., Kazakov Y., Killer C., Lazerson S., Mayer M., McNeely P., Naujoks D., Neelis T., Kontula J., Kurki-suonio T., Niemann H., Ogawa K., Pisano F., Poloskei P., Sitjes A., Rahbarnia K., Rust N., Schmitt J., Sleczka M., Vano L., Vuuren A., Wurden G., Wolf R., W7-x team T.

Validating the ASCOT modelling of NBI fast ions in Wendelstein 7-X stellarator
Journal of Instrumentation 14 C10012

2 Akata N., Hasegawa H., Sugihara S., Tanaka M., Furukawa M., Kurita N., Kovács T., Shiroma Y., Kakiuchi H.

Tritium, hydrogen and oxygen isotope compositions in monthly precipitation samples collected at Toki, JAPAN
Radiation Protection Dosimetry 184 3-4 338-341

3 Akata N., Tanaka M., Iwata C., Kato A., Nakada M., Kovács T., Kakiuchi H.

Isotope Composition and Chemical Species of Monthly Precipitation Collected at the Site of a Fusion Test Facility in Japan
International Journal of Environmental Research and Public Health 16 20 3883

4 Arakawa H., Sasaki M., Inagaki S., Kosuga Y., Kobayashi T., Kasuya N., Yamada T., Nagashima Y., Kin F., Fujisawa A., Itoh K., Itoh S.

Roles of solitary eddy and splash in drift wave–zonal flow system in a linear magnetized plasma
Physics of Plasmas 26 5 26-5, 052305

5 Chen H., Ikesue A., Noto H., Uehara H., Hishinuma Y., Muroga T., Yasuhara R.

Nd^{3+}-activated CaF_2 ceramic lasers
Optics Letters 44 13 3378-3381

6 Chen H., Uehara H., Kawase H., Yasuhara R.

Efficient Pr:$YAlO_3$ lasers at 622 nm, 662 nm, and 747 nm pumped by semiconductor laser at 488 nm
Optics Express 28 3 3017-3024

7 Chen J., Ida K., Yoshinuma M., Murakami I., Kobayashi T., Ye Y., Lyu B.

Effect of Energy Dependent Cross-section on Flow Velocity Measurements with Charge Exchange Spectroscopy in Magnetized Plasma
Physics Letters A 383 12 1293-1299

8 Chikada T., Kimura K., Mochizuki J., Horikoshi S., Matsunaga M., Fujita H., Okitsu K., Tanaka T., Hishinuma Y., Sakamoto Y., Someya Y., Nakamura H.

Surface oxidation effect on deuterium permeation in reduced activation ferritic/martensitic steel F82H for DEMO application
Fusion Engineering and Design 146 PartA 450-454

9 Dinklage A., McCarthy K., Suzuki C., Tamura N., Wegner T., Yamada H., Baldzuhn J., Brunner K., Buttenschön B., Damm H., Drewelow P., Fuchert G., Hirsch M., Hoefel U., Kasahara H., Knauer J., Maier D., Miyazawa J., Motojima G., Oishi T., Rahbarnia K., Pedersen T., Sakamoto R., Wolf R., Zhang D., W7-x team T., The LHD Experimental Group., Tj-ii team T.

Plasma termination by excess pellet fueling and impurity injection in TJ-II, the Large Helical Device and Wendelstein 7-X
Nuclear Fusion 59 7 76010

10 Fujita K., Satake S., Kanno R., Nunami M., Nakata M., Garcia-regana J.

Global effects on the variation of ion density and electrostatic potential on the flux surface in helical plasmas
Plasma and Fusion Research 14 Special Issue 2 3403102

11 Fujiwara Y., Kamio S., Ogawa K., Yamaguchi H., Seki R., Nuga H., Nishitani T., Isobe M., Osakabe M.

Enhancement of an E parallel B type neutral particle analyzer with high time resolution in the Large Helical Device
Journal of Instrumentation 15 C02021

12 Fukuda T., Otsuka T., Sentoku Y., Nagatomo H., Sakagami H., Kodama R., Yugami N.

Experiments of forward THz emission from femtosecond laser created plasma with applied transverse electric field in air
Japanese Journal of Applied Physics 59 2 20902

13 Futatani S., Suzuki Y.

Non-linear magnetohydrodynamic simulations of plasma instabilities from pellet injection in Large Helical Device plasma
Plasma Physics and Controlled Fusion 61 95014

14 Garcia-Munoz M., Sharapov S., Zeeland M., Ascasibar E., Cappa A., Chen L., Ferreira J., Galdon-Quiroga J., Geiger B., Gonzalez-martin J., Heidbrink W., Johnson T., Lauber P., Johanna mantsinen M., Melnikov A., Nabais F., Rivero-rodriguez J., Sanchis-sanchez L., Schneider P., Stober J., Suttrop W., Todo Y., Vallejos P., Zonca F.

Active control of Alfvén eigenmodes in magnetically confined toroidal plasmas
Plasma Physics and Controlled Fusion 61 5 054007 (12pp)

15 Goto M., Ishikawa R., Iida Y., Tsuneta S.

Analytical Solution of the Hanle Effect in View of CLASP and Future Polarimetric Solar Studies
Atoms 7 2 55

16 Goto M., Nimavat N.

Modeling of Lyman-α line polarization in fusion plasma due to anisotropic electron collisions
Journal of Physics: Conference Series 1289 12011

17 Goto M., Uyama H., Ogawa T., Matra K., Motojima G., Oishi T., Morita S.

Dependence of Plasma Parameters in Hydrogen Pellet Ablation Cloud on the Background Plasma Conditions
Plasma and Fusion Research 14 Special Issue 2 3402053

18 Goto T., Miyazawa J., Tamura H., Tanaka T., Sakamoto R., Suzuki C., Seki R., Satake S., Nunami M., Yokoyama M., Yanagi N., Sagara A., Group F.

Conceptual design of a compact helical fusion reactor FFHR-c1 for the early demonstration of year-long electric power generation
Nuclear Fusion 59 7 76030

19 Goto T., Ohgo T., Miyazawa J.

Experimental study on MHD effect of liquid metal sheath jet for the liquid metal divertor REVOLVER-D
Plasma and Fusion Research 14 Regular Issue 1405092

20 Goto Y., Kubo S., Igami H., Nishiura M., Shimozuma T., Yoshimura Y., Takahashi H., Tsujimura T.

Development of the calibration method for a fast steering antenna for investigating the mode conversion window used in EBW heating in the LHD plasma
Japanese Journal of Applied Physics 58 10 106001

21 Goto Y., Kubo S., Tsujimura T.

Cyclotron Emission with a Helical Wavefront from an Electron Accelerated by the Circularly Polarized Wave
Journal of Advanced Simulation in Science and Engineering 7 1 34-50

22 Goto Y., Tsujimura T., Kubo S.

Diffraction Patterns of the Millimeter Wave with a Helical Wavefront by a Triangular Aperture
Journal of Infrared, Millimeter and Terahertz Waves 40 9 943–951

23 Goya K., Uehara H., Konishi D., Sahara R., Murakami M., Tokita S.

Stable 35-W Er: ZBLAN fiber laser with CaF_2 end caps
Applied Physics Express 12 10 102007

24 Haba Y., Nagaoka K., Tsumori K., Kisaki M., Nakano H., Ikeda K., Osakabe M.

Characterisation of negative ion beam focusing based on phase space structure
New Journal of Physics 22 2 23017

25 Hasegawa H., Ishiguro S.

Impurity Ion Transport by Filamentary Plasma Structures
Nuclear Materials and Energy 19 473-478

26 Hasegawa H., Ishiguro S.

Three-dimensional Effect of Particle Motion on Plasma Filament Dynamics
Physics of Plasmas 26 6 062104-1-062104-5

27 Hayashi Y., Nishikata H., Ohno N., Kajita S., Tanaka H., Ohshima H., Seki M.

Double – probe measurement in recombining plasma using NAGDIS – II
Contributions to Plasma Physics 59 7 e201800088

28 Hayashi Y., Ohno N., Meiden H., Scholten J., Kajita S., Berg J., Perillo R., Vernimmen J., Morgan T.
Application of Ion Sensitive Probe to High Density Plasmas in Magnum-PSI
Plasma and Fusion Research 14 Regular Issue 1202135

29 Hollmann E., Nishijima D., Patino M., Chrobak C., Doerner R., Nagata D., Tokitani M.
Observation of increased nanostructure cone growth on Cr due to grazing-incidence Ta seed atom deposition in a He plasma
Journal of Applied Physics 126 7 73301

30 Horiuchi R., Usami S., Moritaka T., Ono Y.
Particle Simulation Studies of Merging Processes of Two Spherical-Tokamak-Type Plasmoids
Physics of Plasmas 26 9 92101

31 Ichiguchi K., Suzuki Y.
Vacuum Configurations of D Shape Heliotron
Plasma and Fusion Research 14 Special Issue 2 3403100

32 Ida K.
Summary of the 27th IAEA Fusion Energy Conference in the categories of EX/W, EX/D, and ICC
Nuclear Fusion 59 11 117001

33 Ida K.
On the interplay between MHD instabilities and turbulent transport in magnetically confined plasmas
Plasma Physics and Controlled Fusion 62 1 14008

34 Ida K., Nakata M., Tanaka K., Yoshinuma M., Fujiwara Y., Sakamoto R., Motojima G., Masuzaki S., Kobayashi T., Yamasaki K.
Transition between Isotope-Mixing and Nonmixing States in Hydrogen-Deuterium Mixture Plasmas
Physical Review Letters 124 43878 25002

35 Ida K., Sakamoto R., Yoshinuma M., Yamasaki K., Kobayashi T., Fujiwara Y., Suzuki C., Fujii K., Chen J., Murakami I., Emoto M., Mackenbach R., Yamada H., Motojima G., Masuzaki S., Mukai K., Nagaoka K., Takahashi H., Oishi T., Goto M., Morita S., Tamura N., Nakano H., Kamio S., Seki R., Yokoyama M., Murakami S., Nunami M., Nakata M., Morisaki T., Osakabe M.
The isotope effect on impurities and bulk ion particle transport in the Large Helical Device
Nuclear Fusion 59 5 56029

36 Ida K., Yoshinuma M., Kobayashi T., Fujiwara Y., Chen J., Murakami I., Kisaki M., Osakabe M.
Verification of Carbon Density Profile Measurements with Charge Exchange Spectroscopy Using Hydrogen and Deuterium Neutral Beams
Plasma and Fusion Research 14 Regular Issue 1402079

37 Ida K., Yoshinuma M., Yamasaki K., Kobayashi T., Fujiwara Y., Chen J., Murakami I., Satake S., Yamamoto Y., Murakami S., Kobayashi M.
Measurements of radial profile of hydrogen and deuterium density in isotope mixture plasmas using bulk charge exchange spectroscopy
Review of Scientific Instruments 90 9 93503

38 Idei H., Onchi T., Mishra K., Zushi H., Kariya T., Imai T., Watanabe O., Ikezoe R., Hanada K., Ono M., Ejiri A., Qian J., Nakamura K., Fujisawa A., Nagashima Y., Hasegawa M., Matsuoka K., Fukuyama A., Kubo S., Yoshikawa M., Sakamoto M., Kawasaki S., Higashijima A., Ide S., Takase Y., Murakami S.
Electron heating of over-dense plasma with dual-frequency electron cyclotron waves in fully non-inductive plasma ramp-up on the QUEST spherical tokamak
Nuclear Fusion 60 1 16030

39 Ikeda K., Miyamoto K., Oguri H., Kashiwagi M.
Front Runner: Negative ion source was not made in a day, Expansion of Studies for Negative Ion Beam and Source
Journal of Plasma and Fusion Research 95 7 328-349

40 Ikeda K., Tsumori K., Nagaoka K., Nakano H., Kisaki M., Fujiwara Y., Kamio S., Haba Y., Masaki S., Osakabe M.
Extension of high power deuterium operation of negative ion based neutral beam injector in the large helical device
Review of Scientific Instruments 90 11 113322

41 Ikeda K., Tsumori K., Nakano H., Kisaki M., Nagaoka K., Kamio S., Fujiwara Y., Haba Y., Osakabe M.

Exploring deuterium beam operation and the behavior of the co-extracted electron current in a negative-ion-based neutral beam injector
Nuclear Fusion 59 7 76009

42 Imagawa S., Obana T., Takada S., Hamaguchi S., Chikaraishi H.

Study on Configuration of Conductor Samples for 13 T – 700 mm Test Facility
Plasma and Fusion Research 14 Special Issue 2 3405060

43 Isobe M., Shimizu A., Liu H., Liu H., Xiong G., Yin D., Ogawa K., Yoshimura Y., Nakata M., Kinoshita S., Okamura S., Tang C., Xu Y.

Current Status of NIFS-SWJTU Joint Project for Quasi-Axisymmetric Stellarator CFQS
Plasma and Fusion Research 14 Special Issue 2 3402074

44 Ito A., Nakajima N.

Magnetic flux coordinates for analytic high-beta tokamak equilibria with flow
Plasma Physics and Controlled Fusion 61 10 105006

45 Iwamoto A., Fujimura T., Norimatsu T.

Void free fuel solidification in a foam shell FIERX target
Plasma and Fusion Research 15 Special Issue 1 2404006

46 Kamio S., Fujiwara Y., Ogawa K., Isobe M., Seki R., Nuga H., Nishitani T., Osakabe M., The LHD Experimental Group.

Development of NPA Array Using Single Crystal CVD Diamond Detectors
Journal of Instrumentation 14 C08002

47 Kanno R., Kawamura G., Nunami M., Homma Y., Hatayama A., Hoshino K.

Global modelling of tungsten impurity transport based on the drift-kinetic equation
Nuclear Fusion 60 1 16033

48 Kariya T., Minami R., Imai T., Okada M., Motoyoshi F., Numakura T., Nakashima Y., Idei H., Onchi T., Hanada K., Shimozuma T., Yoshimura Y., Takahashi H., Kubo S., Oda Y., Ikeda R., Sakamoto K., Ono M., Nagasaki K., Eguchi T., Mitsunaka Y.

Development of high power gyrotrons for advanced fusion devices
Nuclear Fusion 59 6 066009 (10pp)

49 Kawase H., Uehara H., Chen H., Yasuhara R.

Passively Q-switched 2.9 μm Er:YAP single crystal laser using graphene saturable absorber
Applied Physics Express 12 10 102006

50 Kawase H., Yasuhara R.

2.92-μm high-efficiency continuous-wave laser operation of diode-pumped Er:YAP crystal at room temperature
Optics Express 27 9 12213

51 Kenmochi N., Nishiura M., Nakamura K., Yoshida Z.

Tomographic Reconstruction of Imaging Diagnostics with a Generative Adversarial Network
Plasma and Fusion Research 14 Regular Issue 1202117

52 Kin F., Fujisawa A., Itoh K., Kosuga Y., Sasaki M., Inagaki S., Nagashima Y., Yamada T., Kasuya N., Yamasaki K., Hasamada K., Zhang B., Kawachi Y., Arakawa H., Kobayashi T., Itoh S.

Observations of radially elongated particle flux induced by streamer in a linear magnetized plasma
Physics of Plasmas 26 4 26-4, 042306

53 Kin F., Itoh K., Happel T., Birkenmeier G., Fujisawa A., Inagaki S., Itoh S., Stroth U.

Comparison of Conditional Average Using Threshold and Template Methods for Quasi-Periodic Phenomena in Plasmas
Plasma and Fusion Research 14 Regular Issue 14, 1402114

54 Kinoshita S., Shimizu A., Okamura S., Isobe M., Xiong G., Liu H., Xu Y.

Engineering Design of the Chinese First Quasi-Axisymmetric Stellarator (CFQS)
Plasma and Fusion Research 14 Special Issue 2 3405097

55 Kobayashi M., Ogawa K., Isobe M., Nishitani T., Kamio S., Fujiwara Y., Tsubouchi T., Yoshihashi S., Uritani A., Sakama M., Osakabe M., The LHD Experimental Group.

Thermal neutron flux evaluation by a single crystal CVD diamond detector in LHD deuterium experiment
Journal of Instrumentation 14 C09039

56 Kobayashi M., Saze T., Miyake H., Ogawa K., Isobe M., Tanaka M., Akata N., Nishimura K., Hayashi H., Kobuchi T., Yokota M., Osuna M., Nakanishi H., Osakabe M., Takeiri Y., LHD Experiment Group.

Radiation control in LHD and radiation shielding capability of the torus hall during first campaign of deuterium experiment
Fusion Engineering and Design 143 180-187

57 Kobayashi M., Seki R., Masuzaki S., Morita S., Zhang H., Narushima Y., Tanaka H., Tanaka K., Tokuzawa T., Yokoyama M., Ido T., Yamada I., The LHD Experimental Group.

Impact of a resonant magnetic perturbation field on impurity radiation, divertor footprint, and core plasma transport in attached and detached plasmas in the Large Helical Device
Nuclear Fusion 59 9 96009

58 Kobayashi M., Tanaka T., Nishitani T., Ogawa K., Isobe M., Motojima G., Kato A., Yoshihashi S., Osakabe M., LHD Experiment Group.

Neutron flux distributions in the Large Helical Device torus hall evaluated by an imaging plate technique in the first campaign of the deuterium plasma experiment
Nuclear Fusion 59 12 126003

59 Kobayashi T., Ida K., Suzuki Y., Takahashi H., Takemura Y., Yoshinuma M., Tsuchiya H., Sanders M., LHD Experiment Group.

Electron temperature profile collapse induced by double-odd-parity MHD mode in the Large Helical Device
Nuclear Fusion 60 3 36017

60 Kobayashi T., Kobayashi M., Iwama N., Kuzmin A., Goto M., Kawamura G., The LHD Experimental Group.

Three dimensional distribution of impurity emission in the edge region of LHD obtained by single field-of-view tomography
Nuclear Materials and Energy 19 239

61 Kobayashi T., Losada U., Liu B., Estrada T., Milligen B., R G., Sasaki M., Carlos H.

Frequency and plasma condition dependent spatial structure of low frequency global potential oscillations in the TJ-II stellarator
Nuclear Fusion 59 4 44006

62 Kobayashi T., Takahashi H., Nagaoka K., Sasaki M., Nakata M., Yokoyama M., Seki R., Yoshinuma M., Ida K.

Isotope effects in self-organization of internal transport barrier and concomitant edge confinement degradation in steady-state LHD plasm
Scientific Reports 9 15913

63 Kobayashi T., Takahashi H., Nagaoka K., Sasaki M., Yokoyama M., Seki R., Yoshinuma M., Ida K.

Definition of the profile gain factor and its application for internal transport barrier analysis in torus plasmas
Plasma Physics and Controlled Fusion 61 8 85005

64 Kodama N., Himura H., Azuma K., Tsumori K., Nakano H.

Effect of a Magnetic Filter Across the Exit Hole of a Flat Oxygen Plasma Source
Plasma and Fusion Research 14 Regular Issue 1206088

65 Laube R., Bussiahn R., Tamura N., McCarthy K.

Integration of the TESPEL injection system at W7-X
Fusion Engineering and Design 150 111259

66 Liu B., Dai S., Kawamura G., Zhang L., Feng Y., Wang D.

3D effects of neon injection positions on the toroidally symmetric/asymmetric heat flux distribution on EAST
Plasma Physics and Controlled Fusion 62 35003

67 Maeda T., Hasegawa H., Ishiguro S., Hoshino K., Hatayama A.

Effects of the Plasma Blob Nonlinear Formation/Transport on Impurity Transport in the SOL Regions
Plasma and Fusion Research 14 Special Issue 2 3403133

68 Masaki S., Maeshiro K., Tsumori K., Wada M.

Electric Potential Structure in the Extraction Region of the Negative Hydrogen Ion Source
Plasma and Fusion Research 14 Special Issue 2 3401136

69 Mase A., Kogi Y., Maruyama T., Tokuzawa T., Sakai F., Kunugida M., Koike T., Hasegawa H.

Non-Contact and Real-Time Measurement of Heart Rate and Heart Rate Variability Using Microwave Reflectometry
Review of Scientific Instruments 91 1 14704

70 Masuzaki S., Otsuka T., Ogawa K., Yajima M., Tokitani M., Zhou Q., Isobe M., Oya Y., Yoshida N., Nobuta Y.

Investigation of Remaining Tritium in the LHD Vacuum Vessel after the First Deuterium Experimental Campaign
Physica Scripta T171 14068

71 Matoike R., Kawamura G., Ohshima S., Kobayashi M., Suzuki Y., Nagasaki K., Masuzaki S., Kobayashi S., Yamamoto S., Kado S., Minami T., Okada H., Konoshima S., Mizuuchi T., Tanaka H., Matsuura H., Feng Y., Frerichs H.

First Application of 3D Peripheral Plasma Transport Code EMC3-EIRENE to Heliotron J
Plasma and Fusion Research 14 Special Issue 2 3403127

72 Matsuo K., Higashi N., Iwata N., Sakata S., Lee S., Johzaki T., Sawada H., Iwasa Y., Law K., Morita H., Ochiai Y., Kojima S., Abe Y., Hata M., Sano T., Nagatomo H., Sunahara A., Alessio M., Yogo A., Nakai M., Sakagami H., Ozaki T., Yamanoi K., Norimatsu T., Nakata Y., Tokita S., Kawanaka J., Shiraga H., Mima K., Azechi H., Kodama R., Arikawa Y., Sentoku Y., Fujioka S.

Petapascal Pressure Driven by Fast Isochoric Heating with a Multipicosecond Intense Laser Pulse
Physical Review Letters 124 3 35001

73 Matsuyama M., Zushi H., Tokunaga K., Kuzmin A., Hanada K.

Effect of Re-Deposition Layers in Plasma-Facing Wall on Tritium Retention and Tritium Depth Profile
Plasma and Fusion Research 14 Regular Issue 1405125

74 Mito T., Onodera Y., Hirano N., Takahata K., Yanagi N., Iwamoto A., Hamaguchi S., Takada S., Baba T., Chikumoto N., Kawagoe A., Kawanami R.

Development of FAIR conductor and HTS coil for fusion experimental device
Journal of Physics Communications 4 3 35009

75 Miura H., Yang J., Gotoh T.

Hall magnetohydrodynamic turbulence with a magnetic Prandtl number larger than unity
Physical Review E 100 6 63207

76 Miyazawa J., Tamura H., Tanaka T., Hamaji Y., Kobayashi M., Murase T., Nakagawa S., Goto T., Yanagi N., Sagara A., Group F.

Improved Design of a Cartridge-Type Helical Blanket System for the Helical Fusion Reactor FFHR-b1
Plasma and Fusion Research 14 Regular Issue 1405163

77 Moon C., Kobayashi T., Ida K., Tokuzawa T., Hidalgo C., Yoshinuma M., Ogawa K., Itoh K., Fujisawa A., LHD Experiment Group.

Spatial Structure of Low-Frequency Fluctuations throughout the Transition of Poloidal Flow Velocity in Edge Plasmas of LHD
Physics of Plasmas 26 9 92302

78 Mori T., Nishiura M., Yoshida Z., Kenmochi N., Katsura S., Nakamura K., Yokota Y., Tsujimura T., Kubo S.

Simulation of Electromagnetic Wave Propagation in a Magnetospheric Plasma
Plasma and Fusion Research 14 Special Issue 2 3401134

79 Morishita T., Ito A.

Traveling without dwelling: Extending the timescale accessible to molecular dynamics simulation
Physical Review Research 1 3 33032

80 Morita S., Dong C., Kato D., Liu Y., Zhang L., Cui Z., Goto M., Kawamoto Y., Murakami I., Oishi T.

Quantitative analysis on tungsten spectra of W^{6+} to W^{45+} ions
Journal of Physics: Conference Series 1289 12005

81 Moritaka T., Hager R., Cole M., Lazerson S., Chang C., Ku S., Matsuoka S., Satake S., Ishiguro S.

Development of a Gyrokinetic Particle-in-Cell Code for Whole-Volume Modeling of Stellarators
Plasma 2 2 179

82 Motojima G., Masuzaki S., Morisaki T., Tanaka H., Sakamoto R., Murase T., Schmitz O., Kobayashi M., Shoji M., Tokitani M., Tsuchibushi Y., Yamada H., Takeiri Y., LHD Experiment Group.

New approach to the control of particle recycling using divertor pumping in the Large Helical Device
Nuclear Fusion 59 8 86022

83 Motojima G., Murase T., Shoji M., Ogawa H., Yokota M., Maccallini E., Siviero F., Ferrara A., Mura M., Sakurai H., Masuzaki S., Morisaki T.

New installation of in-vessel Non Evaporable Getter (NEG) pumps for the divertor pump in the LHD
Fusion Engineering and Design 143 226-232

84 Motojima G., Okada H., Okazaki H., Kobayashi S., Nagasaki K., Sakamoto R., Yamada H., Kado S., Ohshima S., Minami T., Kenmochi N., Ohtani Y., Nozaki Y., Yonemura Y., Nakamura Y., Konoshima S., Yamamoto S., Mizuuchi T., Watanabe K.

High-density experiments with hydrogen ice pellet injection and analysis of pellet penetration depth in Heliotron J
Plasma Physics and Controlled Fusion 61 7 75014

85 Muroga T., Fukada S., Hayashi T.

Overview of Fusion Engineering Research in Japan Focusing on Activities in NIFS and Universities
Fusion Science and Technology 75 7 559-574

86 Nagaoka K., Hotta S., Hidaka Y., Kobayashi T., Terasaka K., Yoshimura S.

Characteristics of electroconvection turbulence and proposal of its application to turbulent transport experiment in a rotating spherical shell
High Energy Density Physics 31 79-82

87 Nagaoka K., Takahashi H., Nakata M., Satake S., Tanaka K., Mukai K., Yokoyama M., Nakano H., Murakami S., Ida K., Yoshinuma M., Ohdachi S., Bando T., Nunami M., Seki R., Yamaguchi H., Osakabe M., Morisaki T., The LHD Experimental Group.

Transport characteristics of deuterium and hydrogen plasmas with ion internal transport barrier in the Large Helical Device
Nuclear Fusion 59 10 106002

88 Nagasaka T., Muroga T., Tanaka T., Sagara A., Fukumoto K., Zheng P., Kurtz R.

High-temperature creep properties of NIFS-HEAT-2 high-purity low-activation vanadium alloy
Nuclear Fusion 59 9 96046

89 Nakamura H., Miyanishi H., Yasunaga T., Fujiwara S., Mizuguchi T., Nakata A., Miyazaki T., Otsuka T., Kenmotsu T., Hatano Y., Saito S.

Molecular dynamics study on DNA damage by tritium disintegration
Japanese Journal of Applied Physics 59 SA SAAE01

90 Nimavat N., Goto M., Oishi T., Morita S.

Polarization measurement of hydrogen Lyman-α in the Large Helical Device
Journal of Physics: Conference Series 1289 12038

91 Nimavat N., Goto M., Oishi T., Morita S.

Study of Lyman-α Polarization due to Anisotropic Electron Collisions in LHD
Plasma and Fusion Research 14 Special Issue 2 3402083

92 Nishijima D., Tokitani M., Patino M., Nagata D., A G., Doerner R.

Effect of a Cr-rich surface layer on D retention in various RAFM steels
Physica Scripta T171 14005

93 Nishimura A.

Study on Butt Weld Joint of Thick Plate Superconducting Coil Structure to Reduce Welding Residual Deformation
Plasma and Fusion Research 14 Special Issue 2 3405062

94 Nishitani T., Arikawa Y., Kishimoto H., Murata I., Ogawa K., Pu N., Isobe M.

Development of capillary plate neutron detector filed with liquid scintillator by using recoiled-particle trajectory analyses
Journal of Instrumentation 14 C10026

95 Nishitani T., Ozaki T., Saito K., Kamio S., Ogawa K., Isobe M., Osakabe M.

Neutronics analyses for shield upgrading of the compact neutral particle analyzer for LHD deuterium plasma experiments
Plasma and Fusion Research 14 Special Issue 2 3405048

96 Nishitani T., Roman R., Krasilnikov V., Aakanksha S., Laura C., Luciano B.

Neutronics assessment of a compact D-D neutron generator as a neutron source for the neutron calibration in magnetic confinement fusion devices
Plasma and Fusion Research 15 Special Issue 1 2402017

97 Nishiura M., Yoshida Z., Kenmochi N., Sugata T., Nakamura K., Mori T., Katsura S., Shirahata K., HOWARD J.

Experimental analysis of self-organized structure and transport on the magnetospheric plasma device RT-1
Nuclear Fusion 59 9 96005

98 Nojiri K., Ashikawa N.

Collaboration Works of JSPS Bilateral Joint Research Projects (Japan (NIFS) – China (ASIPP))
Journal of Plasma and Fusion Research 96 3 149-151

99 Noto H., Hishinuma Y., Muroga T.

Transformation super plasticity deformation of reduced activation ferritic/martensitic steel
Fusion Engineering and Design 145 94-99

100 Nuga H., Seki R., Ogawa K., Kamio S., Fujiwara Y., Osakabe M., Isobe M., Nishitani T., Yokoyama M.

Analysis of energetic particle confinement in LHD using neutron measurement and simulation codes
Plasma and Fusion Research 14 Special Issue 2 3402075

101 Obana T., Terazaki Y., Yanagi N., Hamaguchi S., Chikaraishi H., Takayasu M.

Self-field measurements of an HTS twisted stacked-tape cable conductor
Cryogenics 105 103012

102 Ogawa K., Bozhenkov S., Akaslompolo S., Isobe M., Nuga H., Seki R., Kamio S., Fujiwara Y., Nishitani T., Osakabe M., The LHD Experimental Group.

Effect of Resonant Magnetic Perturbation Field on Energetic Ion Behavior in the Large Helical Device
Plasma and Fusion Research 14 Regular Issue 1202159

103 Ogawa K., Bozhenkov S., Akaslompolo S., Killer C., Grulke O., Nicolai D., Satheeswaran G., Isobe M., Osakabe M., Yokoyama M., Wolf R., W7-x team T.

Energy-and-pitch-angle-resolved escaping beam ion measurements by Faraday-cup-based fast-ion loss detector in Wendelstein 7-X
Journal of Instrumentation 14 C09021

104 Ogawa K., Isobe M., Nishitani T., Murakami S., Seki R., Nuga H., Kamio S., Fujiwara Y., Yamaguchi H., Saito Y., Maeta S., Osakabe M., LHD Experiment Group.

Energetic ion confinement studies using comprehensive neutron diagnostics in the Large Helical Device
Nuclear Fusion 59 7 76017

105 Ogawa K., Seki R., Yamaguchi H., Murakami S., Isobe M., Shimizu A., Kinoshita S., Okamura S., Liu H., Xu Y.

Feasibility Study of Neutral Beam Injection on Chinese First Quasi-axisymmetric Stellarator (CFQS)
Plasma and Fusion Research 14 Special Issue 2 3402067

106 Ohdachi S.

Special Topic Articles: Plasma Informatics – Application of Data Driven Science to Plasmas 5.Inverse problems in the imaging diagnostics and its relation to data science
Journal of Plasma and Fusion Research 95 11 554-559

107 Ohdachi S., Yamamoto S., Suzuki Y., Purohit S., Iwama N.

Tomographic inversion technique using orthogonal basis patterns
Plasma and Fusion Research 14 Special Issue 2 3402087

108 Ohgo T., Goto T., Miyazawa J.

A New Divertor System Using Fusible Metal Pebbles
Plasma and Fusion Research 14 Special Issue 2 3405050

109 Okamoto A., Yoshimura S., Terasaka K., Tanaka M.

Variation of Doppler Broadening in High-Temperature Bubbles Created in an ECR Plasma
Plasma and Fusion Research 14 Regular Issue 1201165

110 Olevskaia V., Kobayashi T., Ida K., Yoshinuma M., Wenqing H.

Multi-channel scanning filter spectrometer for the beam emission spectroscopy
Plasma and Fusion Research 14 Regular Issue 1305118

111 Ozaki T., Kamio S., Nishitani T., Saito K., Ogawa K., Isobe M., Osakabe M., Kobayashi M.

Reduction of the neutron induced noise in the compact neutral particle analyzer for LHD deuterium plasma experiments
Plasma and Fusion Research 14 Special Issue 2 3402142

112 Pu N., Nishitani T., Isobe M., Ogawa K., Matsuyama S., Miwa M.

Evaluation of scintillating-fiber detector response for 14 MeV neutron measurement
Journal of Instrumentation 14 P10015

113 Purohit S., Suzuki Y., Ohdachi S., Yamamoto S.

Capability studies of the Heliotron -J soft X-ray tomographic diagnostic
Plasma and Fusion Research 14 Special Issue 2 3402056

114 Purohit S., Suzuki Y., Ohdachi S., Yamamoto S.

Soft x-ray tomographic reconstruction of Heliotron J plasma for the study of magnetohydrodynamic equilibrium and stability
Plasma Science and Technology 21 6 65102

115 Reman B., Dendy R., Akiyama T., Chapman S., Cook J., Igami H., Inagaki S., Saito K., Yun G.

Interpreting observations of ion cyclotron emission from Large Helical Device plasmas with beam-injected ion populations
Nuclear Fusion 59 9 96013

116 Saito K., Wang S., Wi H., Kim H., Kamio S., Nomura G., Seki R., Seki T., Kasahara H., Mutoh T.

Development of power combination system for high-power and long-pulse ICRF heating in LHD
Fusion Engineering and Design 146 PartA 256-260

117 Saito T., Tanaka S., Shinbayashi R., Tatematsu Y., Yamaguchi Y., Fukunari M., Kubo S., Shimozuma T., Tanaka K., Nishiura M.

Oscillation Characteristics of a High Power 300 GHz Band Pulsed Gyrotron for Use in Collective Thomson Scattering Diagnostics
Plasma and Fusion Research 14 Regular Issue 1406104

118 Sasaki A., Richard M., Fujii K., Kato D., Murakami I.

Atomic kinetics calculations of complex highly-charged ions in plasmas in non-local thermodynamic equilibrium by using a Monte-Carlo approach
High Energy Density Physics 32 1-7

119 Sasaki M., Camenen Y., Escarguel A., Inagaki S., Kasuya N., Itoh K., Kobayashi T.

Formation of spiral structures of turbulence driven by a strong rotation in magnetically cylindrical plasmas
Physics of Plasmas 26 4 42305

120 Sasaki M., Itoh K., Kosuga Y., Dong J., Inagaki S., Kobayashi T., Cheng J., Zhao K., Itoh S.

Parallel flow driven instability due to toroidal return flow in high-confinement mode plasmas
Nuclear Fusion 59 6 66039

121 Sasaki M., Kasuya N., Kosuga Y., Kobayashi T., Yamada T., Arakawa H., Inagaki S., Itoh K.

Turbulence simulation on zonal flow formations in the presence of parallel flows
Plasma and Fusion Research 14 Regular Issue 1401161

122 Sato M., Todo Y.

Effect of precession drift motion of trapped thermal ions on ballooning modes in helical plasmas
Nuclear Fusion 59 9 94003

123 Seguineaud G., Motojima G., Narushima Y., Goto M.

Non-CLTE spectral modeling approach for hydrogen pellet ablation cloud in the Large Helical Device
Journal of Physics: Conference Series 1289 conference 1 12039

124 Seki R., Ogawa K., Isobe M., Yokoyama M., Murakami S., Nuga H., Kamio S., Fujiwara Y., Osakabe M.

Evaluation of Neutron emission rate with FIT3D-DD code in large helical device
Plasma and Fusion Research 14 Special Issue 2 3402126

125 Seki R., Todo Y., Suzuki Y., Spong D., Ogawa K., Isobe M., Osakabe M.

Comprehensive magnetohydrodynamic hybrid simulations of Alfvén eigenmode bursts and fast-ion losses in the Large Helical Device
Nuclear Fusion 59 9 96018

126 Sergeev V., Dnestrovskij A., Frolov V., Pustovitov V., Tamura N.

Modeling of heat pulse propagation during TESPEL injection into the LHD plasma
Plasma and Fusion Research 14 Special Issue 2 3402121

127 Shimizu A., Liu H., Kinoshita S., Isobe M., Okamura S., Ogawa K., Nakata M., Satake S., Suzuki C., Xiong G., Xu Y., Liu H., Zhang X., Huang J., Wang X., Tang C., Yin D., Wan Y.

Consideration of the influence of coil misalignment on the Chinese First Quasi-Axisymmetric Stellarator magnetic configuration
Plasma and Fusion Research 14 Special Issue 2 3403151

128 Shiroma Y., Hirao S., Akata N., Furukawa M., Miyake H., Hayashi H., Saze T., Tanaka M.

Measurement of Absorbed Dose Rate in Air at NIFS Site after the First Deuterium Plasma Experiment in LHD
Plasma and Fusion Research 14 Regular Issue 1305130

129 Shoji M., Kawamura G.

Comparative Analysis of Impurity Transport in the Peripheral Plasma in the Large Helical Device for Carbon and Tungsten Divertor Configurations with EMC3-EIRENE
Plasma and Fusion Research 14 Special Issue 2 3403057

130 Sugama H., Matsuoka S., Satake S., Nunami M., Watanabe T.

Improved linearized model collision operator for the highly collisional regime
Physics of Plasmas 26 10 102108

131 Sugama H., Research project T.

Recent Progress in the Numerical Simulation Reactor Research Project
Plasma and Fusion Research 14 Special Issue 2 3503059

132 Sugiyama S., Matsuura H., Goto T., Nishitani T., Isobe M., Ogawa K.

Prediction of Neutron Emission Anisotropy for Validation of an Analysis Model for Neutron Spectra in Beam-Injected LHD Deuterium Plasmas
Plasma and Fusion Research 14 Special Issue 2 3403123

133 Suzuki C., Emoto M., Ida K.

Special Topic Articles: Data Analysis Infrastructures in Plasma Experiments 2. Automatic Data Compilation / Analysis Infrastructure in LHD -AutoAna-
Journal of Plasma and Fusion Research 95 5 208-212

134 Suzuki C., Koike F., Murakami I., Tamura N., Sudo S., O'Sullivan G.

Soft X-ray Spectroscopy of Rare-Earth Elements in LHD Plasmas
Atoms 7 3 66

135 Suzuki C., Mukai K., Masuzaki S., Kobayashi M., Peterson B., Akiyama T., Murakami I., LHD Experiment Group.

Spectroscopic studies on the enhanced radiation with high Z rare gas seeding for mitigating divertor heat loads in LHD plasmas
Nuclear Materials and Energy 19 195-199

136 Suzuki C., Murakami I., Koike F., Higashiguchi T., Sakaue H., Tamura N., Sudo S., O'Sullivan G.

Development of an Experimental Database of EUV Spectra from Highly Charged Ions of Medium to High Z Elements in the Large Helical Device Plasmas
X-Ray Spectrometry 49 1 78-84

137 Tachibana Y., Tanaka M., Nogami M.

Crown ether-type organic composite adsorbents embedded in high-porous silica beads for simultaneous recovery of lithium and uranium in seawater
Journal of Radioanalytical and Nuclear Chemistry 322 2 717-730

138 Taimourzadeh S., Bass E., Chen Y., Collins C., Gorelenkov N., Könies A., Lu Z., Spong D., Todo Y., Austin M., Bao J., Biancalani A., Borchardt M., Bottino A., Heidbrink W., Kleiber R., Lin Z., Mishchenko A., Shi L., Varela J., Waltz R., Yu G., Zhang W., Zhu Y.

Verification and validation of integrated simulation of energetic particles in fusion plasmas
Nuclear Fusion 59 6 066006 (17pp)

139 Takada E., Amitani T., Fujisaki A., Ogawa K., Nishitani T., Isobe M., Jo J., Matsuyama S., Miwa M., Murata I.

Design optimization of a fast-neutron detector with scintillating fibers for triton burnup experiments at fusion experimental devices
Review of Scientific Instruments 90 4 43503

140 Takada S.

A Review of Pool boiling in Superfluid Helium under microgravity condition
International Journal of Microgravity Science and Application 36 4 360401

141 Takahashi K., Tsuyoshi I., Ishitomi M., Nagaoka K., Haba Y., Nakano H., Ando A., Kisaki M., Tsumori K., Ikeda K.

Spatiotemporal oscillation of an ion beam extracted from a potential-oscillating plasma source
New Journal of Physics 21 93043

142 Takemura Y., Watanabe K., Sakakibara S., Ohdachi S., Narushima Y., Ida K., Yoshinuma M., Tsuchiya H., Tokuzawa T., Yamada I.

Study of slowing down mechanism of locked-mode-like instability in helical plasmas
Nuclear Fusion 59 6 66036

143 Tamura H., Goto T., Yanagi N., Miyazawa J., Tanaka T., Sagara A., Ito S., Hashizume H.

Effect of coil configuration parameters on the mechanical behavior of the superconducting magnet system in the helical fusion reactor FFHR
Fusion Engineering and Design 146 Part A 586-589

144 Tamura H., Yanagi N., Goto T., Miyazawa J., Tanaka T., Sagara A., Ito S., Hashizume H.

Mechanical Design Concept of Superconducting Magnet System for Helical Fusion Reactor
Fusion Science and Technology 75 384-390

145 Tamura Y., Kobayashi M., Kobayashi T., Omori W., Nakamura H., Ohtani H., Fujiwara S., The LHD Experimental Group.

Volume Rendering Method Applied to 3D Edge Impurity Emission in LHD to Produce Projection Image in Arbitrary Plane
Plasma and Fusion Research 14 Special Issue 2 3406084

146 Tanaka H., Kawamura G., Hoshino K., Kobayashi M., Matsunaga G., Suzuki Y., Lunt T., Feng Y., Ohno N.

First EMC3-EIRENE modelling of JT-60SA edge plasmas with/without resonant magnetic perturbation field
Contributions to Plasma Physics e201900114

147 Tanaka H., Masuzaki S., Kawamura G., Kobayashi M., Suzuki Y., Morisaki T., Ohno N.

Analysis of indefinite divertor footprint with proper orthogonal decomposition in hydrogen/deuterium plasmas in LHD
Nuclear Materials and Energy 19 378-383

148 Tanaka K., Ohtani Y., Nakata M., Warmer F., Tsujimura T., Takemura Y., Kinoshita T., Takahashi H., Yokoyama M., Seki R., Igami H., Yoshimura Y., Kubo S., Shimozuma T., Tokuzawa T., Akiyama T., Yamada I., Yasuhara R., Funaba H., Yoshinuma M., Ida K., Goto M., Motojima G., Shoji M., Masuzaki S., Michael C., Vacheslavov L., Osakabe M., Morisaki T.

Isotope effects on energy, particle transport and turbulence in electron cyclotron resonant heating plasma of the Large Helical Device
Nuclear Fusion 59 12 126040

149 Tanaka M., Akata N., Iwata C.

Environmental tritium around a fusion test facility
Radiation Protection Dosimetry 184 43894 324-327

150 Tanaka T., Kobayashi M., Yoshihashi S., Uritani A., Watanabe K., Yamazaki A., Nishitani T., Ogawa K., Isobe M.

Measurement of Thermal and Epithermal Neutron Flux Distribution in the Torus Hall of LHD using Activation Method in the First Deuterium Experiment Campaign
Plasma and Fusion Research 14 Special Issue 2 3405162

151 Tanaka T., Noto H., Sato F., Hishinuma Y., Sakaue H., Yoshino M.

Examination of Transmutation Effect on Responses of K-Type and N-Type Thermocouples at Fusion Blanket
Fusion Science and Technology 75 8 1076–1083

152 Tanaka T., Sagara A., Yagi J., Muroga T.

Liquid Blanket Collaboration Platform Oroshhi-2 at NIFS with FLiNaK/LiPb Twin Loops
Fusion Science and Technology 75 8 1002-1009

153 Tanaka T., Yoshihashi S., Kobayashi M., Uritani A., Watanabe K., Yamazaki A., Nishitani T., Ogawa K., Isobe M.

Measurement of Neutron Spectrum using Activation Method in Deuterium Plasma Experiment at LHD
Fusion Engineering and Design 146 Part A 496-499

154 Terasaka K., Yoshimura S.

Front Runner:Characteristics of High-Temperature Bubbles Observed in an ECR Plasma
Journal of Plasma and Fusion Research 95 9 461-466

155 Toda S., Nakata M., Nunami M., Ishizawa A., Watanabe T., Sugama H.

Transport Simulation for Helical Plasmas by use of Gyrokinetic Transport Model
Plasma and Fusion Research 14 Special Issue 2 3403061

156 Todo Y.

Critical energetic particle distribution in phase space for the Alfvén eigenmode burst with global resonance overlap
Nuclear Fusion 59 9 96048

157 Toida M., Igami H., Saito K., Akiyama T., Kamio S., Seki R.

Simulation study of energetic ion driven instabilities near the lower hybrid resonance frequency in a plasma with increasing density
Plasma and Fusion Research 14 Special Issue 2 3401112

158 Tokitani M., Hamaji Y., Hiraoka Y., Masuzaki S., Tamura H., Noto H., Tanaka T., Muroga T., Sagara A., Group F.

Leak tight joint procedures for ODS-Cu/ODS-Cu by the advanced brazing technique
Fusion Engineering and Design 148 111274

159 Tsuchiya H., Iwama N., Yamaguchi S., Takenaka R., Koga M.

Feasibility Study of Holography Using Microwave Scattering
Plasma and Fusion Research 14 Special Issue 2 3402146

160 Ueda Y., Hatano Y., Yokomine T., Hinoki T., Hasegawa A., Oya Y., Muroga T.

Project Review: Japan-US Joint Research Project PHENIX-Accomplishments of 6 Years Project and the Next Program-1. Overview of PHENIX Project
Journal of Plasma and Fusion Research 96 3 129-148

161 Uehara H., Konishi D., Goya K., Sahara R., Murakami M., Tokita S.

Power scalable 30-W mid-infrared fluoride fiber amplifier
Optics Letters 44 19 4777-4780

162 Usami S., Horiuchi R., Ohtani H.

Horn-Shaped Structure Attached to the Ring-Shaped Ion Velocity Distribution during Magnetic Reconnection with a Guide Field
Plasma and Fusion Research 14 Special Issue 2 3401137

163 Usami S., Horiuchi R., Ohtani H., Ono Y., Inomoto M., Tanabe H.

Dependence of the Pickup-Like Ion Effective Heating on the Poloidal and Toroidal Magnetic Fields during Magnetic Reconnection
Physics of Plasmas 26 10 102103

164 Varela J., Cooper A., Nagaoka K., Watanabe K., Spong D., Garcia L., Cappa A., Azegami A.
Effect of the tangential NBI current drive on the stability of pressure and energetic particle driven MHD modes in LHD plasma
Nuclear Fusion 60 2 26016

165 Varela J., Spong D., Garcia L., Ohdachi S., Watanabe K., Seki R.
Analysis of the MHD stability and energetic particles effects on EIC events in LHD plasma using a Landau-closure model
Nuclear Fusion 59 4 46008

166 Voermans S., Ida K., Kobayashi T., Yoshinuma M., Tsuchiya H., Akiyama T., Emoto M.
Characteristics of tongue-shaped deformations in hydrogen and deuterium plasmas in the Large Helical Device
Nuclear Fusion 59 10 106041

167 Wang H., Todo Y., Osakabe M., Ido T., Suzuki Y.
Simulation of energetic particle driven geodesic acoustic modes and the energy channeling in the large helical device plasmas
Nuclear Fusion 59 9 96041

168 Watanabe K., Sakakibara S., Narushima Y., Ohdachi S., Suzuki Y., Takemura Y., Ida K., Yoshinuma M., Yamada I.
Dependence of the resonant magnetic perturbation penetration threshold on plasma parameters and ions in helical plasmas
Nuclear Fusion 59 8 86049

169 Yajima M., Hatano Y., Ohno N., Kuwabara T., Toyama T., Takagi M., Suzuki K.
Kinetics of Deuterium Penetration into Neutron-Irradiated Tungsten under Exposure to High Flux Deuterium Plasma
Nuclear Materials and Energy 21 100699

170 Yamada H., Tanaka K., Seki R., Suzuki C., Ida K., Fujii K., Goto M., Murakami S., Osakabe M., Tokuzawa T., Yokoyama M., Yoshinuma M.
Isotope effect on energy confinement time and thermal transport in neutral-beam-heated stellarator-heliotron plasmas
Physical Review Letters 123 18 185001

171 Yamaguchi H.
A quasi-isodynamic magnetic field generated by helical coils
Nuclear Fusion 59 10 104002

172 Yanagihara K., Kubo S., Tsujimura T., Dodin I.
Mode purity of electron cyclotron waves after their passage through the peripheral plasma in the Large Helical Device
Plasma and Fusion Research 14 Special Issue 2 3403103

173 Yang J., Gotoh T., Miura H., Watanabe T.
Intermittency of an incompressible passive vector convected by isotropic turbulence
Physical Review Fluids 4 11 114602

174 Yang J., Gotoh T., Miura H., Watanabe T.
Statistical properties of an incompressible passive vector convected by isotropic turbulence
Physical Review Fluids 4 6 64601

175 Yokoyama M.
Statistical induction of a thermal transport model based on the transport analyses database
Nuclear Fusion 59 9 94004

176 Yokoyama M., Yamaguchi H.
Practicability of a statistically induced thermal transport model based on TASK3D-a transport analyses database
Plasma and Fusion Research 14 Regular Issue 1303095

177 Yokoyama S., Takahashi T., Ota M., Kakiuchi H., Hirao S., Momoshima N., Tamari T., Shima N., Atarashi-Andoh M., Fukutani S., Nakasone S., Furukawa M., Tanaka M., Akata N.
Development of Field Estimation Technique and Improvement of Environmental Tritium Behavior Model
Plasma and Fusion Research 14 Special Issue 2 3405099

178 Yoshida K., Miura H., Tsuji Y.
Spectrum in the Strong Turbulence Region of Gross–Pitaevskii Turbulence
Journal of Low Temperature Physics 196 43832 211–217

179 Yoshimura S., Aramaki M., Otsubo Y., Yamashita A., Koga K.

Controlling feeding gas temperature of plasma jet with Peltier device for experiments with fission yeast
Japanese Journal of Applied Physics 58 SE SEEG03

180 Yoshimura S., Terasaka K., Tanaka M.

Intermittent Magnetic Fluctuations Associated with High-Temperature Bubbles in an ECR Plasma
Plasma and Fusion Research 14 Special Issue 2 3401081

※ This list was compiled as of March 31, 2021

National Institute for Fusion Science

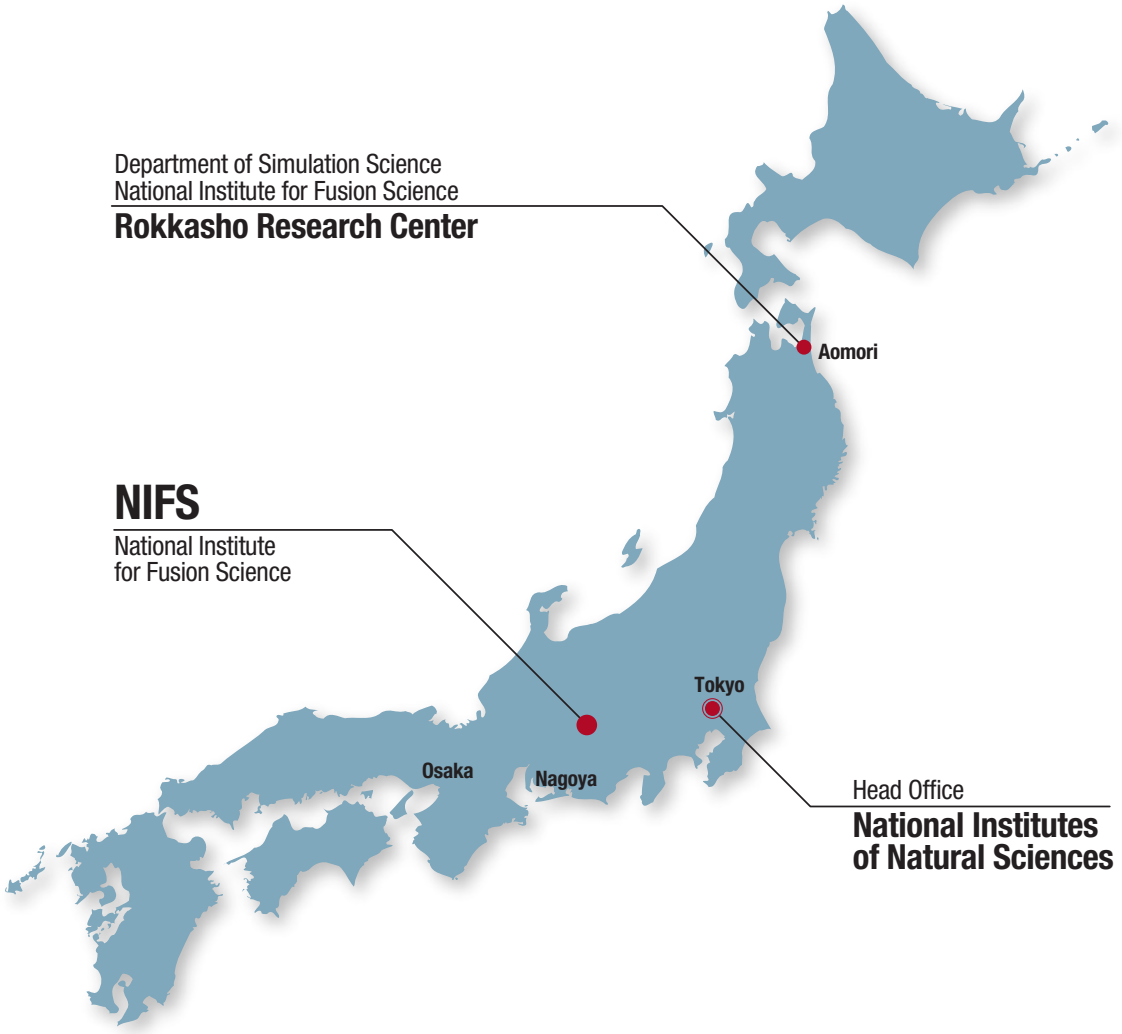

National Institute for Fusion Science
National Institutes of Natural Sciences
(TOKI Area)

322-6 Oroshi-cho
Toki-city, GIFU
509-5292

TEL: 0572-58-2222 FAX: 0572-58-2601

Rokkasho Research Center
Department of Helical Plasma Research
Located in the Aomori Research and Development Center
Japan Atomic Energy Agency

2-166 Oaza-Obuchi-Aza-Omotedate,
Rokkasho-mura, Kamikita-gun,
AOMORI
039-3212

TEL/FAX: 0175-73-2151

How to Reach National Institute for Fusion Science

☐ACCESS

When you use the public transportation facility

◇from Centrair (Central Japan International Airport)

Centrair – (μ-sky) – Meitetsu Kanayama Sta. (36km)
about 25min

JR Kanayama Sta. – (JR Chuo Line) – JR Tajimi Sta. (33km)
about 33min (express)

JR Tajimi Sta. – (Totetsu Bus) – Kenkyuugakuentoshi (7km)
about 15min

◇from JR Nagoya Sta.

JR Nagoya Sta. – (JR Chuo Line) – JR Tajimi Sta. (36km)
about 22min (limited express) / about 30min (lapid) / about 40min (local)

JR Tajimi Sta. – (Totetsu Bus) – Kenkyuugakuentoshi (7km)
about 15min

◇from Nagoya Airport

(Obihiro•Akita•Yamagata•Niigata•Kouchi• Matsuyama•Fukuoka•Kumamoto•Nagasaki)

Nagoya Airport – (Taxi) – JR Kachigawa Sta. (4km)
about 10min

Nagoya Airport – (Meitetsu Bus) – JR Kachigawa Sta. (4km)
about 19min

JR Kachigawa Sta. – (JR Chuo Line) – JR Tajimi Sta. (21km)
about 20min

JR Tajimi Sta. – (Totetsu Bus) – Kenkyuugakuentoshi (7km)
about 15min

When you use a car

from Chuo Expressway Toki I.C. or Tajimi I.C. (8km)
about 20min

from Tokai-Kanjo Expressway Tokiminami Tajimi I.C. (2km)
about 5min

How to Reach Rokkasho Research Center

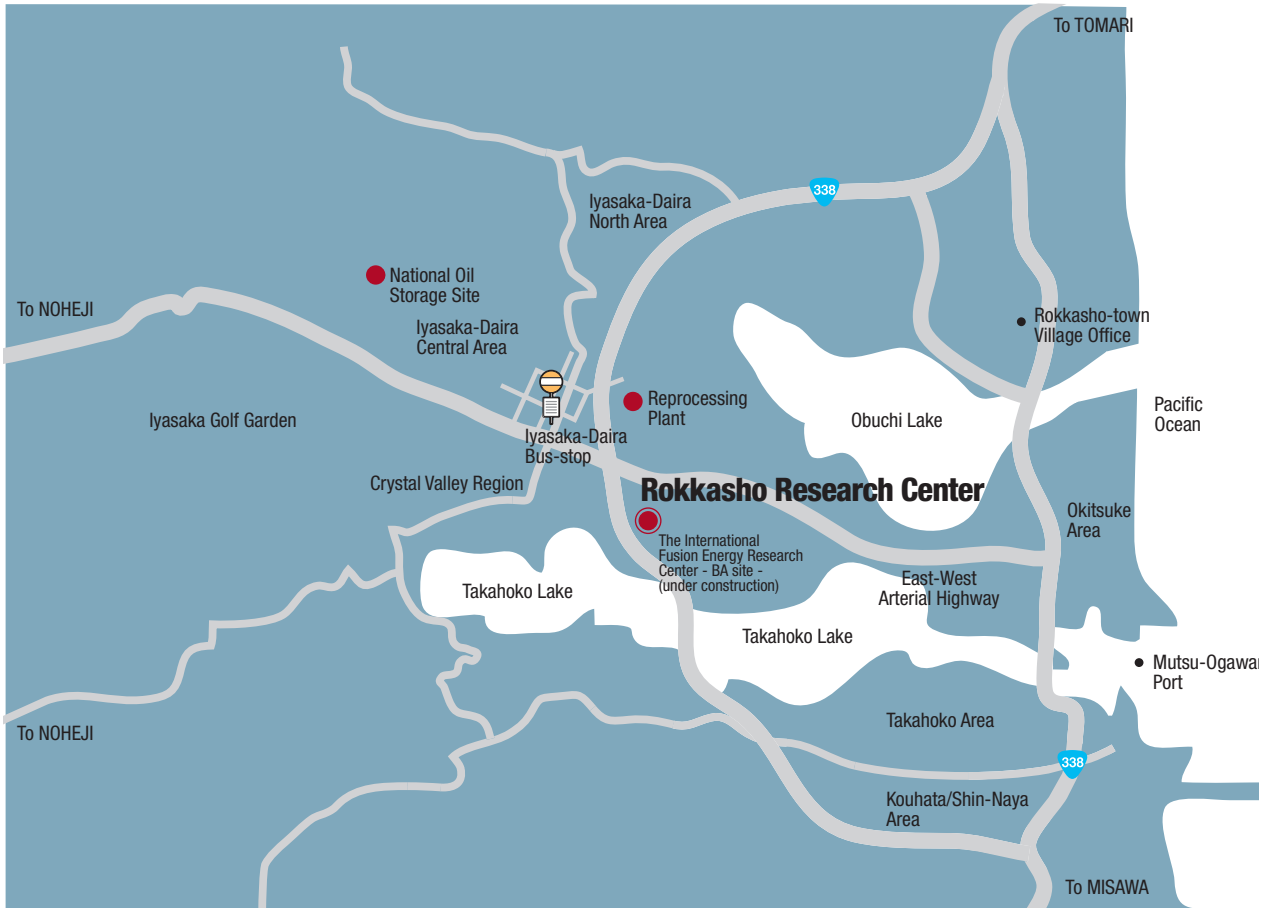

☐ACCESS

When you use the public transportation facility

◇from Tokyo

Tokyo – (Tohoku-Shinkansen) – Hachinohe Sta. (630km)
about 3hr

Hachinohe Sta. – (JR Tohoku Limited Express) – Noheji (51km)
about 30min

Noheji – (Shimokita Koutsu Bus) – Iyasaka-Daira (10km)
about 40min

Iyasaka-Daira .....on foot..... Rokkasho Research Center (0.7km)
about 8min

◇from Misawa Airport

Misawa Airport – (Bus) – Misawa (2km)
about 13min

Misawa – (JR Tohoku Limited Express) – Noheji (30km)
about 20min

Noheji – (Shimokita Koutsu Bus) – Iyasaka-Daira (10km)
about 40min

Iyasaka-Daira .....on foot..... Rokkasho Research Center (0.7km)
about 8min

◇from Aomori Airport

Aomori Airport – (Bus) – Aomori (12km)
about 40min

Aomori – (JR Tohoku Limited Express) – Noheji (45km)
about 30min

Noheji – (Shimokita Koutsu Bus) – Iyasaka-Daira (10km)
about 40min

Iyasaka-Daira .....on foot..... Rokkasho Research Center (0.7km)
about 8min

National Institute for Fusion Science

Building Arrangement

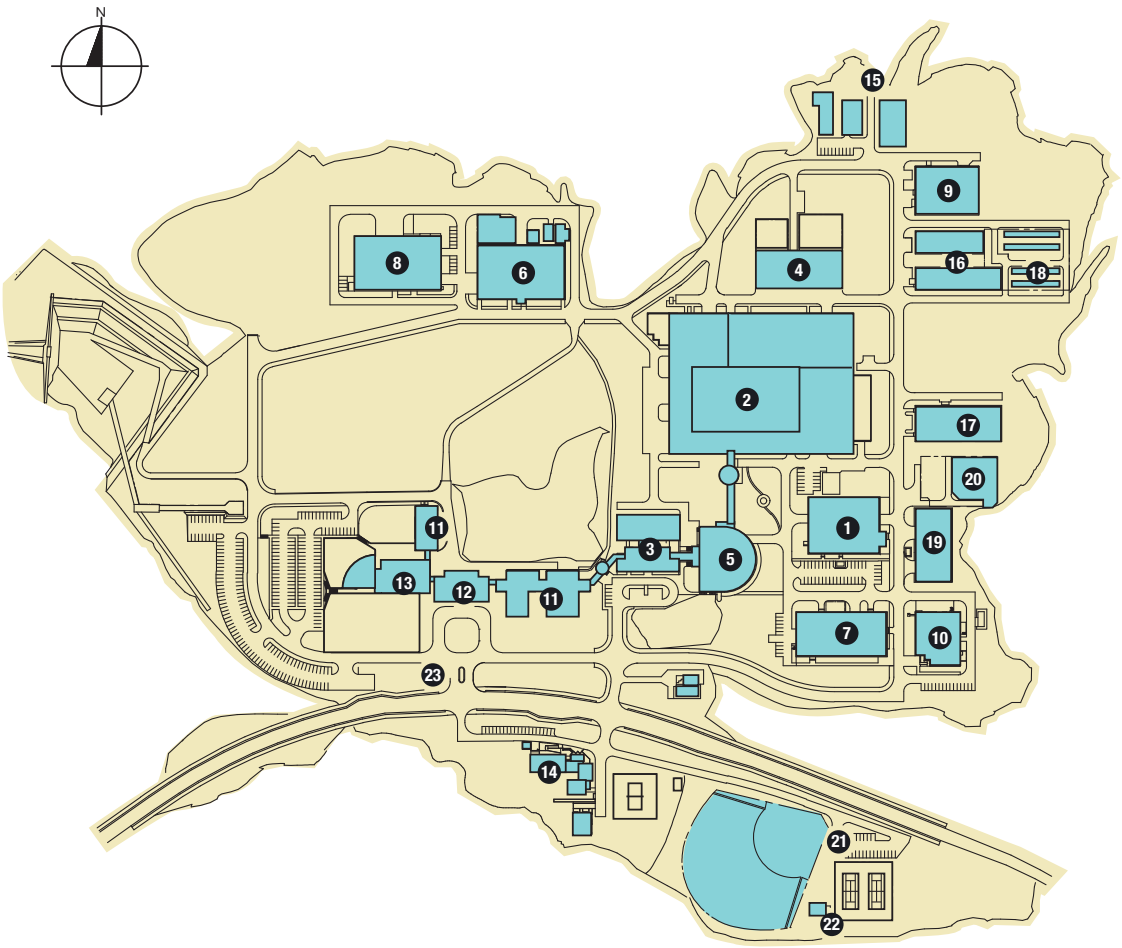

NIFS plot plan

1. Superconducting Magnet System Laboratory
2. Large Helical Device Building
3. Simulation Science Research Laboratory
4. Heating and Power Supply Building
5. LHD Control Building
6. Fusion Engineering Research Laboratory
7. Plasma Diagnostics Laboratories
8. R & D Laboratories
9. Motor-Generator Building
10. Central Workshops
11. Research Staff Building
12. Library Building
13. Administration Building
14. Helicon Club (Guest Housing)
15. High-Voltage Transformer Station
16. Cooling Water Pump Building
17. Helium Compressor Building
18. Cooling Tower
19. Equipments Room
20. Helium Tank Yard
21. Recreation Facilities
22. Club House
23. Guard Office